

Luís Miguel Antunes de Sousa

Licenciatura em Bioquímica

**Elucidating the role of synucleins in retinal
neurodegeneration in Parkinson's Disease, Diabetes
and Ageing**

Dissertação para obtenção do Grau de Mestre em
Bioquímica para a Saúde

Orientador: Sandra Tenreiro , PhD, Cell and Molecular Neuroscience Lab,
CEDOC | NOVA Medical School, Faculdade de Ciências Médicas da
Universidade Nova de Lisboa

Setembro de 2018

Luís Miguel Antunes de Sousa

Licenciatura em Bioquímica

**Elucidating the role of synucleins in retinal
neurodegeneration in Parkinson's Disease, Diabetes
and Ageing**

Dissertação para obtenção do Grau de Mestre em
Bioquímica para a Saúde

Orientador: Sandra Tenreiro , PhD, Cell and Molecular Neuroscience Lab,
CEDOC | NOVA Medical School, Faculdade de Ciências Médicas da
Universidade Nova de Lisboa

Júri:

Presidente: Prof. Doutor António Sebastião Rodrigues

Arguente(s): Doutor João Filipe da Costa Martins

Vogal(ais): Doutora Sandra Isabel Nogueira Tenreiro

Prof^a. Doutora Teresa Catarino

**Faculdade de Ciências Médicas da Universidade Nova de Lisboa
CEDOC | NOVA Medical School**

Setembro de 2018

Elucidating the role of synucleins in retinal neurodegeneration in Parkinson's Disease, Diabetes and ageing

Copyright © Luís Miguel Antunes de Sousa, FCM/UNL

Todas as afirmações efetuadas no presente documento são de exclusiva responsabilidade do seu autor, não cabendo qualquer responsabilidade à Faculdade de Ciências Médicas da Universidade Nova de Lisboa pelos conteúdos nele apresentados.

Acknowledgements

A year went by and it is overwhelming how things have changed, the new people I met, the bonds I strengthened, the values I learned and the skills I developed. What is even more astonishing is the fact that I overcame personal limitations which I believed I would never cross. However, I am fully aware that all the accomplishments I have gathered this passing year would not be possible without the following people, to whom I will be forever grateful. It is a honour to have you carved in my own life story. From the bottom of my heart: **thank you!**

First of all, I would like to thank my dear supervisor **Dr. Sandra Tenreiro**. From all the researchers I contacted for a master thesis position, you were the first to take a step and to accept me as your pupil. You opened the first door of my professional growth in science and gave me the opportunity to shine and to do my best. You have always cared for me (almost like a mother when I cut myself) and trusted me to do my work, you taught me many great things, gave me the chance to become more independent and even to teach others on your behalf. A part of my scientist persona comprises a bit of you. Countless more things can be said, but take note that I will cherish you forever in my heart.

I would like to thank you **Dr. Tiago Outeiro** for giving me the chance to join your lab, this opportunity provided me long lasting memories and skills that are very special to me.

To you **Dr. Hugo Miranda**, I present you my sincere acknowledgments for all the support you have given me this whole year. Thank you for all the brainstorming conversations on the hallway and criticism on my work, I deeply treasure your opinion and mindset. I hope I can repay you someday such kindness. Thank you for being a good friend and for teaching me many things!

Prof. Dr. Teresa Catarino you too deserve my honest acknowledgments for accepting me in the Master of Biochemistry for Health and for that contagious good mood you always have.

I would also like to thank to **CEDOC**, as I was so well accepted in this research institute which provided me excellent opportunities to meet other scientists and to learn.

I also would like to thank to my whole **lab team**. I would have never guessed I would make such good friends and so powerful memories at this point of my life. **Gabriela Santos**, aka Gabs, you deserve a special thank you. One year ago, you let me be your shadow, you let me learn from you and never frowned whenever you had to teach me something while having the stress with your own thesis. You have been my partner in crime this whole year and we both form “o pessoal dos olhinhos” group! Thank you for always being there to hear me and advise me, to answer my doubts, for waiting for me to lunch with you despite your hungry tummy. I will not ever be able to pay you back what you have done for me and I am extremely proud to call you my dear friend! **Ana Chegão**, the great-great-great-granny of our lab, you know how much I look up to you! That is why I am always teasing you, to see if you get down from that throne of yours. But seriously, thank you for your assertive attitude and advice that helped me mature both as a human and as a scientist., I truly value your warm heart! Whenever I would be almost shutting down from low energy you always found a way to cheer me up. I learned a lot from you, do not ever forget that! **Bárbara Gomes**, aka Babita Caganita, we have such good memories trying to change Ana’s PC wallpaper (we should have done an album of that by the way!); Thank you for this awesome year, whenever any issue would come up you would be always ready to give me a solution (amazing how quickly you were the first to always text back), or, ready to laugh with me of my own misery! “Terrível!” as you would say! You do not know how much I value you letting me in your life, I sincerely thank you! **Joana Rodrigues**, impressive how far way you have been and it seems as though you are still here at CEDOC. Unfortunately, we hung up very little, but you made sure to always send me Swedish strength and good vibes, thank you for your awesome personality, for your support and for that chocolate you gave me on your thesis presentation day (yes I have not eaten it, it is a special gift)! To you **Tiago Coelho**, aka Lapin (yes I have not forgotten), it is mesmerizing how we started from barely talking, as you were extremely shy, to talking so regularly to the point you would keep me company throughout the night while I was writing my thesis! I cannot thank you enough for all the support, for the awesome drawings, for the 1000 gels I needed (oh god...) and other stuff! I hope our friendship lasts way more than Neji’s life (bro love, no homo)! **Andreia Monteiro**, aka owner of the Bobby Zimurski laugh, you were the last member to enter the team, but I have to confess that things would have not been the same without you! Thank you for all the support you always gave me, for the positive words comforting my

sleepless nights in the confocal microscope, for all the gels you made for me, for your home as place to host a very special event of a Harry Potter film marathon, and so many more things! You too played a big role on my journey! To you **Dr. Angela Castela**, I thank you for the precious help you offered by teaming up with me during 3 months! I seriously do not know how I would have managed to make those western blots if it was not for your help! A part of my thesis contains a bit of you! Thank you for all the advice and pro-activity, I do take your opinion very seriously. I hope someday fate joins us to work together again and for a beer! To you **Dr. João Martins**, even at hundreds of kilometres away you still managed to be helpful and to promptly answer my questions. I do not know how can I thank you, more than being helpful, you left me material to work on, a scientific direction, a logic and reasoning to follow, as you were the propeller of this work.

Sarah Dias and **Mariana Guarda**, you both played a role in the development of my thesis! Your appearance in my story encouraged me to keep on working hard on my thesis and to keep and maintain my enthusiasm while I was teaching you! Thank you for the awesome memories!

To you **Dr. Rita Oliveira**, thank you for your daily good mood, you always knew how to put a smile on my face with your compliments every day. I am very grateful for all the caring, work-related suggestions, late night conversations before my confocal microscopy sessions, and all the help you provided me!

To the **Drs. Luísa Lopes, Paula Macedo, Sílvia Conde, Diana Cunha-Reis, Marcelo Mendonça and Rui Costa**, I sincerely thank you for providing the animals that made possible this whole thesis.

I would also like to thank to all my **friends**, whenever I needed a brake on the thesis or a boost on my confidence, you were always ready to support me and ready to cheer me up.

To my **girlfriend's family**, I thank you for the constant support you gave me, all the advice and heart-warming words, definitely helped me in this journey. Thank you for never doubting me.

To all my **8 birds and dog**, I thank you for the smile you can put on my life every day when I arrive home, even when things seemed to be tearing apart, you knew how to cheer me up.

To all my **family**, I deeply thank you for the constant support you gave me, you always showed to be very interested in my work and wished me the best! But specially, I have to thank my parents **António Sousa** and **Florabela Sousa**, all the accomplishments I have achieved so far are 100% consequence of the amazing education and values in which you brought me up, you are the most influent people in my life, I look up to you every day and hope to become the type of persons you are today. I aspire to achieve the same greatness you have. You are the real proof that commitment and hard work pays off even without any higher education degrees, thank you for being my parents, I proudly acknowledge that. I love you!

Finally, I want to acknowledge my **beautiful girlfriend Diana Moita**. You know you are my role model, I have said it countless times! I cannot imagine how my life would be without you, you always encouraged me to do my best and not for a millisecond ever doubted my abilities or my strength. You are the fuel that boost my life, the light that points me the way, the person that I want to be! Thank you for always being there for me, you have never failed me. I trust you and your opinion more than anything, you are my most precious thing in the whole universe, I truly love you! Thank you for everything and for believing in me!

Thank you everyone, I feel so blessed for having you in my life.

Funding: iNOVA4Health Research Unit (LISBOA-01-0145-FEDER-007344), which is cofunded by Fundação para a Ciência e Tecnologia (FCT) / Ministério da Ciência e do Ensino Superior, through national funds, and by FEDER under the PT2020 Partnership Agreement. FCT SFRH/BPD/101646/2014 (ST).

Abstract

Retinal neurodegeneration occurs in Parkinson's disease (PD), *Diabetes Mellitus* (DM) and with ageing. Aside from the thinning of the ganglion cell layer (GCL) and inner nuclear layer (INL) in the retina, the dopaminergic system, crucial for global retina function, is also affected in these three circumstances.

Diabetic and ageing cellular environments share several cellular environments known to be present in PD, whose pathogenicity in the brain is associated with the synuclein family, which is composed by alpha-synuclein (aSyn), beta-synuclein (bSyn) and gamma-synuclein (gSyn). As synucleins are also present in the retina, they may also play neurotoxic roles by impairing synaptic activity and cell survival.

Therefore, this study aimed to characterize the synucleins distribution profile in the retina by immunohistochemistry, and their protein levels through western blot, in the MitoPark PD mouse model, in DM animal models (high-fat diet (HFD) mouse and Zucker diabetic fatty (ZDF) rat), and in naturally ageing and accelerated ageing rats (D-Galactose treatment). This characterization was used to test a correlation with retinal neurodegeneration, by evaluating protein levels by western blot of synaptic and cell survival markers as readouts.

The results show that MitoPark mice retina have increased bSyn protein levels and decreased Synaptophysin levels. Naturally ageing rats only present, of all the parameters tested, reduced thickness of retinal layers and cell density in the GCL, whereas the D-Galactose rats exhibit increased GCL cell density. D-Galactose rats also show a decreased aSyn-bSyn colocalization in the GCL and reduced protein levels of NF- κ B. HFD mice do not show any alteration on the tested parameters, which contrasts with the observation of increased gSyn-positive cell bodies in the GCL of ZDF rats.

Altogether, this work enlightened synucleins retinal distribution in all these animal models and global results point to subtle changes, which may correlate with neurodegeneration.

Keywords: Synucleins, Retinal neurodegeneration, Parkinson's Disease, *Diabetes Mellitus*, Ageing

Resumo

A Neurodegeneração retiniana ocorre na doença de Parkinson (PD), em *Diabetes Mellitus* (DM) e com o envelhecimento. Além da diminuição da espessura da camada de células ganglionares (GCL) e da camada interna nuclear (INL) na retina, o sistema dopaminérgico, indispensável ao funcionamento global retiniano, é afetado nestas situações.

Os ambientes celulares diabético e envelhecido partilham ambientes celulares com a PD, cuja patogenicidade no cérebro está associada à família das sinucleínas, composta pela alfa-sinucleína (aSyn), beta-sinucleína (bSyn) e gama-sinucleína (gSyn). As sinucleínas também são expressas na retina, onde podem adquirir neurotoxicidade e comprometer a atividade sináptica e sobrevivência celular.

Deste modo, este estudo pretendeu caracterizar o perfil de distribuição das sinucleínas na retina por imunohistoquímica, e os níveis proteicos por *western blot*, em murganhos MitoPark modelos de PD, modelos de DM (murganhos alimentados com uma dieta rica em gordura (HFD) e ratos obesos diabéticos *Zucker* (ZDF)), ratos naturalmente envelhecidos e com envelhecimento precoce (tratados com D-Galactose). Posteriormente, procuraram-se correlações entre esta caracterização e a neurodegeneração retiniana, através da avaliação de níveis proteicos de marcadores sinápticos e sobrevivência celular por *western blot*.

Os resultados obtidos na retina de murganhos MitoPark demonstram um aumento e diminuição dos níveis proteicos da bSyn e Sinaptofisina, respetivamente. Em ratos naturalmente envelhecidos, dos vários parâmetros testados, há apenas uma redução da espessura de várias camadas retinianas e da densidade celular na GCL, contrariamente a ratos precocemente envelhecidos que mostram aumento da colocalização aSyn-bSyn e menores níveis proteicos de NF- κ B. Os murganhos HFD não apresentam qualquer alteração nos parâmetros testados, enquanto que em ratos ZDF se observa o aumento dos corpos celulares na GCL positivos para gSyn.

Globalmente, este trabalho elucidou a distribuição das sinucleínas na retina nestes modelos animais e os resultados obtidos apontam para alterações subtis que podem estar correlacionadas com neurodegeneração retiniana.

Palavras-chave: Sinucleínas, Neurodegeneração retiniana, Doença de Parkinson, *Diabetes Mellitus*, Envelhecimento

Table of contents

Acknowledgements.....	iii
Abstract.....	vii
Resumo	viii
Table of contents.....	x
Index of figures.....	xiii
Index of tables.....	xv
Abbreviations.....	xvi
1. Introduction.....	1
1.1. The synuclein family	1
1.1.1. Insights into synucleins structure.....	1
1.1.2. aSyn - The central player	3
1.1.2.1. Physiological role	3
1.1.2.2. Pathological role	5
1.1.3. bSyn	7
1.1.3.1. Physiological role	7
1.1.3.2. Pathological role	8
1.1.4. gSyn	9
1.1.4.1. Physiological role	9
1.1.4.2. Pathological role	10
1.1.5. Synergistic effect between synucleins	11
1.2. Parkinson's Disease	11
1.2.1. Clinical features of PD.....	12
1.2.2. Etiopathogenesis of PD.....	13
1.2.2.1. aSyn implications in PD	14
1.2.3. Animal models of PD	15
1.2.3.1. MitoPark mouse model.....	16
1.3. Synucleins importance in the retina.....	16
1.3.1. Retinal architecture and physiology	17
1.3.2. Synucleins localization in ocular tissues	20
1.3.3. The retina in PD.....	20
1.4. Ageing.....	21
1.4.1. Hallmarks of ageing.....	22
1.4.2. Animal models of ageing.....	24
1.4.2.1. Accelerated ageing - D-Gal administration model	24
1.4.3. The ageing retina	25
1.5. <i>Diabetes Mellitus</i>	26

1.5.1. Diabetic retinopathy.....	27
1.5.1.1. Non-proliferative and proliferative DR	28
1.5.1.2. Retinal neurodegeneration – the prequel of vascular alterations	30
1.5.2. Animal models of diabetes	31
1.5.2.1. High Fat Diet mouse model	31
1.5.2.2. Zucker Diabetic Fatty rat model	32
1.6. Triangulation between PD, DM and Ageing – common pathophysiology.....	32
1.7. Scientific direction and aim	33
2. Materials and Methods.....	35
2.1. Animal handling	35
2.1.1. High-Fat diet mouse model.....	35
2.1.2. Zucker Diabetic Fatty rat model	35
2.1.3. MitoPark mouse model.....	36
2.1.4. Naturally aged rat model.....	36
2.1.5. D-Galactose rat model	36
2.2. Eye harvesting and sampling	36
2.3. Localization of markers of interest by immunohistochemistry	37
2.4. Assessment of protein levels of markers of interest by Western Blot.....	38
2.5. Statistical analysis.....	40
3. Results and Discussion	41
3.1. Cre recombinase protein levels in the retina of MitoPark mice model of PD.....	41
3.2. Synucleins levels in the retina of MitoPark mice model of PD.....	42
3.3. Synaptic markers levels in the retina of MitoPark mice model of PD	43
3.4. Cell death markers levels in the retina of MitoPark mice model of PD	44
3.5. The synucleins family in the retina of ageing rat models	45
3.5.1. Synucleins levels in whole retina protein extracts of ageing and and D-Gal rats	45
3.5.2. Synucleins distribution profile in the retina of ageing and D-Gal rats	47
3.6. Synaptic markers in the retina of ageing rat models.....	56
3.7. Cell survival markers in the retina of ageing rat models	58
3.7.1. Cell survival marker levels in the retina of ageing and D-Gal rats.....	58
3.7.2. Retinal layers integrity in ageing and D-Gal rats	60
3.8. Body weight and glycaemic characterization of T2DM animal models	62
3.9. The synucleins family in the retina of T2DM animal models	63
3.9.1. Synucleins levels in whole retina extracts of HFD mice and ZDF rats.....	63
3.9.2. Synucleins distribution profile in the retina of HFD mice and ZDF rats	65
3.10. Synaptic markers in the retina of T2DM animal models.....	72

3.11. Cell survival markers in the retina T2DM animal models.....	74
3.11.1. Cell survival markers levels in the retina of HFD mice and ZDF rats	74
3.11.2. Retinal layers integrity in HFD mice and ZDF rats.....	77
4. Conclusion	79
5. References.....	85
6. Appendices.....	101

Index of figures

Figure 1.1. - Schematic structure of the members of the synuclein family.	2
Figure 1.2. – Composition of the presynaptic fusion machinery.	4
Figure 1.3. – Scheme of the several pathogenic mechanisms by which aSyn is able to mediate neurodegeneration.	7
Figure 1.4. – Timeline of the clinical symptoms described in PD patients.	12
Figure 1.5. – Sketch of the mammalian retina.	18
Figure 1.6. - Core pathogenic events in diabetic retinopathy.	29
Figure 3.1. – Assessment of synucleins levels in Control and MitoPark mice whole retina protein extracts.	42
Figure 3.2. – Assessment of synaptic markers levels in Control and MitoPark mice whole retina protein extracts.	43
Figure 3.3. – Assessment of cell death markers levels in Control and MitoPark mice whole retina protein extracts.	45
Figure 3.4. – Assessment of synucleins levels in ageing and accelerated ageing rats whole retina protein extracts.	46
Figure 3.5. – Immunohistochemistry of the synuclein family distribution profile in the retina of 1, 6, 10 and 19 months old rats.	48
Figure 3.6. – Immunohistochemistry of the colocalization between aSyn and bSyn in the retina of 1, 6, 10 and 19 months old rats.	49
Figure 3.7. – Immunohistochemistry of the colocalization between aSyn and gSyn in the retina of 1, 6, 10 and 19 months old rats.	50
Figure 3.8. – Immunohistochemistry of the synuclein family distribution profile in the retina of Sham and D-Gal rats.	52
Figure 3.9. – Immunohistochemistry of the colocalization between aSyn and bSyn in the retina of Sham and D-Gal rats.	52
Figure 3.10. – Immunohistochemistry of the colocalization between aSyn and gSyn in the retina of Sham and D-Gal rats.	53
Figure 3.11. – Quantification of the synucleins distribution in the IPL and GCL in ageing and accelerated ageing rats.	55

Figure 3.12. – Assessment of synaptic markers protein in ageing and accelerated ageing rats whole retina protein extracts.	57
Figure 3.13. – Assessment of cell survival and inflammation markers levels in ageing and accelerated ageing rats whole retina protein extracts.	59
Figure 3.14. – Quantification of retinal layers' thickness and GCL cell density in ageing and accelerated ageing.	61
Figure 3.15. – Assessment of synucleins levels in HFD mice and ZDF rats whole retina protein extracts.	64
Figure 3.16. – Synuclein family distribution profile in the retina of NCD and HFD mice and Lean and ZDF rats.	66
Figure 3.17. – Immunohistochemistry of the colocalization between aSyn and bSyn in the retina of NDC and HFD mice and also Lean and ZDF rats.	67
Figure 3.18. – Immunohistochemistry of the colocalization between aSyn and gSyn in the retina of NDC and HFD mice and also Lean and ZDF rats.	68
Figure 3.19. - Quantification of the synucleins distribution in the INL, IPL and GCL in HFD mice and ZDF rats. N=3 for NCD and HFD mice and for Lean and ZDF rats.	70
Figure 3.20. – Assessment of synucleins levels in HFD mice and ZDF rats whole retina protein extracts.	73
Figure 3.21. – Assessment of cell survival and inflammation markers levels in HFD mice and ZDF rats whole retina protein extracts	75
Figure 3.22. – Quantification of retinal layers' thickness and GCL cell density in HFD mice and ZDF rats.	77
Supplementary Figure 1 – Assessment of Cre recombinase levels by Western Blot in control and MitoPark mice whole retina protein extracts.	101
Supplementary Figure 2 – Body weight and glycaemic characterization of NCD and HFD mice.	101
Supplementary Figure 3 – Body weight and glycaemic characterization of Lean and ZDF rats.	101

Index of tables

Table 2.1. – Primary antibody description used in immunohistochemistry assays.	37
Table 2.2. – Primary antibody description used in western blot assays.	39
Table 2.3. – Secondary antibody description used in western blot assays.	39

Abbreviations

AChE	Acetylcholinesterase	FELASA	Federation of European Laboratory Animal Science Associations
AD	Alzheimer's disease	GABA	Gamma-aminobutyric acid
AGE	Advanced glycation end-product	GCL	Ganglion cell layer
ALP	Autophagy-lysosomal pathway	GFAP	Glial fibrillar acidic protein
AMPK	Adenosine monophosphate-activated protein kinase	GH	Growth hormone
aSyn	Alpha-Synuclein	GPCR	G protein-coupled receptor
BSA	Bovine serum albumine	gSyn	Gamma-Synuclein
BRB	Blood-retinal barrier	GWAS	Genome-wide association studies
bSyn	Beta-Synuclein	HFD	High-fat diet
cAMP	Cyclic adenosine monophosphate	HSP	Heat-shock protein
CFS	Cerebrospinal fluid	IGF-1	Insulin growth factor 1
CNS	Central Nervous System	IIS	Insulin/insulin growth factor 1 signalling
DA	Dopaminergic amacrine	INL	Inner nuclear layer
DAPI	4',6-diamidino-2-phenylindole	IPL	Inner plexiform
DAT	Dopamine transporter	KO	Knock-out
D-Gal	D-Galactose	LB	Lewy Body
DLB	Dementia with Lewy Bodies	MSA	Multiple System Atrophy
DM	<i>Diabetes Mellitus</i>	MODY	Maturity-onset diabetes in youth
DR	Diabetic retinopathy	mTOR	Mammalian target of rapamycin
ER	Endoplasmic Reticulum	NAC	Non-amyloid- β component

NAD⁺	Nicotinamide adenine dinucleotide+	SD	Standard deviation
NCD	Normal chow diet	SDS	Sodium dodecyl sulfate
ONL	Outer nuclear layer	SD-OCT	Spectral domain optical coherence tomography
OPL	Outer plexiform layer	SNAP-25	Synaptosomal-associated protein 25
OCT-A	Optical coherence tomography angiography	SNARE	Soluble N-ethylmaleimide-sensitive factor attachment protein receptor
OCT	Optical coherence tomography	SNP	Single nucleotide polymorphism
PFA	Paraformaldehyde	SNpc	Substantia Nigra <i>pars compacta</i>
PBS	Phosphate buffer saline	SOD	Superoxide dismutase
PBS-T	Triton in PBS	SPR	Surface plasmon resonance
PI	Phosphatidylinositol	T1DM	Type 1 <i>diabetes mellitus</i>
PINK1	Phosphatase and tensin homolog-induced putative kinase 1	T2DM	Type 2 <i>diabetes mellitus</i>
PKC	Protein kinase C	TBS	Tris-buffered saline
PSD95	Postsynaptic density 95	TBS-T	Tween-20 in TBS
PTM	Posttranslational modification	TH	Tyrosine hydroxalase
RGC	Retinal ganglion cell	UPR	Unfolded protein response
RIPA	Radioimmunoprecipitation	VAMP2	Vesicle-associated membrane protein 2
RNFL	Retinal nerve fibre layer	VEGF	Vascular endothelial growth factor
ROS	Reactive Oxygen Species	VMAT2	Vesicular monoamine transporter 2
RPE	Retinal pigment epithelium	ZDF	Zucker diabetic fatty
RT	Room temperature		

1. Introduction

1.1. The synuclein family

The synuclein protein family, whose name originally derived from its apparent restricted cellular localization in synaptic nerve terminals and in the nuclear envelope (Maroteaux L et al., 1998), is composed by three members: alpha-synuclein (aSyn), beta-synuclein (bSyn) and gamma-synuclein (gSyn) (Lavedan C, 1998). These proteins with an average molecular weight of 14 kDa, belong to a family of intrinsically unfolded proteins due to the absence of a well-defined secondary structure (Bertoncini W et al., 2007), (Wales P et al., 2013). The encoding genes, *SNCA*, *SNCB* and *SNCG*, were respectively mapped in the human chromosomes 4q21, 5q35 and 10q23 (Spillantini MG et al., 1995), (Lavedan C et al., 1998).

In 1988, Maroteaux *et al.*, identified the first synuclein, gSyn, by screening an expression library with an anti-serum against cholinergic vesicles, from the electric organ of the Pacific electric ray *Torpedo californica*. A cDNA clone was also isolated from a rat brain cDNA library, which encoded a highly homologous protein, the aSyn protein. Later in 1993, bSyn was firstly isolated from a bovine brain (Nakajo S et al., 1993), (Lavedan C, 1998).

In humans, both aSyn and bSyn are preferentially localized in the Central Nervous System (CNS), including the retina (Surguchov A et al., 2001), more specifically in presynaptic nerve terminals (Nakajo S et al., 1994), but not so abundantly in the peripheral nervous system, where gSyn is predominantly rich (Akopian AN et al., 1995), (Lavedan C et al., 1998), but also in other tissues such as in the ovaries, testis and heart (Clayton DF and Geroge JM, 1998).

1.1.1. Insights into synucleins structure

Concerning synucleins' amino acid sequence, all three members share a high homology, especially due to the identical first 42 amino acids that compose their sequence. However, aSyn and bSyn, which are composed by 140 and 134 amino acids, respectively, are more closely related to each other than with gSyn, which only has 127 residues (Lavedan C, 1998).

All the three proteins are mainly constituted by three domains (Fig. 1.1.): a highly conserved amphipathic region in the N-terminal, a hydrophobic central region named non-amyloid- β component (NAC) domain and lastly an acidic tail containing the C-terminal (George JM, 2002), (Emamzadeh FN, 2016).

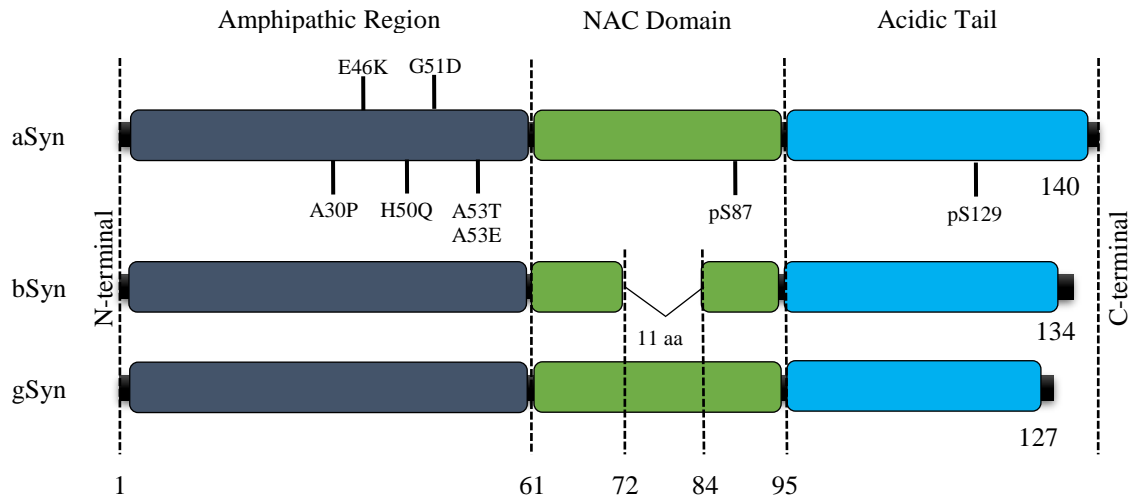


Figure 1.1. - Schematic structure of the members of the synuclein family. The three members aSyn, bSyn and gSyn share high homology between them and are composed by an amphipathic region, a NAC domain and an acidic tail. bSyn exhibits a truncation of 11 aminoacids in the NAC domain and gSyn has a shorter tail than the other synucleins. aSyn and bSyn share the highest homology (Adapted from Wales P et al., 2013).

Synucleins N-terminal has a series of repeats of 11 amino acids containing a variable number of imperfect hexameric (KTKEVG)-repeats. In solution, the amphipathic region remains unstructured, but in the presence of lipids it folds into an apolipoprotein-like class A₂ helix which helps binding to lipid's polar head (Emamzadeh FN, 2016), (George JM, 2002), (Perrin RJ et al., 2000). Furthermore, the N-terminal can also bind to high molecular weight complexes (Sang M et al., 2002).

Regarding the central domain NAC, it has amyloidogenic properties that allow the conversion of random coils to β -sheet structures. This phenom is essential for fibril formation and aggregation (George JM, 2002), (Emamzadeh FN, 2016).

Lastly, the acidic tail appears to solubilize high molecular weight complexes, thus revealing a chaperone-like function of the synucleins (Souza JM et al., 2000), (Sang M et al., 2002). In addition, the flexibility of this tail seems to be important for interactions with other proteins, as seen in other small molecular chaperones, such as clusterin (Humpherys DT et al., 1999). Moreover, it was shown that the truncation of this domain impairs the chaperone activity of the synucleins (Souza JM et al., 2000). Nevertheless,

this domain by itself does not exhibit chaperone-like activity, since the presence of the N-terminal for protein binding, as well as the synucleins' current conformation, are important factors for its solubilizing activity (Sang M et al., 2002).

Structurally comparing the three proteins, the most notable difference is the absence of 11 amino acid residues in the NAC region in bSyn, which makes it less prone to aggregate and form fibrils, but also, gSyn has a shorter acidic tail than the rest of the synucleins (Sung Y and Eliezer D, 2007).

1.1.2. aSyn - The central player

1.1.2.1. Physiological role

Among the three proteins, aSyn has been the most studied and the one in the centre of the spotlight, as it seems to be the most implicated in several neurodegenerative diseases, termed synucleinopathies. Even though its physiological role still remains to be elucidated, there are considerable evidences pointing to an involvement in neurotransmitter release, due to the preferential localization in synaptic terminals (Zhang L et al., 2008) where it binds to synaptic vesicle pools (Nuscher B et al., 2004). Moreover, an *in vitro* study in hippocampal neurons with impaired aSyn expression showed a size reduction of the distal vesicle pools (Murphy DD et al., 2000). In contrast, overexpression of aSyn in mice causes a deficient synaptic vesicle exocytosis both in hippocampal and dopaminergic neurons (Nemani VM et al., 2010).

It has been proposed that aSyn is a curvature-sensing and stabilizing protein, which is triggered to fold, from its unstructured conformation to an amphipathic helix, by lipid packaging defects in curved membranes. This binding to natively charged lipids provides stabilization (Middleton ER and Rhoades E, 2010). Furthermore, through a double-anchor mechanism, aSyn is able to cluster synaptic vesicles (Fusco G et al., 2016), thus it is likely that it can also modulate the proximity of these vesicles to voltage-gated calcium channels in the plasma membrane (Cárdenas AM and Marengo F, 2016).

In addition, a recent study shows that the highly coordinated membrane fusion machinery, composed by the soluble N-ethylmaleimide-sensitive factor attachment protein receptor (SNARE) and Sec1/Munc18-like proteins, demands the chaperone activity mediated by synucleins for the assembly of the SNARE-complex. This process

happens via the binding of the synucleins' C terminal to the SNARE-protein named synaptobrevin-2/vesicle-associated membrane protein 2 (VAMP2) (confirmed through immunoprecipitation assays) and also by the binding of the N terminus to membrane phospholipids (Burré J et al., 2010). In turn, VAMP2, a v-SNARE located on the vesicle, interacts with the t-SNAREs Syntaxin and Synaptosomal-associated protein 25 (SNAP-25) that are located on the plasma membrane. This interaction forms a four-helix bundle that zips up concomitant with bilayer fusion, allowing neurotransmitter release (Söllner T et al., 1993.) (Fig. 1.2).

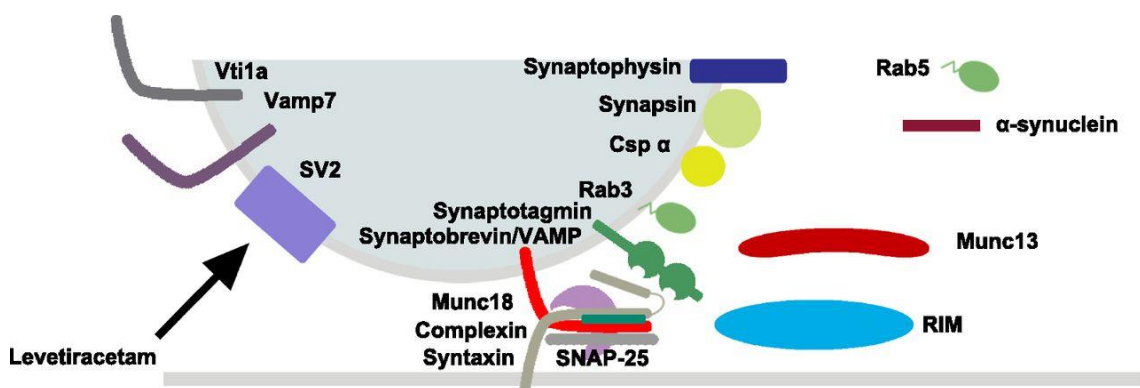


Figure 1.2. – Composition of the presynaptic fusion machinery. The SNARE-complex is composed by several proteins with v-SNARE or t-SNARE function, chaperones and others. aSyn is a key protein in this process as SNARE-complex assembly requires the chaperone-like activity of this protein, so that the synaptic vesicle membrane can merge with the plasma membrane, thus releasing the vesicular content, which includes neurotransmitters (Adapted from Ying C and Ege TK).

Furthermore, mice with a simultaneous knock-out (KO) for the three synucleins (triple abg-Syn KO) display age-dependent alterations in the levels of SNARE-complex proteins, and consequently altered synaptic structural organization and diminished neurotransmission, which correlate with the reduced survival and age-dependent neuronal dysfunction of the hippocampus and retina observed in these mice (Greten-Harrison B et al., 2010).

On the other hand, *in vitro* aSyn overexpression studies show an inhibition of the docking and fusion of endoplasmic reticulum (ER) vesicles with Golgi membranes, thus it can affect the exocytosis (Cooper AA et al., 2006), (Thayanidhi N et al., 2010). Lou X and colleagues (2017) have even shown by single-vesicle/fusion assays that aSyn promoted vesicle docking at low concentrations (<2.5 μ M), but that inhibited docking at high concentrations (>4 μ M).

Altogether, there are divergent evidences that point to a positive or negative regulator role of aSyn in exocytosis. Nevertheless, aSyn is able to influence the maintenance of the synaptic vesicle pool for neurotransmitter release.

1.1.2.2. Pathological role

Neurodegenerative diseases are a group of chronic and progressive disorders characterized by the gradual loss of neurons, typically in discrete areas of the CNS. Most neurodegenerative diseases are seen as a combination of several interrelated events that can comprise protein aggregation, neuronal dysfunction, neuronal death, sustained neuroinflammation and others (Gao H and Hong J, 2016), (Wales P et al., 2013). Protein aggregation has been one the major focus of research nowadays, because it is crucial to understand and determine the underlying conformational species with neurotoxic potential.

Regarding aSyn, the NAC domain is believed to be required for oligomerization and fibrillation of the protein. Indeed, the deletion of 12 amino acids in the middle of the NAC domain of aSyn abrogates its aggregation (Giasson BI et al., 2001). On the other hand, these aggregation processes hardly happen with bSyn as it has a deletion in the NAC domain.

Misfolding of aSyn leads to aggregation-prone conformations that afterwards give rise to amyloid-like fibrils and lastly to Lewy Bodies (LBs), which are essentially protein aggregates and hallmarks of Parkinson's disease (PD) and other synucleinopathies. This process happens in a nucleation-dependent manner, in which intermediate species are produced (Wood SJ et al., 1999). However, recently, aSyn was suggested to exist in a stable tetrameric state, which is less susceptible to aggregate, in contrast to the previous documented soluble monomeric conformation (Bartels T et al., 2011).

Misfolded aSyn can accumulate in the ER and lead to an impaired docking and fusion of ER vesicles with Golgi membranes, hence triggering an unfolded protein response (UPR) (Cooper AA et al., 2006).

Recent studies indicate that aSyn protofibrils strongly inhibit the 26S proteasome-mediated protein degradation system, which is one of the pathways responsible for clearing misfolded aSyn (Zhang N et al., 2008). Nonetheless, the cell still has the

autophagy-lysosomal pathway (ALP) to deal with the larger oligomeric aSyn species (Lee HJ et al., 2004). Several *in vitro* and *in vivo* experiments have shown that aSyn oligomers might also be transmitted between neuronal cells through a prion-like mechanism (Hansen C et al., 2011).

aSyn is also translocated into the mitochondria where it associates with complex I (Reeve AK et al., 2015). Increased aSyn protein levels impairs complex I activity, increases mitochondrial calcium (Parihar MS et al., 2008), and promotes mitochondrial fragmentation in the SH-SY5Y cell line (Xie and Chung 2012). As a result, cells start accounting for bioenergetic deficits and increased production of reactive oxygen species (ROS), which ultimately contribute to cell death of dopaminergic neurons in a PD mouse model (Chinta SJ et al., 2010).

Other reports have demonstrated that aSyn is able to interact with histones in single copies of DNA. These interactions may lead to a perturbation of nucleosomes, thus compromising the stability of DNA, which can have deregulated transcriptional implications (Hedge ML and Jagannatha RKS, 2003). Additionally, aSyn aggregates are able to sequester nuclear proteins in the cytoplasm, which further strengthens aSyn's role in transcriptional deregulation (Wales P et al., 2013).

There are major evidences pointing to posttranslational modifications (PTMs) as drivers for aSyn aggregation such as phosphorylation, truncation, ubiquitination, glycation, acetylation and others (Oueslati A et al., 2010).

More specifically, aSyn phosphorylated at serine 129 (pS129) in PD composes 90% of total aSyn present in LB, and it is also presente in other synucleinopathies such as Dementia with Lewy Bodies (DLB) and Multiple System Atrophy (MSA) (Fujiwara H et al., 2002). On the other way around, phosphorylation at Y125, Y133 and Y136 indicated an inversely correlated propensity for aggregation (Tenreiro S et al., 2014).

On the other hand, since aSyn is a lysine-rich protein, both the PTMs glycation and acetylation in this protein are likely to happen, especially in the N terminal (Miranda MV and Outeiro TF, 2010). Recently, it was demonstrated that glycation, which is highly increased in PD patients, in aged individuals, and in diabetics, exacerbates aSyn toxicity and aggregation both in yeast and in human cell lines (Miranda HV et al., 2017). Conversely, Sirtuin 2 (SIRT2), a deacetylase whose levels are known to be increased with ageing (Maxwell MM et al., 2011), is known to interact and remove acetyl groups from

aSyn, which in turn promotes aSyn toxicity and aggregation. Thus, acetylation in aSyn acts as a neuroprotective PTM (Oliveira RM et al., 2017).

In summary, aSyn is capable of interfering with numerous cell processes and organelles that may compromise cell survival (Fig.1.3.)

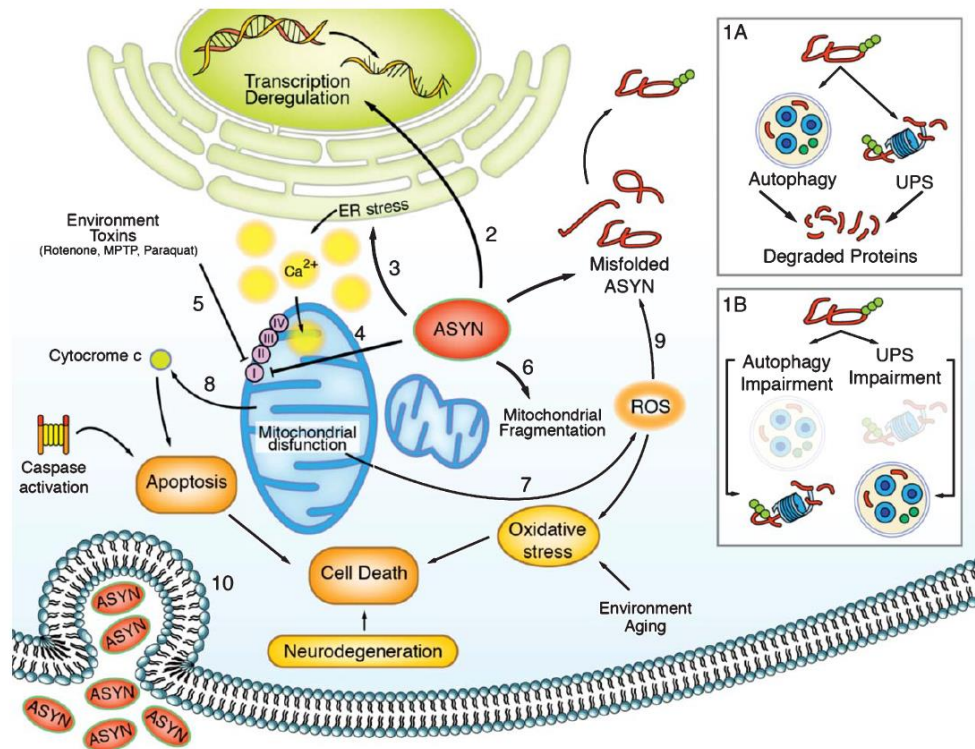


Figure 1.3. – Scheme of the several pathogenic mechanisms by which aSyn is able to mediate neurodegeneration. Under physiological conditions, proteins are directed to the ubiquitin-proteasome system UPS and ALP to be degraded (1A), however the efficiency of these mechanisms in synucleinopathies is compromised (1B) leading to accumulation of misfolded aSyn that can cause transcriptional deregulation (2), ER stress and consequently an imbalanced intracellular Ca^{2+} level (3), and impaired activity of the mitochondrial complex I (4). Some toxins such as the MPTP, Paraquat and rotenone can inhibit the activity of the mitochondrial complex I (5), which also seems to be able to induce mitochondrial fragmentation (6). These damages to the mitochondria cause dysfunction and increased levels of ROS (7), cytochrome c release to trigger cell death (8). Both mitochondria dysfunction and increased ROS levels promote aSyn misfolding, later leading to the formation of oligomeric species that can be transmitted from cell-to-cell through a prion-like mechanism (10) (Adapted from Wales P. et al., 2013).

1.1.3. bSyn

1.1.3.1. Physiological role

bSyn is very similar to aSyn regarding their structure and localization, as previously mentioned. Therefore, an analogous role of bSyn could perhaps be expected.

However, bSyn has shown other particularities. It has been hypothesised to decrease aSyn aggregation, as transgenic mice expressing human aSyn develop aSyn inclusions, while transgenic mice simultaneously expressing both human aSyn and bSyn have reduced accumulation of aSyn and fewer motor deficits (Hashimoto M et al., 2001). Furthermore, *in vitro* studies using HEK293 cells transfected with both aSyn and bSyn do not show any presence of aggregates and demonstrate that they co-immunoprecipitate, indicating a possible interaction between the two. Nevertheless, it remains to be determined if this direct interaction is preventing aSyn aggregation, which is consistent with bSyn chaperon-like activity, or if bSyn is able to interact with other molecules, hence consequently producing a neuroprotective effect (Hashimoto M et al., 2001). Furthermore, bSyn has also been observed to decrease the fibrillation rate of gSyn promoted by seeds of aSyn (Jain MK et al., 2018).

Recent evidence points to a binding activity of bSyn to Akt, leading to a stabilization of the Akt protein, further promoting its activation. This serine/threonine-specific protein kinase is involved in cellular processes such as glucose metabolism, cell proliferation and death, neurite outgrowth, among others. By transfecting B103 neuroblastoma cells with bSyn, Hashimoto M and his colleagues noticed an increased activity of Akt, which protected neurons from rotenone-induced toxicity, and also discovered a direct interaction between them as they co-immunoprecipitated (Hashimoto M et al., 2004).

Thus, bSyn is able to directly promote cell survival by binding to aSyn and decreasing its aggregation, indirectly through the phosphatidylinositol 3 (PI3)/Akt pathway.

Altogether, there is a potential role for bSyn in regulating the conformational state of aSyn.

1.1.3.2. Pathological role

bSyn was once thought not to be able to aggregate due to the deletion in the NAC domain, which is important for fibrillation events. However, this protein has been discovered to aggregate under certain conditions such as macromolecular crowding, metal ions and pesticides (Yamin G et al., 2005).

A recent study showed that bSyn overexpression in rat leads to dopaminergic neurodegeneration, probably due to mitochondrial damages, in the substantia nigra *pars compacta* (SNpc), almost to the same extent as aSyn in PD. Moreover, the same study also demonstrated the presence of bSyn aggregates in the surviving neurons and in rat primary cortical neurons *in vitro* (Taschenberger G et al., 2013). Another report in yeast revealed that bSyn can be toxic, form heterodimers with aSyn, originate aSyn-like inclusions and disrupt the some of the cellular events that aSyn affects (Tenreiro S et al., 2016). Following these evidence, bSyn can no longer be seen only as a scavenger of aSyn-mediated neurotoxicity, thus further studies on this protein are critical.

In addition, there are two known point mutations in the human bSyn encoding-gene *SNCB* that are correlated with an increased risk of developing rare forms of DLB - V70M and P123H. Patients with these mutations reveal LB pathology with aggregates containing aSyn, but not bSyn (Ohtake H et al., 2004).

Similar to aSyn, PTMs also play a role in defining bSyn cytotoxicity. It is known that downregulation of sumoylation impairs bSyn clearance by the UPS in yeast, although it does not increase bSyn aggregation nor does it compromise the ALP activity (Popova B et al., 2018).

1.1.4. gSyn

1.1.4.1. Physiological role

Regarding neuronal tissues, gSyn can be found predominantly in primary sensory, sympathetic and motor neurons, which compose the peripheral nervous system, but it can also be found in the brain and in the retina (Geroge JM, 2002).

Little is known about this protein, in contrast to the other members of the synuclein family, but there are some studies associating its function with different cellular events. It is known, for instance, that in several types of human interphasic cells and in bovine retinal pigment epithelium cells, gSyn is present in the perinuclear area and is localized to centrosomes (Surguchov A et al., 2001). In contrast, in neuronal cells gSyn has other function, where it binds to synaptic vesicles, but not to the SNARE-complex proteins as the other synucleins (Lytkina OA et al., 2014).

Moreover, gSyn has been found to modulate monoamine transporters such as of serotonin (Wersinger C and Sidhu A 2009), but not the dopamine transporter (DAT) (Senior SL et al., 2008), to have chaperone-like activity (Jiang Y et al., 2004) and to regulate microtubule-mediated organelle trafficking (Zhang H et al., 2011).

Another report suggested that gSyn could inhibit aSyn aggregation by binding to oligomeric intermediates, which by becoming stabilized, halt the fibrillation process, thus preventing the evolution into fibrils, but instead into amorphous structures (Uversky VN et al., 2002).

1.1.4.2. Pathological role

A recent study showed that under certain conditions such as high temperature, low pH and high concentrations of this synuclein, there is an increase in the rate of fibrillation of gSyn (Jain MK et al., 2018), which was once thought to be incapable of forming fibrils as well (Geroge JM, 2002).

As gSyn-KO mice exhibit low frequency of anxious behaviours (Kokhan VS et al., 2011), it is thought that gSyn has a role in cognitive function, which is one of the altered faculties in PD and Alzheimer's disease (AD) (Varanese S et al., 2011).

Overexpression of this protein in transgenic mice under the Thy-1 promoter leads to accumulation and aggregation of gSyn in the spinal cord and further neurodegeneration. These transgenic mice develop severe age- and transgene dose-dependent neuropathology, motor deficits and exhibit decreased survival (Ninkina N et al., 2009). Moreover, these animals exhibit some amyotrophic lateral sclerosis (ALS) features - selective damage and loss of discrete populations of upper and lower motor neurons and their axons (Peters OM et al., 2012). Another recent report demonstrated that gSyn oxidised at Met38 formed inclusions in the amygdala and substantia nigra, while colocalizing with aSyn, in humans (Surgucheva I et al., 2014).

Furthermore, gSyn has also been found in LBs in hippocampal regions of DLB and PD patients (Galvin JE et al., 1999).

Interestingly, glaucoma patients exhibit decreased gSyn mRNA and protein levels along with a redistribution of gSyn in the optic nerve (Surgucheva I et al., 2002), which

is similar to AD patients who exhibit a decreased gSyn immunoreactivity in the retinal nerve fiber layer (Surguchov A et al., 2001).

Regarding non-neuronal tissues, gSyn overexpression in breast tissue has been linked to breast cancer (Ji H et al., 1997).

1.1.5. Synergistic effect between synucleins

Surface Plasmon Resonance (SPR) data shows that interaction between aSyn-bSyn, bSyn-gSyn and aSyn-gSyn are weak to moderate in nature. However, they can be physiologically relevant to collectively understand the synucleins behaviour and to tackle the hostile conditions in neurons that trigger their accumulation and aggregation, which can potentially affect PD pathology progression (Jain MK et al., 2018).

In case of neuronal damage, aSyn and bSyn colocalize and quickly accumulate in injured neurons, afterwards promoting axonal transport and cytoskeletal reorganizations (Quilty MC et al., 2003). However, other reports showed that co-expression of aSyn and bSyn exacerbates synucleins toxic effect in yeast and promotes inclusion formation. Thus, there can be a positive or negative synergistic effect between them. In addition, heterodimers of aSyn and bSyn were reported to be formed both in yeast and mammalian cells (Tenreiro S et al., 2016).

1.2. Parkinson's Disease

PD is the second most common neurodegenerative disease worldwide after AD (Dorsey ER et al., 2005). It was first described as a neurological syndrome by James Parkinson in 1817 (Kalia LV and Lang AE, 2015). The incidence of PD ranges from 10 to 18 per 100 000 person-years and is twice more frequent in males than females (Van den Eeden SK et al., 2003). Familial forms of PD are known to contribute nearly to 10% of all PD cases, whereas sporadic PD forms account for 90% (Kalia LV and Lang AE, 2015).

1.2.1. Clinical features of PD

PD presents an early loss of dopaminergic neurons in the SNpc as the biggest hallmark of the disorder, leading to a severe decrease in the levels of the neurotransmitter dopamine (Sideworf A and Lang AE, 2012).

Currently, PD is seen as a slowly progressing disease that has various implications regarding motor abilities, but also non-motor features. Typically, PD patients are described to have motor features such as bradykinesia, rigidity, postural instability, tremors, among others, in which physicians rely on to establish the diagnosis of the disease (Kalia LV and Lang AE, 2015). In addition, results of clinical-pathological correlation studies show that moderate to severe dopaminergic neuronal loss within the SNpc is possibly the underlying cause of the motor features (Dickson DW et al., 2009). However, other PD manifestations such as constipation, olfactory dysfunction, ophthalmologic complications and others start in the prodromal period, several years before the occurrence of the first motor features (Fig.1.4.) (Khoo TK et al., 2013).

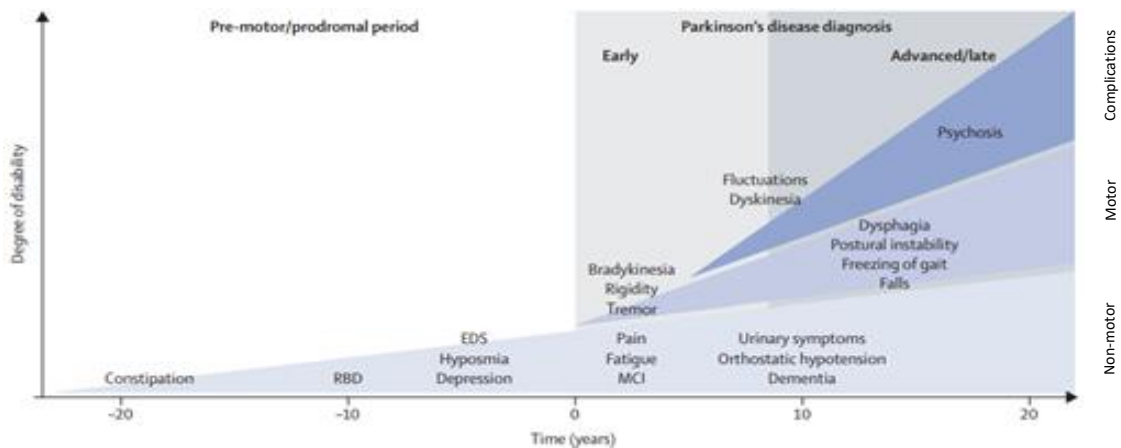


Figure 1.4. – Timeline of the clinical symptoms described in PD patients. The first clinical symptoms start roughly 20 years before the first motor features are diagnosed, such as constipation, visual dysfunction and others, that later progress to the well-known tremors, bradykinesia and others (Adapted from Kalia LV and Lang AE, 2015).

The current therapies are not able to slow down the disease progression, they are merely improving the quality of life of patients by tackling the motor features. The existing therapies are based on increasing the intracerebral concentration of dopamine or on stimulating dopamine receptors; therefore, physicians are prescribing levodopa, dopamine agonists, monoamine oxidase type B inhibitors and others (Fox SH et al.,

2011). In addition, deep brain stimulation is also an alternative and a well-established treatment for PD patients (Kalia SK et al., 2013).

1.2.2. Etiopathogenesis of PD

PD etiology still remains to be determined, however there are several evidences pointing to risk factors such as ageing, genetics, environmental factors (Lesage D and Brice A 2009) and immunological conditions (Liu B et al., 2003).

In the last decade, several causative genes and susceptibility factors have been identified in rare families with Mendelian inheritance, which suggested that abnormal handling of misfolded proteins by the UPS and ALP, increased oxidative stress, mitochondrial and lysosomal dysfunctions, and other pathogenic dysfunctions, contribute to PD (Kalia LV and Lang AE, 2015).

The human aSyn encoding gene *SNCA* was the first gene to be associated with monogenic autosomal dominant forms of PD (Polymeropoulos MH et al., 1997). The *LRRK2* gene, encoding for the Leucine-rich repeat kinase 2 (LRRK2), is associated with autosomal dominant forms of PD as well. This serine-threonine kinase is present in various cellular processes such as neurite outgrowth, synaptic morphogenesis, autophagy and even protein synthesis (Li J et al., 2014).

Regarding autosomal recessive forms, which tend to be correlated with an early onset of the disease (Lücking CB et al., 2008), some of the known causative genes are the *parkin*, *PINK1* that encodes for the phosphatase and tensin homolog (PTEN)-induced putative kinase 1 (PINK1) and *DJ-1* (Kalia LV and Lang AE, 2015). Both parkin, an E3 ubiquitin ligase, and PINK1 proteins are highly associated with mitophagy of damaged mitochondria (Mccoy ML and Cookson MR., 2012), while DJ-1 is related with mitochondrial protection from oxidative stress (Kalia LV and Lang AE, 2015).

Environmental factors such as prior head injury, pesticide exposure like the Paraquat (1,1'-dimethyl4,4'-bipyridinium dichloride), well water drinking, tobacco smoking, coffee drinking, non-steroidal inflammatory drug use, and others, have been described in the literature as environmental agents that increase the risk of developing PD (Noyce AJ et al., 2012). Recent studies also indicate that diabetes is associated with increased risk of developing PD by about 38% (Yue X et al., 2016).

Moreover, neuroinflammation is also present in PD. It is known that these patients have a significant increase in the levels of innate immune components such as the complement and cytokines like IL-1, IL-2, IL-6 and TNF, not only in the substantia nigra but also in the cerebrospinal fluid (CSF) (Liu B et al., 1994).

1.2.2.1. aSyn implications in PD

There are several known missense mutations in the region of the *SNCA* gene encoding for the N-terminal of aSyn that are associated with familial PD: Ala53Thr, Ala30Pro, Glu46Lys, His50Gln, Gly51Asp, and Ala53Glu (Dehay B et al., 2015). The Glu46Lys, His50Gln and Ala53Glu mutations promote aSyn insolubility and, therefore, oligomer production and aggregation (Xu L and Pu J 2016). Furthermore, through a gene dosage effect, the duplication and triplication of the *SNCA* gene are also other forms of aSyn-mediated familial PD (Dehay B et al., 2015). With the overexpression of aSyn there is an increased proneness for aggregation events.

Similarly, recent genome-wide association studies (GWAS) revealed a single-nucleotide polymorphism (SNP) associated with the *SNCA* gene causing increased expression levels of aSyn that altered the risk for sporadic PD (Nalls MA et al., 2014).

LBs are majorly composed by aSyn and by other various proteins with different functions (Wakabayashi K et al., 2103). However, there is an increasing number of evidence showing that perhaps the most toxic forms of aSyn are its oligomer conformations (Outeiro TF et al., 2008). LB pathology found in neurons in the striatum of PD patients is hypothesized to be a biomarker for neurodegeneration (Kalia LV and Lang AE, 2015). Nonetheless, not all PD patients exhibit LBs (Doherty Km et al., 2013) and furthermore, it has been debated whether LBs actually have a role in neuronal loss or if they are neuroprotective, since they are only found in the surviving neurons (Fahn S and Sulzer D 2004).

Nigral dopaminergic neurons are thought to be mainly vulnerable to metabolic and oxidative stress (Boalm JP and Pissadaki EK 2012), which are further exacerbated by the increased levels of cytosolic dopamine and its metabolites (Mosharov EV et al., 2009). Their remarkably long unmyelinated axons with large numbers of synapses,

requiring aSyn to modulate dopamine release (Poewe Werner et al., 2017), have great bioenergetic demands (Pissadaki EK and Bolam JP 2013).

In addition, recent studies highlight the modulator effect that aSyn can have in the rate-limiting enzyme of dopamine synthesis, which is the tyrosine hydroxylase (TH). Furthermore, aSyn also modulates the vesicular monoamine transporter 2 (VMAT2) and DAT (Butler B et al., 2016). Increased aSyn levels have been shown to decrease the dopamine synthesis and activity of TH via direct interaction (Perez et al., 2002), by preventing its phosphorylation and therefore activation (Peng et al., 2005). Overexpression of aSyn also reduces the VMAT2 activity (Ulusoy et al., 2012), and contrasting evidences state that aSyn overexpression either increases (Lee et al., 2001) or decreases (Wersinger and Sidhu 2003) DAT levels. Nevertheless, aSyn appears to have an important role in regulating dopamine synthesis, storage, clearance and efflux (Butler B et al., 2016).

Progressive ageing, which is the greatest risk factor for PD, is linked with reduced ALP and UPS functions (Kaushik S and Cuervo AM 2015), which is consistent with the observations of augmented levels of aSyn in dopaminergic neurons during normal ageing (Chu Y and Kordower JH 2007). As aSyn accumulates and aggregates in these neurons, and taking into account the previously mentioned pathological mechanisms by which aSyn mediates neurodegeneration – mitochondrial and lysosomal dysfunction, UPS inhibition, impaired neurotransmission and others (Fig. 1.3.) – it seems that in fact, aSyn actually plays a central role in defining the dopaminergic neuronal susceptibility.

1.2.3. Animal models of PD

In order to study and unveil the etiopathogenesis of PD, animal models are a great tool for this purpose, as they comprise some of the already known cellular events and also a few motor and non-motor manifestations of PD (Blesa J et al., 2016).

Essentially, animal models of PD can be classified into three main categories: neurotoxin-based, genetically manipulated (relevant to PD), and in the “others” category. The neurotoxic models, which inhibit the mitochondrial complex I in catecholaminergic neurons, comprise the pesticide model MPTP and Paraquat models, for instance. In regard to the genetic models there are, among others, the Thy1-aSyn model, which overexpresses

human α Syn, and the Parkin model, which involves mutations in the *Parkin* gene. Lastly, the “others” category is composed by the MitoPark model, an animal described to have an induced mitochondrial dysfunction in dopaminergic neurons, and several other models (Gubellini P and Kachidian P 2015).

1.2.3.1. MitoPark mouse model

Several lines of evidence point to mitochondrial dysfunction in dopaminergic neurons as being one of the several underlying causes of PD (Dauer Wet al., 2003).

The MitoPark mouse model is based on the specific deletion of the mitochondrial transcription factor A (*TFAM*) gene in dopaminergic neurons (Ekstrand MI and Galter D, 2009). Taking advantage of a *Cre*-mouse line expressing the Cre-recombinase under the DAT gene promoter, and a mouse line with a floxed *TFAM* gene, the MitoPark mouse ($\text{DAT}^{+/cre}\text{-TFAM}^{\text{loxP/loxP}}$) has a lower transcription and maintenance of the mitochondrial DNA (mtDNA) selectively in dopaminergic neurons, causing a dysfunctional respiratory chain (Ekstrand MI et al., 2007), due to the absence of the TFAM binding activity to the mtDNA (Ekstrand MI and Galter D, 2009)

Despite the mtDNA being severely decreased as early as 6 weeks, the decreased locomotion and rearing behaviour only appear near the 14 weeks of age, when a few TH-positive midbrain neurons have already been lost. Motor features progressively worsen with ageing and can be ameliorated with L-DOPA administration (Ekstrand MI et al., 2007). Moreover, this mouse model develops intraneuronal inclusions not constituted by α Syn, but immunoreactive for the mitochondrial protein ATP synthase (Ekstrand MI et al., 2007).

1.3. Synucleins importance in the retina

As previously mentioned, synucleins are expressed across the nervous system including the retina, albeit their physiological role in this tissue is yet to be unveiled.

Nevertheless, there is an important evidence pointing to an important role of synucleins in vision, as the triple α g-Syn KO develops blindness with ageing (Gretchen-Harrison B et al., 2010).

Interestingly, patients affected by synucleinopathies such as DLB, PD and MSA seem to present clinical features that involve the retina. Although the retina is differently affected by these diseases (Armstrong AR, 2012), (Archibald NK et al., 2009), (Mendoza-Santiesteban C et al., 2017), a strong common factor is precisely the pathologic condition of synucleins. Furthermore, inclusions containing aSyn have been reported in the human retina of aged individuals (Leger F et al., 2011), AD, PD and DLB patients (Surguchov A et al., 2009), (Price DL et al 2016), (Bodis-Wollner I et al., 2014). However, before one can be conscious of the implications of synucleinopathies in the retina, it is important to understand the physiognomy and physiology of the retinal tissue.

1.3.1. Retinal architecture and physiology

The retina is a neuronal tissue able to transduce light signals into neuronal representations with specific information about movement, colour and contrast of the images being perceived (Kolb H 2003). Aside from neuronal cells, the retina is also composed of vascular cells such as pericytes and endothelial cells, by microglia (the immunocompetent cells of the CNS) and macroglia (Müller cells and astrocytes) (Vecino E et al., 2016).

Two main arteries provide blood supply to the retina, namely the central retinal artery and the choroidal blood vessels, which are crucial for maintenance of the outer retina, particularly the photoreceptors (Henkid P et al., 1979).

Three layers containing neuron cell bodies, labelled as nuclear layers, and two layers of synapses, entitled plexiform layers, compose all vertebrate retinas. The outer nuclear layer (ONL) comprises the cell bodies of rod and cone photoreceptors. Overlying the ONL is the retinal pigment epithelium (RPE), which absorbs stray light, prevents light backscatter into the retina and digests damaged photoreceptor outer segments due to photooxidation (Kolb H 1995). The ONL is followed by the inner nuclear layer (INL) composed by the cell bodies of bipolar, horizontal and amacrine cells. In between these two layers, synaptic contact occurs between cones and rods with bipolar and horizontal cells, forming the neuropil termed outer plexiform layer (OPL). Lastly, the ganglion cell layer (GCL) is formed by retinal ganglion cells (RGCs) that have axonic projections into the retinal nerve fibre layer (RNFL), which in fact only become myelinated at the optic

nerve head. The GCL also contains displaced amacrine cells. Synaptic connections with neurons from the INL is made in the neuropil named inner plexiform layer (IPL) (Fig.1.5.) (Kolb H 2003), (Kolb H 1995).

Retinal signalling occurs in two directions: vertically and horizontally. Vertical signalling takes place from photoreceptor to bipolar cells and then to RGCs, whereas horizontal neurotransmission is mediated by horizontal and amacrine cells that modulate interactions between photoreceptor and bipolar cells in the OPL, and bipolar cells and RGCs in the IPL, respectively (Archibald NK et al., 2009).

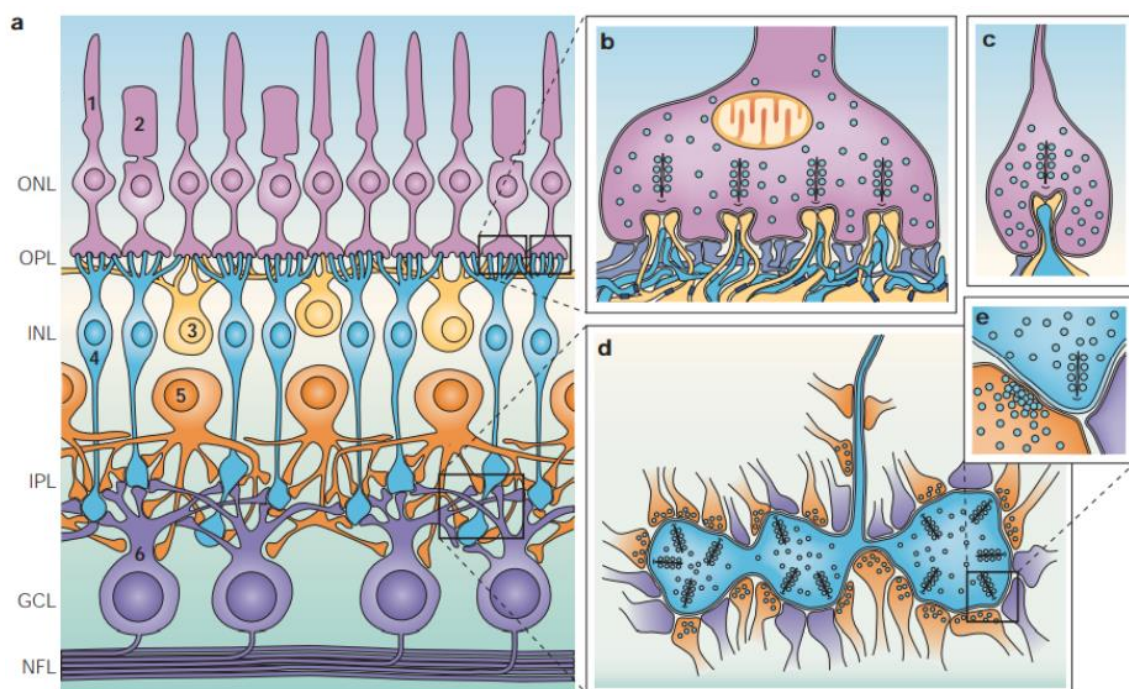


Figure 1.5. – Sketch of the mammalian retina. a | There are six types of neurons in the mammalian retina: rods (1), cones (2) distributed in the ONL, horizontal cells (3), bipolar cells (4), amacrine cells (5) in the INL and RGCs (6) in the GCL. In between these nuclear layers there are the neuropils OPL and IPL. b | Cone terminal contact with bipolar and horizontal cells. c | Rod terminal contact with bipolar and horizontal cells. d | Synaptic contact between amacrine, bipolar cells and RGCs. e | Magnified view of the synaptic contact in the IPL (Adapted from Wässle H 2014).

The main neurotransmitter in vertical neurotransmissions is glutamate, which acts via excitatory ionotropic and inhibitory metabotropic glutamate receptors, while horizontal signalling is primarily mediated by the inhibitory neurotransmitters gamma-aminobutyric acid (GABA) and glycine, but also through electrical gap junctions (Archibald NK et al., 2009).

While in the dark, photoreceptors remain depolarized and incessantly release glutamate and only hyperpolarize, when in light conditions, due to alterations in

membrane potentials which further lead to a decrease in glutamate release. These events can either activate or inhibit different subtypes of bipolar cells, termed ON or OFF bipolar cells, respectively. In turn, cone ON bipolar cells stimulate ON RGCs, while OFF bipolar cells conversely contact with OFF RGCs. Afterwards, RGCs are able to create a 'centre and surround' response that will provide information on contrast to the visual cortex, thus enabling the ability to distinguish shapes and contours (Bloomfield SA and Dacheux 2001).

Like horizontal cells, amacrine cells work horizontally. In spite of affecting the input of rods and cones to bipolar cells as horizontal cells do, amacrine cells regulate the output of bipolar cells to ganglion cells (Bloomfield SA and Völgyi B, 2009).

Amacrine cells, which account for at least 33 known different subtypes, can be categorized accordingly to their neurotransmitter type (GABAergic, glycinergic or neither) or length of dendritic arbours (Blomfield SA and Völgyi B, 2009). A subset of amacrine cells deserves a special mention, which is the dopaminergic amacrine (DA) cell, also known as A18 that localizes in the INL, although with a far less density (Kolb H et al., 1995).

DA cells have a widespread dendritic arborisation that overlaps neighbouring DA and other amacrine cells (Kolb H et al., 1990). These dopamine-producing neurons receive glutamatergic inputs from bipolar cells and GABAergic and glycinergic signals from amacrine cells. Together, these inputs modulate the action potential fire rate of dopamine release (Gustinchi S et al., 1997). Dopamine, in turn, binds to G protein-coupled receptors (GPCR) that regulate the production of cyclic adenosine monophosphate (cAMP). Dopamine receptors subtypes D1 and D5 increase the cAMP levels and activate horizontal, bipolar, amacrine and RGCs (Muresan Z and Besharse JC, 1993), whereas D2, D3 and D4 receptors inhibit rod and cone photoreceptors (Nguyen-Legros J et al., 1997). DA cells can also autocrinally modulate their own dopamine release as they possess the latter dopamine receptors that exhibit inhibitory activity (Veruki ML, 1997). Altogether, increased dopamine levels reduce gap junction permeability between neurons, thus controlling the amount of input that reaches RGCs during the day or in intense light conditions (Ribelayga C et al., 2008).

1.3.2. Synucleins localization in ocular tissues

Although in lower amounts than those found in the brain, data shows that the synuclein family is also present in the ocular tissues. Specifically, these findings demonstrate that they are mainly expressed in the retina and optic nerve, but also exist in the lens, cornea, iris and RPE (Surguchov A et al., 2001). Nonetheless, their physiological role still remains elusive.

In humans, aSyn and bSyn are located in the IPL, which is coherent with the already known preferential localization of synucleins in synapses. However, gSyn exhibits a different expression pattern, as it is not present in the IPL. One could possibly expect that the synucleins would be present in the OPL as well, however, none of the three members are present in this layer, probably because this neuropil is constituted by ribbon synapses, instead of conventional synapses as the IPL is (Surguchov a et al., 2001).

aSyn is also localized in cell bodies of the INL in the human retina, mostly in the proximal region where usually amacrine cells are located, whereas bSyn is more widespread across the INL, therefore it is likely that is present in horizontal, bipolar and amacrine cells. In turn, gSyn seems to be only present in the GCL and RNFL (Surguchov A et al., 2001), and therefore it can potentially be considered a marker of RGCs (Surgucheva I et al., 2008).

Altogether, these evidences point to a difference in transcriptional regulation of the gene expression of each synuclein, which explains the differences in expression patterns (Surguchov A et al., 2001).

1.3.3. The retina in PD

Evidence exists of ocular manifestations in PD as a non-motor feature of the disease. This visual dysfunction includes psychophysical (contrast sensitivity and visual acuity aspects), electrophysiological and morphological changes in the retina function and structure (Archibald NK et al., 2009).

Common visual symptoms range from dry eyes, reading difficulties, perceptual disturbances (feelings of presence and passage) and even visual hallucinations (Archibald

NK et al., 2009), which is in fact an indicator of cognitive impairment (Biousse V et al., 2004).

Previous studies show a dopamine deficiency in the human retina upon decreased immunoreactivity of TH, a classical marker of dopaminergic neurons (Nguyen-Legros 1988). Considering the complexity of connections of DA cells, which suggests multiple roles, changes in the dopamine production will affect several surrounding retinal cells, thus contributing to visual dysfunction at several levels (Archibald NK et al., 2009). In fact, this lack of dopamine is thought to be the cause of reduced contrast sensitivity, as levodopa administration rescues this psychophysical feature (Bulens et al., 1987).

It has also been observed thinning of the RNFL (Inzelberg et al 2004) and INL (Hajee et al., 2009) in the retina of PD patients, which could indicate neurodegeneration in this tissue. A recent study proposes a correlation between the INL thinning and the loss of DA cells (Ahn J., et al 2018).

Moreover, aSyn accumulation (Surguchov A et al., 2001), as well as aggregates containing aSyn, have been found in cells of the INL, GCL and RNFL in the Thy1-aSyn mouse model of aSyn overexpression (Bodis-Wollner I et al., 2004).

1.4. Ageing

Over the last centuries, humanity's lifespan has progressively been increasing due to improved lifestyles, quality of life and healthcare (López-Otín C et al., 2013), (Aunan JR et al., 2015). Factors such as the quality and amount of healthcare during the course of a lifetime, the type of diet, genetic background, and habits such as physical activity, and tobacco and alcohol consumption affect the rate of biological ageing, making the research in the etiology of ageing in human populations more complex (López-Otín C et al., 2013).

Ageing is the inevitable process of physiological integrity of an organism dampening over time, which eventually leads to death. Although organisms can healthily age, various cellular processes can in the long run become so heavily compromised that ageing-associated complications arise such as visual and auditory dysfunctions, but also diseases as diabetes, neurodegenerative disorders like PD and AD, cancer, cardiovascular diseases and others. Thus, the ageing topic has begun to take a place in the vanguard of

researchers' interests, not only to understand which molecular mechanisms are more important for the natural process of ageing and which have a greater pathological potential, but also to identify promising pharmaceutical targets that can improve human's longevity (López-Otín C et al., 2013), (Aunan JR et al., 2015).

1.4.1. Hallmarks of ageing

Ageing is characterized by numerous cellular mechanisms that disturb the homeostasis. Some of the hallmarks proposed by López-Otín C et al. (2013) are cellular senescence, stem cell exhaustion, genomic instability, telomere attrition, epigenetic alterations, loss of proteostasis, deregulated nutrient-sensing, mitochondrial dysfunction and altered intercellular communication (López-Otín C et al., 2013).

The main goal of senescence is to prevent propagation of damaged cells, by arresting the cell cycle, and to initiate cell clearance mechanisms by the immune system. This means that a proper cell replacement system is required to ensure normal cell numbers. However, with ageing, the efficiency of this turnover mechanism declines, due to stem cell exhaustion, which results from the progressive maintenance of tissue homeostasis over time. Thus, eventually, damaged tissues will no longer retain their normal physiological activity to the fullest, resulting in the accumulation of senescent cells, that aggravate the damage and contribute to ageing (López-Otín C et al., 2013), (Kuilamn T et al., 2010).

Genomic and epigenetic alterations are some of the various damages that cells may suffer. These include DNA breaks, DNA methylations and acetylations, histone modification, chromatin remodelling and telomere shortening. The consequences that arise are transcriptional noise, RNA processing aberrations and chromosomal instability. One could also consider the mutations in genomic DNA and mtDNA that accumulate throughout time and that may lead to impaired protein functions. Some genetic alterations may even lead to progeria (accelerated ageing diseases) (López-Otín C et al., 2013), (Kuilamn T et al., 2010), as Cockayne syndrome patients exhibit, for instance (Rapin I et al., 2014).

The quality control mechanisms that preserve the stability and functionality of the proteomes also decline with ageing. Therefore, taking into account that cells are

constantly receiving endogenous and exogenous stress stimuli, they will accumulate misfolded, aggregated and damaged proteins. In physiological conditions, cells would rely on heat-shock proteins (HSP) to refold misfolded proteins and on the UPS and ALP for protein degradation, but with ageing there is a loss of proteostasis, which culminates in proteotoxicity and eventually cell death (Koga H et al., 2011).

The ageing process is exacerbated by anabolism and metabolically characterized by insulin resistance, reduced growth hormone (GH) and insulin growth factor 1 (IGF-1), the latter being largely associated with type 2 diabetes, osteoporosis and other complications (Barzilai N et al., 2012).

In addition to the insulin/insulin growth factor 1 (IGF-1) signalling (IIS) pathway that mediates glucose-sensing, other three important and interconnected nutrient-sensing systems play an important metabolic role: the mammalian target of rapamycin (mTOR), the adenosine monophosphate-activated protein kinase (AMPK) and sirtuins (Barzilai N et al., 2012).

In fact, AMPK and sirtuins, act in the opposite direction to IIS and mTOR. This means that they sense nutrient shortage and promote catabolism, instead of nutrient abundance and anabolism, which contributes to ageing. In other words, the mTOR senses high amino acid concentrations, the AMPK detects low energy states through high AMP levels, and lastly, sirtuins sense high nicotinamide adenine dinucleotide⁺ (NAD⁺) levels as indicator of low energy levels. Directly modulating these pathways has been reported to impact life span (Barzilai N et al., 2012).

Mitochondrial deficiencies may affect several cellular mechanisms. Impaired function of the respiratory chain leads to diminished production of ATP and increased production of ROS which can target and damage many types of biomolecules. Dysfunctional mitochondria also promote apoptotic signalling and trigger ROS-mediated inflammation and further activation of inflammasomes (Green DR, 2011).

Lastly, intracellular communication, including neurohormonal signalling (e.g., renin-angiotensin, adrenergic and IIS) become deregulated with ageing. Moreover, as inflammatory processes are increased, whereas immunosurveillance against pathogens and premalignant cells dampens. (López-Otín C et al., 2013).

1.4.2. Animal models of ageing

Ageing-related complications or diseases are time-dependent events, therefore the best animal model for research in the ageing field is a healthily aged animal. Some old animals, such as rodents, may even spontaneously exhibit features such as cataracts, sarcopenia, cancer, tissue dysfunction, and others (Köks S et al., 2016)

Age-associated diseases can be seen as a process that involves a first step of ageing, followed by a homeostasis imbalance of a tissue. In time, by accumulating losses of functions, a disease may eventually develop.

Several animal models of ageing rely on genomic and mitochondrial mutations or telomere shortening that lead to progeria and other similar syndromes with accelerated ageing. For instance, the mouse model *Polγ*^{D257A/D257A}, presents a mutation in polymerase γ , which is responsible for mtDNA replication. This mutation has implications that compromise mitochondrial homeostasis, which further leads to energetic deficits and increased ROS production. In turn, ROS are inflammation mediators and can promote protein aggregation (Trifunovic A et al., 2004). All these factors are hallmarks of ageing.

1.4.2.1. Accelerated ageing - D-Gal administration model

D-Galactose (D-Gal) is known to accelerate ageing and has been used in rodents for studying the ageing brain, accounting for 500 publications until 2014 regarding the use of this reducing sugar for increasing the rate of ageing (Hao L et al., 2014).

D-Gal is an abundant monosaccharide in fruits, vegetables, milk and others (Gropper SS et al., 2000). In normal concentrations, this sugar is metabolized into glucose, however in higher concentrations galactose oxidase converts D-Gal into aldose and hydroperoxide, which in turn results in increased ROS production. These sugars can non-enzymatically react with the N-terminal of proteins resulting in the accumulation of advanced glycation end-products (AGE) (Wu DM et al., 2008), which are known to have an impact on the development of cataracts, renal failure, PD, oxidative damages in the brain and many other pathologies (Tian J et al., 2005). Thus, neurotoxicity results from increased ROS and AGEs.

Rodents that were intoxicated with D-Gal, either orally fed or through intraperitoneal injection, display a shortened lifespan accompanied by a range of complications highly associated with ageing: cognitive dysfunction, probably due to increased acetylcholinesterase (AChE) activity, memory impairment as well as depressogenic and anxiogenic behaviours. It was also shown an increased lipoperoxidation and superoxide dismutase (SOD) levels whereas catalase and glutathione oxidase activity was decreased. In addition, the levels of biogenic amines are reduced in the brain (Haider S et al., 2015). One important factor to take into account is that usually only males are used because females seem to be not so affected by the stress stimulus of D-Gal administration, probably due to female hormones having neuroprotective roles (Hao L et al., 2014).

1.4.3. The ageing retina

Visual changes have been reported in aged humans, which comprehend reduced visual acuity, visual field sensitivity, contrast sensitivity and delayed dark adaptation (Nadal-Nicolás F et al., 2018). It was also described that electroretinographic amplitudes of the a- and b-waves decrease with ageing (Birch DG and Anderson JL 1992).

In regard to cell function, it was observed the occurrence of mitochondrial damage (El-Sayada HI et al., 2014), decreased dopamine activity (Hankins MW, 2000) and para-inflammation (Xu H et al., 2009) in the retina.

Furthermore, the retina also suffers age-related structural changes. The size of the retina increases linearly with age and body weight. This continuous growth leads to a proportional retinal thinning and cell density reduction, as previously reported for albino rats (Braekevelt CR and Hollenberg MJ, 1970).

In albino but not in pigmented rats, there is an age-related cell loss in the ONL, probably due to a higher susceptibility to damage from light exposure, and to a less extent in the INL (Nadal-Nicolás F et al., 2018). In aged humans, photoreceptor loss has also been observed (Owsley C et al., 2001). Rod bipolar cells exhibit dendrites sprouting into the ONL, although with no evident axonic alterations (Samuel MA et al., 2011). Dendritic arbour size of amacrine cells in the INL does not significantly change in rats with ageing,

however the thinning of the INL may suggest amacrine cell loss (Nadal-Nicolás F et al., 2018).

The two plexiform layers, OPL and IPL, are thinner in aged albino rats, mostly the OPL, but not in a pigmented rat strain, which could suggest a lower number of synapses that ultimately leads to a reduced neuronal function (Nadal-Nicolás F et al., 2018).

In female Sprague Dawley rats the RNFL does not lose volume during ageing, which is in agreement with the maintenance of all cells belonging to the GCL (Nadal-Nicolás F et al., 2018). However, other reports suggest the opposite, a decrease in the RGC number in the same rat strain (Cano J et al., 1986), and also in humans (Harthew RS et al., 2008). In mice, it seems that there is an age-related decrease in the size and complexity of RGC arborisation, which means that the coverage of their receptive field is far less low (Samuel MA et al., 2011)

Altogether, these data show that even within a circuit, different neurons can experience distinct ageing programs and that gender, age and genetic background of the target organism (mice, rat or humans) have impact on the results.

Furthermore, the dopaminergic system efficiency in rats retina was described to lose efficiency throughout ageing, leading to an impaired light/dark adaptation (DjamGoz B et al., 1997).

1.5. *Diabetes Mellitus*

Diabetes Mellitus (DM) is a metabolic disorder essentially characterized by chronic hyperglycaemia, resulting from deficits in insulin secretion, insulin action or both (Kharroubi AT and Darwish HM, 2015), (Baynest HW, 2015). This disease is also accompanied by an impaired carbohydrate, lipid and protein metabolism. (Ahmed AM 2002).

Worldwide epidemiological data shows that in 2011, 366 million people had DM and that by 2030 this number might increase to 552 million (Wild S et al., 2004).

Classifying the type of diabetes a patient may have is important and determines which therapeutic approaches should be used, although it is not easy to specifically place a diabetic individual in a single class. DM can be classified into four different categories:

type 1, type 2, “other specific types” and gestational diabetes (Kharroubi AT and Darwish HM, 2015), (Haynes HW, 2015).

Type 1 DM (T1DM), which makes up an estimated 5-10% of all diabetic patients, can be classified as of autoimmune origin, idiopathic and as fulminant (Kharroubi AT and Darwish HM, 2015). Autoimmune type 1 DM consists of pancreatic β -cell loss, source of insulin production, due to the presence of autoantibodies reactive for insulin and other targets that can be recognized by T cells. This leads to hypoinsulinemia and hyperglycaemia. T1DM patients develop microvascular complications such as nephropathy, neuropathy and retinopathy, but also macrovascular like coronary heart disease and cerebrovascular disease. These patients are insulin dependent (Katsarou A et al., 2017).

Type 2 DM (T2DM), which roughly accounts for 90% of all patients (Haynes HW, 2015), results from the interplay between genetic, environmental and behavioural risk factors (Wild S et al., 2004). Obesity is a major risk factor for developing insulin resistance which is responsible for T2DM. Conversely, insulin resistance promotes obesity and hyperglycaemia (Khan BB and Flier JS, 2000). T2DM is a time-dependent progressive disorder with long-term complications quite similar to T1DM, however without pancreatic β -cell loss. These patients are not insulin-dependent, however, over time insulin secretion decreases with the increased demand for insulin due to the gradual dysfunction of β cells, and thus patients become insulin dependent. (Halban PA et al., 2014), (Haynes HW, 2015).

Gestational diabetes occurs in women with T1DM or asymptomatic T2DM. The “other” category comprises cases with several etiologies including genetic defects of β -cell function, also known as maturity-onset diabetes in youth (MODY), compromised insulin action or impaired pancreatic physiology due to infections and drugs (Kharroubi AT and Darwish HM, 2015).

1.5.1. Diabetic retinopathy

Diabetic retinopathy (DR) is the most common microvascular complication of DM and is a leading cause of vision loss in middle-aged and elderly people (Duh EJ et al., 2017). Epidemiological data reveals that one third of the diabetic patients develops

DR (Wong TW et al., 2016). This ocular complication comprehends an early phase entitled non-proliferative stage that later progresses into the proliferative stage. DR diagnosis relies on an ophthalmoscopy analysis (Duh EJ et al., 2017).

1.5.1.1. Non-proliferative and proliferative DR

It is known that several molecular features of DM can be found in the diabetic eye, namely hyperglycaemia, increased oxidative stress, inflammation, AGEs and protein kinase C (PKC) levels, mitochondrial dysfunction, and others, which have an impact in neuronal cells fitness (Das A, 2016).

However, some of these cellular events also occur in non-neuronal cells such as Müller cells, endothelial cells and others. Due to the hostile environment, Müller cells present upregulated levels of glial fibrillar acidic protein (GFAP) and go through a reactive gliosis process in which pro-inflammatory cytokines are secreted (Bringmann A and Wiedemann P, 2012). These cytokines recruit leukocytes that compromise the permeability of the blood-retinal barrier (BRB) (Noda K et al., 2012). Increased PKC levels also contribute to increased permeability (Tang J and Kern TS, 2011). In addition, augmented AGEs levels are known to induce pericyte loss (Stitt AW et al., 2004), leaving blood vessels without support that along with increased oxidative stress leads to the formation of acellular capillaries. Altogether, these changes disrupt endothelial vascular cells tight junctions, causing leakage to interstitial space, but also vascular frailty, triggering haemorrhages and microaneurysm occurrence. Finally, it culminates in the deposition of hard exudates in the extracellular space that contribute to an ischemic and hypoxic environment in the retina (Das A, 2016).

The disease progresses into the proliferative stage when neovascularization starts occurring. Newly formed blood vessels grow into the vitreous chamber and are thinner and more fragile, which further enhances the probability of haemorrhages and exacerbates retinal inflammation. In addition, these new blood vessels can not only disrupt the retinal architecture and detach the retina, but they can also block the incoming light, thus preventing it from reaching the photoreceptors (Wong TY et al., 2016). The new retinal vascular architecture can be observed through optical coherence tomography (OCT)-Angiography (OCT-A) (Matsunaga D et al., 2014).

Overall, these vascular alterations contribute to vision loss and retinal dysfunction (Fig.1.6).

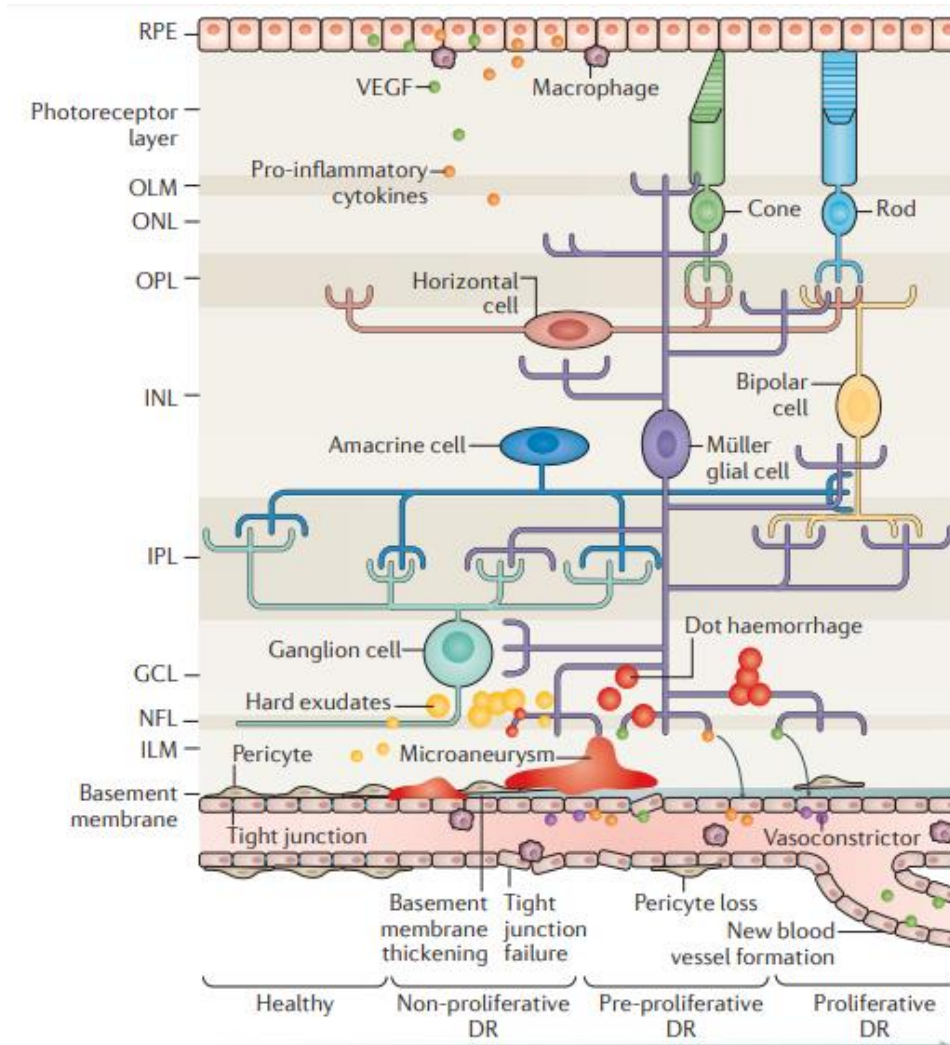


Figure 1.6. - Core pathogenic events in diabetic retinopathy. DR is characterized by specific pathogenic events in the development and progression of diabetic depicted from healthy (left) to an advanced stage (right). Non-proliferative DR comprehends basement membrane thickening, increased endothelial permeability and pericyte loss which culminate in haemorrhages, microaneurysms and hard exudates. The ischemic and hypoxic environment as well as the presence of pro-angiogenic cytokines triggers a neovascularization response, forming new blood vessels into vitreous that are very fragile and can easily get damaged (Adapted from Wong TY et al., 2016). GCL, ganglion cell layer; ILM, inner limiting membrane; INL, inner nuclear layer; IPL, inner plexiform layer; NFL, nerve fibre layer; OLM, outer limiting membrane; ONL, outer nuclear layer; OPL, outer plexiform layer.

In regard to the current therapies, aside from the standard procedure of glycaemic control, diabetic patients may be submitted to an ocular surgery to perform photocoagulation, or may be prescribed with aminoguanidine, a methylglyoxal scavenger and AGEs breakdown agent (Kern TS and Engerman RL 2001), or even be intraocularly injected with anti-vascular endothelial growth factor (VEFG) (Simó R and Hernández C,

2008), which is a protein upregulated in the diabetic environment that promotes vascular permeability and vasculogenesis (Frank RN, 2004)

1.5.1.2. Retinal neurodegeneration – the prequel of vascular alterations

Growing evidence suggest that retinal neurodegeneration is as early event in the pathogenesis of DR that precedes the already known vascular damage and alterations (Duh EJ et al., 2017). This is further strengthened by reports pointing to colour vision loss (Roy MS et al., 1986), reduced contrast sensitivity (Sokol S et al., 1985) and decreased electrical responses on electroretinographic tests (Abcouwer SF and Gardner TW, 2014). Furthermore, structural changes in the retina of diabetic patients have been documented through OCT and spectral domain-OCT (SD-OCT), revealing decreased thickness of the RNFL and GCL-IPL (Carpineto P et al., 2016), but also in the INLin a T1DM animal model (Dijk HW et al., 2009). In addition, cell death of RGCs and amacrine cells has also been observed in diabetic animal models and in *post-mortem* diabetic eyes (Barber AJ et al., 1998). Moreover, photoreceptor loss (Park SH et al., 2003) and abnormalities in bipolar cell response (Bui BV et al., 2009) have been reported in diabetic animals.

Although yet unclear, synapses are known to present high vulnerability to several degenerative stimuli, which is in accordance to recent evidence that often subtle events occurring at the distal synaptic extremities precede neuronal death (Wishart TM et al., 2018). DM plays a role in modulating the content and distribution of exocytotic proteins and neurotransmitters in cultured hippocampal neurons and in the retinal nerve terminals. In the retina, most of the differences reported so far were detected at an early onset of the disease, which faded over time, possibly due to compensatory mechanisms. Both Syntaxin 1A and Synaptophysin levels were reported to decrease, although later recovering to normal levels. Only Synapsin-1 and VAMP-2 remained at lower levels (Gaspar JM et al., 2010), (Batista FI et al., 2011). Moreover, another report shows that for a short period of experimental diabetes there was a decrease in the retinal content of the synaptic proteins Synaptophysin, Synapsin I, VAMP2, SNAP-25 and Postsynaptic density-95 (PSD95) without any recovery (Vanguilder HD et al., 2008). It is possible that these differences derive from the use of different rat strains, which respond differently to diabetes. Nevertheless, DM is compromising the communication between neurons.

1.5.2. Animal models of diabetes

Animal models have been extensively used in diabetes research in order to better understand the etiopathogenesis of the disease, but also to uncover new molecular mechanisms that can be crucial for the disease progression. In addition to all these studies, testing pharmacological interventions is another important aim (King AJ, 2012).

Animal models of T1DM essentially rely on β -cell destruction. It may be chemically induced, through streptozotocin for instance, or it can be due to spontaneous autoimmunity (non-obese diabetic mouse model). These animals can even be genetically modified (the *Ins2^{Akita}* mouse model that has a point mutation the insulin 2 gene) or virally-induced through the Kilham rat virus, for example (King AJ, 2012).

Regarding the animal models of T2DM, they usually rely on induced obesity, either through diet (High-fat diet (HFD) model) or through genetics (Zucker Diabetic Fatty (ZDF) Rat) (King AJ, 2012).

1.5.2.1. High Fat Diet mouse model

The HFD mouse model is characterized by an increased weight, when compared to normal chow diet (NCD) fed mice due to an average 56% caloric content intake instead of 11-26%, that promotes hyperglycaemia (Winzell MS and Ahrén B, 2004).

Within one week of diet metabolic changes are already present. The weight gain is related to insulin resistance that along with the lack of β -cell compensation causes mice to develop impaired glucose tolerance (Winzell MS and Ahrén B, 2004).

Although the genetic background of mice determines the metabolic response to the HFD, this mouse model is thought to be the best T2DM animal as in humans both the disease and obesity are being induced by environmental factors (Survit RS et al., 1995).

The HFD mouse model has been used to study DR (revealing decreased electroretinographic responses), (Chang RC et al., 2015) ageing, chronic inflammation, peripheral artery disease, AD and other complications (Heydemann A, 2016).

1.5.2.2. Zucker Diabetic Fatty rat model

The ZDF *fa/fa* rat model is characterized by a mutation in the leptin receptor gene *fa* that promotes hyperphagia (Philips MS et al., 1996). Therefore, at 4 weeks of age, these rats become obese and, in turn, develop hyperinsulinaemia, hyperlipidaemia, and impaired glucose tolerance (Srinivasan K and Ramarao P 2007). Heterozygous rats do not develop DM and female homozygous rats rarely exhibit hyperglycaemia (Shiota M and Printz 2012). Eventually, this diabetic rat model will exhibit deficient insulin secretion, probably due to β -cell death (Pick A et al., 1998).

Moreover, the ZDF rats develop hydronephrosis, a neuropathy related with a slow motor nerve conduction velocity, DR, systemic cardiovascular complications and impaired wound healing capacity (Shiota M and Printz 2012). These rats are considered to be the non-insulin dependent diabetic rat model with the most severe DM (Peterson RG et al., 1990).

1.6. Triangulation between PD, DM and Ageing – common pathophysiology

Ageing is a biological process that all organisms experience throughout their life. During their lifetime, all cellular events that ensure the physiology of a tissue, of the retina for example, are progressively dampened. This includes, for instance, deregulation/impairment of the electrophysiological activities of neurons and of the molecular switches that modulate metabolic responses (López-Otín C et al., 2013).

Both DM and PD are age-related diseases and recent evidence suggests an underlying common pathophysiology (Tian T et al., 2015), as diabetic patients seem to have an increased risk of developing PD (Yue et al., 2016).

In fact, DM shares several pathogenic molecular features with PD and with ageing, namely increased AGEs, inflammation, oxidative stress, mitochondrial dysfunction, and others (Das A 2016), (Wales P et al., 2013). These alterations can further exacerbate synucleins pathological role (Wales P et al., 2013), especially glycation, which is increased in aged individuals, in PD and in diabetic patients, and that targets aSyn, hence driving its neurotoxic potential (Miranda MV et al., 2017). These pathogenic

mechanisms were described in the brain tissue, where synucleins are present, however these proteins are also found in the retina (Surguchov A et al., 2001), a tissue that is a target of neurodegeneration throughout ageing, in PD and in DM (Wong TY et al., 2016), (Inzelberg et al 2004), (Hajee et al., 2009), (Nadal-Nicolás F et al., 2018).

Although the synucleins physiological role in the retina remains elusive, it is known that the triple abg-Syn KO develops age-dependent blindness, which highlights their role in vision (Greten-Harrinson B et al., 2010).

In addition, aSyn was reported to modulate dopamine synthesis, storage, clearance and efflux (Butler B et al., 2016), which is a key neurotransmitter in the retina important for light adaptation (Ribelayga et al., 2008) and whose shortage in the SNpc is thought to lead to the well-known motor features (Dickson DW et al., 2009). Furthermore, retinal thinning in PD patients is proposed to have a correlation with the loss DA cells (Ahn J., et al 2018). In addition, DM even seems to increase the turnover of dopamine in a diabetic animal model (Kleinridders A et al., 2015).

Considering that there is a decreased dopamine activity in the retina of aged individuals (Hankins MW, 2000) and loss of DA cells in the retina of diabetic animal models (Nishimura C et al., 1985), (Gastinger MJ et al., 2006) and PD patients, it is plausible that the previous molecular events may be triggering synucleins pathogenicity, thus contributing to vision impairment through DA cell dysfunction. However, the synucleins family members are also present in other retinal populations (Surguchov A et al., 2001) that can be a target of their neurotoxicity as well.

Moreover, levodopa administration in a DR mouse model significantly improves retinal function (Aung MH et al., 2014). Conversely, rosiglitazone, an anti-diabetic drug, can efficiently protect retinal neurons in a PD animal model (Normando EM et al., 2016), which further strengthens the crosstalk between the two diseases.

1.7. Scientific direction and aim

Synucleins have been highly associated with neurodegenerative disorders, however their physiologic and pathologic roles are not completely understood (Wales P. et al., 2013).

Neurodegeneration in the retina, a tissue where synucleins are present (Surguchov A et al., 2001), was reported to occur with ageing, in PD and DR (Wong TY et al., 2016), (Inzelberg et al. 2004), (Hajee et al., 2009), (Nadal-Nicolás F et al., 2018). Whether there is a causative role of synucleins or not, it remains elusive. Nevertheless, these three circumstances exhibit shared pathological mechanisms that can trigger synucleins pathogenicity (Tian T et al., 2015), (López-Otín C et al., 2013).

Therefore, our aim is to perform a characterization of the protein levels by western blot of the synuclein family members and to profile their distribution by confocal microscopy in the retina of animal models of PD (MitoPark mouse), T2DM (HFD mouse and ZDF rat) and ageing (naturally aged rats and D-Gal treated rats).

Furthermore, we aim to address by western blot if there is any alteration in the integrity of synaptic markers, either caused by eventual synuclein alterations or by the molecular features that are characteristic of the respective animal model.

As synucleins can cause neurodegeneration, we intend to evaluate by western blot the protein levels of markers related with cell proliferation, cell death and inflammation in these animal models of PD, DM and ageing. Moreover, structural integrity of the retinal layers quantification will be quantified in confocal microscopy images.

Altogether, these experiments aim to unravel how global retinal function, specially related with synucleins, may be affected in DM and ageing, which are risk factors for PD.

2. Materials and Methods

2.1. Animal handling

All animals were handled according with the FELASA (Federation of European Laboratory Animal Science Associations) guidelines. The minimum possible number of animals was used and all efforts were made to minimize animal suffering. These animals were fed with food and water *ad libitum* and submitted to a 12 hour light-dark cycle.

2.1.1. High-Fat diet mouse model

Male C57BL/6 mice with 10 weeks of age obtained from Prof. Paula Macedo's Lab and housed at CEDOC NOVA Medical School in Portugal, were divided into two groups and fed either a high-fat diet (HFD) (Research Diets Inc., D12331) or with a normal chow diet (NCD) (Special Diets Services, 801030), and therefore referred as HFD and NCD groups respectively, until 22 weeks old *ad libitum*. The HFD consisted of 58% fat, 25.5% carbohydrate, and 16.4% protein (total 1000,1 kcal/g), whereas NCD contained 13.7% fat, 14.3% carbohydrate, and 72% protein (total 15,10 kcal/g). Before sacrifice, mice were weighted and glucose blood levels were measured with a glucometer.

2.1.2. Zucker Diabetic Fatty rat model

Experiments were carried out on ZDF inbred rats with 5 months old obtained from Prof. Sílvia Conde's Lab and housed at CEDOC NOVA Medical School, where T2DM and related complications develop due to a leptin receptor gene mutation. Homozygous recessive males (*fa/fa*), here referred as ZDF, develop obesity, fasting hyperglycaemia and Type 2 Diabetes (Srinivasan K and Ramarao P 2007). Homozygous dominant (+/+) and heterozygous (*fa/+*) genotypes, here referred as Lean, remain normoglycemic. Before sacrifice, rats were weighted and glucose blood levels were measured with a glucometer.

2.1.3. MitoPark mouse model

MitoPark mice with 16 weeks were obtained from Prof. Rui Costa's Lab and housed at Champalimaud Centre for the Unknown, Portugal. Male C57BL/6 mice were used to generate a knock-in mouse line that expressed the cre recombinase under the control of DAT promoter, enabling the selective excision of the floxed *TFAM* gene in dopaminergic neurons (Ekstrand MI et al., 2007). MitoPark mice have both *TFAM* alleles floxed, as opposing to control mice that only have one floxed allele.

2.1.4. Naturally aged rat model

Male Wistar rats obtained from Dr. Diana Cunha-Reis' Lab were housed at IMM, Portugal, and raised until they reached the following ages of interest: 1 month, 6 months, 10 months and 19 months old.

2.1.5. D-Galactose rat model

Male Wistar rats obtained from Dr. Diana Cunha-Reis' Lab were housed at IMM, Portugal, and injected intraperitoneally with 250 mg/Kg D-Gal for 6 weeks starting at 10 weeks of age, whereas sham rats were injected with saline, and sacrificed at 6 months

2.2. Eye harvesting and sampling

After animal sacrifice and eye enucleation, eyes planned for microscopic analysis were immersed and fixed in 4% paraformaldehyde (PFA) in phosphate buffer saline (PBS) 1X pH 7.2 for a maximum of 24h. After fixation the eyes were submitted to a 10% and 20 % sucrose gradient in PBS 1X pH 7.2 and stored in 30% sucrose in PBS 1x pH 7.2 at 4°C. Prior to histological sectioning, the eyes were embedded in Optimum Cutting Temperature mounting medium for cryotomy (VWR) and frozen at -80°C. Each eye was vertically cut with a 12 µm thickness in a cryostat (Leica, CM3050 S) at -20°C. Each eye section was sequentially placed in slides and left to dry for 24h and afterwards stored at -20°C.

If the eyes were meant for western blot analysis, the retinas of the harvested eyes were dissected in ice-fresh cold PBS 1X supplemented with protease inhibitors (Roche) and phosphatase inhibitors (Roche) - 1 pill of each per 10 mL of buffer. To extract the protein, each retina was homogenized with a pellet pestle in 50-70 μ L of radioimmunoprecipitation (RIPA) buffer (25 mM Tris, 150 mM NaCl, 0.1% sodium dodecyl sulfate (SDS), 0.5% sodium deoxycholate and 1% NP-40) supplemented with a cocktail of protease and phosphatase inhibitors – 1 pill of each per 10 mL of buffer. Afterwards, the homogenate was centrifuged for 15 min at 15 000 xg at 4°C and collected the supernatant for storage at -20°C.

2.3. Localization of markers of interest by immunohistochemistry

After thawing slides containing retinal sections, retina slices were hydrated in PBS 1X for 30 min. Then, washes with 0.25% Triton X-100 in PBS 1X (PBS-T 0.25%) were performed for 45 min and afterwards blocked in 1% bovine serum albumin (BSA)/Donkey, 3% serum/Goat in 0.25% PBS-T for 1h at Room Temperature (RT), rinsed and incubated overnight with the respective primary antibody (Table 2.1.). After washing for 45 min with 0.25% PSB-T the sections were incubated with the respective secondary antibodies (1:1000) Goat anti-Rabbit Alexa Fluor 488 (Invitrogen, A32731) and Goat anti-Mouse Alexa Fluor 594 (Invitrogen, A11005) for 1h at RT. Washes with 0.25% PBS-T were performed for 30 min before the incubation with 4',6-diamidino-2-phenylindole (DAPI) (Sigma) with a dilution of 1:10 000 in PBS 1x for 10 min at RT. The slides were next rinsed twice in PBS 1X, the fluorescent mounting media (Dako) was added and a coverslip was placed on top of each slide. After 1h of drying, the slides were sealed with nail polish. Images with 10 z-stacks were acquired through the Zeiss LSM710 confocal microscope, under a 40x magnification objective, while also using the Zen 2010 software. Further analyzes of the confocal images was performed through the FIJI software.

Table 2.1. – Primary antibody description used in immunohistochemistry assays.

Antibody	Reference	Species	Dilution (in 0.25% PBS-T)
-----------------	------------------	----------------	----------------------------------

aSyn	BD (610787)	Mouse	1:200
aSyn	Cell signalling (2629S)	Rabbit	1:200
bSyn	Abcam (ab76111)	Rabbit	1:200
gSyn	Abcam (ab55424)	Rabbit	1:200

2.4. Assessment of protein levels of markers of interest by Western Blot

To quantify the protein concentration of each sample the bicinchoninic acid (BCA) protein assay (ThermoScientific) was used, complemented with the use of the spectrophotometer Infinite M200 (Tecan) for absorbance measurements. The samples were denatured by adding 1X concentrated protein sample buffer (0.5 M Tris, 30% glycerol, 10% SDS, 0.6 M dithiothreitol, 0.012% Bromophenol Blue) and by heating at 100 °C during 10 min. PageRuler (ThermoScientific) was the protein ladder used. Equal amounts of protein were loaded into the gel wells (15 µg) and the extracts were separated by SDS gel electrophoresis, using 10–12% bis-acrylamide gels. The proteins were transferred electrophoretically for 7 min under a 25V and 2,5A electric current to nitrocellulose membranes (BioRad) using the Trans-blot Turbo system (Bio-rad Laboratories). The membranes were blocked for 1h at RT, in Tris-buffered saline (137 mM NaCl, 20 mM Tris-HCl, pH 7.6) (TBS) containing 0.1% Tween-20 (TBS-T) and 5% (w/v) Bovine Serum Albumin (BSA) (Nzytech) in TBS-T (5% BSA-T). The membranes were incubated with the primary antibody diluted in 5% BSA-T (Table 2.2.), overnight at 4 °C with agitation. After washing for 30 min in TBS-T, the membranes were incubated for 2h at room temperature with the respective horseradish peroxidase-conjugated secondary antibody (Table 2.3.), prepared in BSA-T 5% and afterwards washed in TBS-T for 30 min. The membranes were processed for protein detection using the Blotting detection reagent ECL (GE Healthcare) and the densitometer ChemiDoc (BioRad). Digital quantification of the bands intensity was performed using ImageLab 5.2.1 software (Bio-Rad Laboratories). The stripping of the membranes was performed with an incubation with a stripping buffer pH 2.0 (200 mM Glycine, 3.5 mM SDS) up to 30 min at RT, followed by 30 min of washes with TBS and 30 min with TBS-T. Before incubating overnight at 4 °C with the respective primary antibody, the membranes the

membranes were blocked again with 5% BSA-T for 1h at RT. The following steps are similar to the previously mentioned.

Table 2.2. – Primary antibody description used in western blot assays.

Antibody	Reference	Species	Dilution (in 5% BSA-T)
β-actin	Sigma (A5441)	Mouse	1:10000
aSyn	BD (610787)	Mouse	1:1000
pS129-aSyn	Wako (015-25191)	Mouse	1:500
bSyn	Abcam (ab76111)	Rabbit	1:1000
gSyn	Abcam (ab55424)	Rabbit	1:1000
Synaptophysin	Sigma (S5768)	Mouse	1:1000
SNAP-25	Labome (111 002)	Rabbit	1:1000
Rab3a	SICGEN (AB10032-200)	Goat	1:1000
Syntaxin 1A	Sigma (S0664)	Mouse	1:1000
PSD95	Milipore (04-1066)	Rabbit	1:1000
TH	Abcam (Ab112)	Rabbit	1:500
STAT3	Cell signaling (12640)	Rabbit	1:2000
pY705-STAT3	Cell signaling (9131)	Rabbit	1:1000
MLKL	Sigma (SAB1302339)	Rabbit	1:250
pMLKL	Abcam (ab196436)	Rabbit	1:1000
Caspase 3	Cell Signaling (8G10)	Rabbit	1:1000
NF-κB	Cell Signaling (4113)	Rabbit	1:1000
GFAP	Millipore (AB5804)	Rabbit	1:1000
Cre	SICGEN (AB0124-200)	Goat	1:2500

Table 2.3. – Secondary antibody description used in western blot assays.

Antibody	Reference	Specie	Dilution (in 5% BSA-T)
Anti-Rabbit	GE Healthcare (NA934V)	Donkey	1:5000
Anti-Mouse	GE Healthcare (NA931V)	Sheep	1:5000
Anti-Goat	Santa Cruz Biotechnology (sc-2620)	Donkey	1:5000

2.5. Statistical analysis

All statistical analysis was performed using the GraphPad Prism 7 software. Results are presented as mean±standard deviation (SD). Before statistical comparisons, Normality tests were conducted in all animal groups using the D'Agostino-Pearson, Shapiro-Wilk and Kolmogorov-Smirnov tests with a Confidence level of 95%. Upon verification that the values came from a Gaussian distribution, statistical comparison between diabetic animals and respective age-matched controls, or between MitoPark mice and control, or between D-Gal injected rats and sham, was performed using the unpaired parametric Student's t-test. If not normal, a Mann-Whitney test was conducted for these data. Regarding the naturally aged rats, a parametric ANOVA test was used if the data had a normal distribution, followed by a multiple comparisons Dunnett's test, using the 1 month old age rats as control. If the data did not have a normal distribution a Kruskal-Wallis test was used, followed by multiple comparisons Dunn's test using the 1 month old age rats as controls. Differences were considered significant as: *p<0.05, **p<0.01, ***p<0.005 and ****p<0.001.

3. Results and Discussion

3.1. Cre recombinase protein levels in the retina of MitoPark mice model of PD

The MitoPark mouse model takes advantage of a Cre-loxP system in order to create a hostile environment through the excision of the *TFAM* gene that causes mitochondrial dysfunction in DA cells, and eventually cell death (Ekstrand MI and Galter D, 2009). However, before one can make any assessments, we assessed the levels of the cre recombinase in whole retina protein extracts of MitoPark mice by western blot, in order to prove that the system had the excision tool present (See Sup. Fig. 1).

Western blot analysis of whole retina protein extracts confirms the presence of cre recombinase both in Control and MitoPark mice retina, however with significantly lower levels in Control regarding MitoPark mice (1.000 ± 0.6729 vs 6.235 ± 2.573) (See Sup. Fig. 1). As Control mice are heterozygous for the floxed allele of interest, *TFAM*, it means that they still retain the *cre* gene, therefore it would be expectable that they exhibit detectable protein levels.

Nevertheless, it still remains elusive whether the cre recombinase is actually working under the influence of the DAT promoter and whether it is excising the *TFAM* gene in the retina. Aside from the already tested cre protein levels, in order to ensure that the Cre-loxP system is working in the retina of MitoPark mice, it would be important to check if they have the *cre* gene and the floxed *TFAM* gene. Hence, it would be required to genotype mice via ear punch biopsy (negative control), genotype harvested midbrain DNA (positive control) and lastly compare with DNA harvested from the retinal tissue. In addition, it is also crucial to check by polymerase chain reaction the mRNA levels specifically of the *cre* and *TFAM* genes in the retina. Finally, immunohistochemistry provides the localization of the cre protein in the retina, and if colocalized with TH or DAT it could mean that at least there is cre recombinase being expressed in DA cells (Versaux-Botteri C et al., 1984), (Cheng Z et al., 2006).

3.2. Synucleins levels in the retina of MitoPark mice model of PD

As the synuclein family is highly associated with the pathogenesis of PD (Wales P et al., 2013), we next addressed if the mitochondrial dysfunction expected to occur in this mouse model had any effect on the synucleins levels in whole retina proteins extracts of MitoPark mice, including pS129-aSyn (Fig. 3.1.).

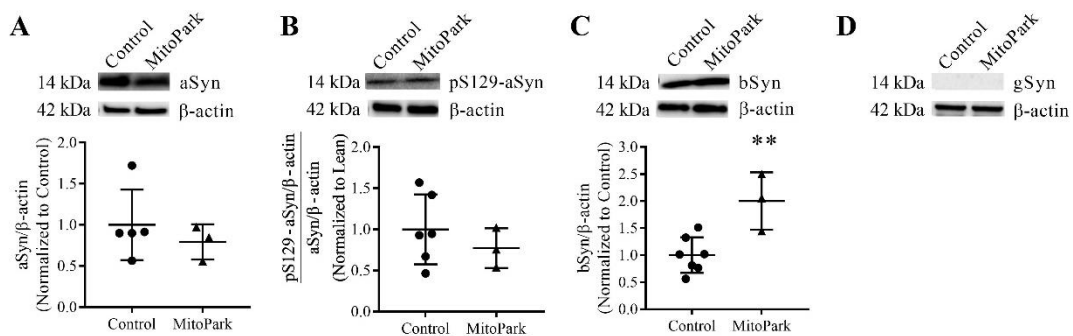


Figure 3.1. – Assessment of synucleins levels in Control and MitoPark mice whole retina protein extracts. A) Western blot for the comparison of aSyn protein levels between Control and MitoPark mice (upper panel) and the corresponding densitometry analysis (lower panel). B) Western blot for the comparison of the proportion of aSyn phosphorylated at S129 over total aSyn protein levels between Control and MitoPark mice (upper panel) and the corresponding densitometry analysis (lower panel). C) Western blot for the comparison of bSyn protein levels between Control and MitoPark mice (upper panel) and the corresponding densitometry analysis (lower panel). D) Western blot for the detection of gSyn protein levels in Control and MitoPark mice. A representative image of the western blot is shown. All Western Blot data are presented as Mean \pm SD. ** $p < 0.01$ MitoPark compared with Control; T-test.

The results obtained show that both aSyn as well as the proportion of pS129-aSyn over total aSyn protein levels do not suffer any variation between Control and MitoPark mice retina (Fig. 3.1.A and B). However, bSyn reveals increased protein levels in MitoPark mice retina in comparison to control mice (2.001 ± 0.5296 vs 1.000 ± 0.3294) (Fig. 3.1.C). Regarding, gSyn, this protein was not detected in both animals in the tested conditions (Fig. 3.1.D).

Although aSyn has been considered among the synucleins the one most implicated in PD progression (Wales P et al., 2013), it seems that in this animal model of PD, bSyn is the only one affected by a cascade of events following mitochondrial dysfunction induced by the deletion of the *TFAM* gene (Ekstrand MI and Galter D, 2009). Whether this increasing event has neuroprotective effects by controlling aSyn aggregation (Hashimoto M et al., 2001), (Hashimoto M et al., 2004) or neurotoxic properties by forming aSyn-like inclusions that compromise cell normal function (Taschenberger G et al., 2013), (Tenreiro S et al., 2016), it relies to be elucidated.

3.3. Synaptic markers levels in the retina of MitoPark mice model of PD

The mouse model MitoPark is described to have a preferential loss of dopaminergic neurons in the brain (Ekstrand MI and Galter D, 2009). It is also known that DA cells in the retina and their role of dopamine production are essential for global retina function, specifically for light/dark adaptation (Ribelayga et al., 2008).

Therefore, the aim was to check by western blot if the levels of proteins whose function is known to be directly related with synaptic function, such as the v- and t-SNAREs Synaptophysin and Syntaxin 1A (Söllner T et al., 1993), were altered. TH levels, the regulator enzyme of dopamine synthesis and marker of dopaminergic neurons (Peng et al., 2005), were also evaluated (Fig. 3.2.).

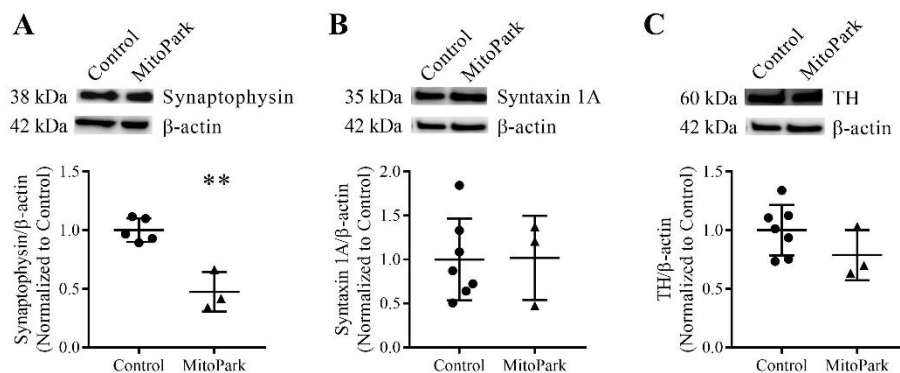


Figure 3.2. – Assessment of synaptic markers levels in Control and MitoPark mice whole retina protein extracts. A) Western blot for the comparison of Synaptophysin protein levels between Control and MitoPark mice (upper panel) and the corresponding densitometry analysis (lower panel). B) Western blot for the comparison of Syntaxin 1A protein levels between Control and MitoPark mice (upper panel) and the corresponding densitometry analysis (lower panel). C) Western blot for the comparison of TH protein levels between Control and MitoPark mice (upper panel) and the corresponding densitometry analysis (lower panel). A representative image of the western blot is shown. All Western Blot data are presented as Mean \pm SD. ** $p < 0.01$ MitoPark compared with Control; T-test.

Regarding Synaptophysin, it is significantly decreased in MitoPark mice retina in comparison to Control mice (0.4738 ± 0.1682 vs 1.000 ± 0.1005) (Fig. 3.2.A), in contrast to Syntaxin 1A whose levels do not suffer any variation between Control and MitoPark mice retina (Fig. 3.2.B). This reduction in Synaptophysin levels can result from an altered turnover of the protein, either through gene downregulation or increased clearance. This change may also reflect less synaptic vesicles carrying Synaptophysin or less Synaptophysin protein per synaptic vesicle. In other words, there could be less neurotransmitters being released or impaired neurotransmission, respectively, in the retina of MitoPark mice.

Lastly, TH levels seem not to be affected in MitoPark mice retina regarding control mice (Fig. 3.2.C). As previously reported in the brain, there is a progressive loss in the number of TH-positive neurons in the brain of MitoPark mice, starting at 12 weeks of age that intensifies with ageing (Ekstrand MI and Galter D, 2009). One could perhaps expect the same events to happen in the retinal tissue as DA cells are TH- and DAT-positive (Versaux-Botteri C et al., 1984), (Cheng Z et al., 2006). which was not observed. Nevertheless, higher number of Mitopark mice would help to clarify if there is any difference.

Altogether, only synaptophysin decreased levels pointed to an impaired synaptic function in MitoPark mice retina.

3.4. Cell death markers levels in the retina of MitoPark mice model of PD

DA cells are expected to be dying through the mitochondrial apoptotic pathway, a caspase dependent event (Wang C and Youle RJ, 2013), however cell death may also be occurring in DA cell neighboring or in other areas of the retina, due to the lack of dopamine activity, an important neurotransmitter (Yamauchi T et a., 2003). Possibly, adjacent cells may even undergo the necroptosis signaling pathway for instance, which is caspase independent (Wang H et al., 2014), as their mitochondrial integrity, hypothetically, is not being challenged nor the cytochrome c being released.

Therefore, our aim was to evaluate the protein levels by western blot of the Mixed Lineage Kinase domain-like (MLKL), the last effector of necroptosis, but also and the proportion of its phosphorylation, pMLKL, that permeabilizes membranes and triggers cell death (Petrie EJ et al., 2018). Caspase 3 protein levels and its cleaved formed, an important effector of the intrinsic apoptotic pathway (Nuñez G et al., 1998), were also tested by western blot in MitoPark mice retina (Fig. 3.3.).

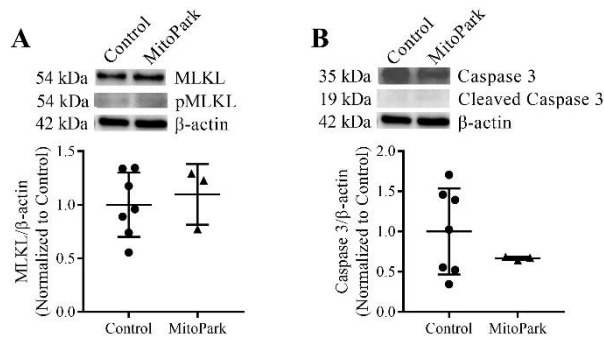


Figure 3.3. – Assessment of cell death markers levels in Control and MitoPark mice whole retina protein extracts. A) Western blot for the comparison of MLKL protein levels between Control and MitoPark mice and detection of pMLKL (upper panel) and the corresponding densitometry analysis (lower panel). B) Western blot for the comparison of caspase 3 protein levels between Control and MitoPark mice and detection of cleaved caspase 3 (upper panel) and the corresponding densitometry analysis (lower panel). A representative image of the western blot is shown. All Western Blot data was analyzed with T-test and are presented as Mean \pm SD.

The obtained results from the western blot analysis show similar MLKL protein levels between Control and MitoPark mice and undetectable pMLKL levels in the tested conditions (Fig. 3.3.A). Conversely, Caspase 3 protein levels remained equal in MitoPark mice retina in comparison to Control and no cleaved caspase 3 was detected in the tested conditions (Fig. 3.3. B).

In summary, in the tested conditions, cell death markers independent and dependent of caspases did not point to any cell death events in the retina of MitoPark mice.

3.5. The synucleins family in the retina of ageing rat models

3.5.1. Synucleins levels in whole retina protein extracts of ageing and D-Gal rats

With ageing, proteins accumulate PTMs and the efficiency of the quality control mechanisms that preserve the stability of the proteome declines (Koga H et al., 2011), hence creating the perfect environment for synucleins misfolding, accumulation and even aggregation (Wales P et al, 2013). Therefore, we next assessed the synucleins levels, including pS129-aSyn, by western blot in whole retina proteins extracts in 1, 6, 10 and 19 months old rats and Sham and D-Gal rats (Fig. 3.4.).

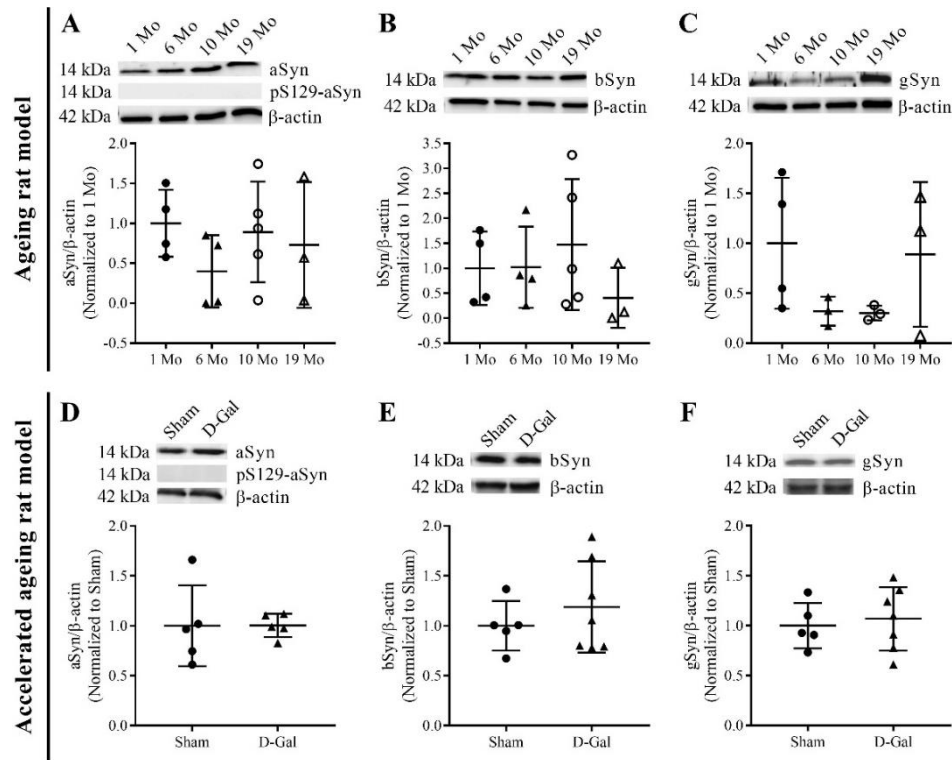


Figure 3.4. – Assessment of synuclein levels in ageing and accelerated ageing rats whole retina protein extracts. A) Western blot for the comparison of aSyn protein levels between 1, 6, 10 and 19 months old rats and detection of pS129-aSyn (upper panel) and the corresponding densitometry analysis (lower panel). B) Western blot for the comparison of bSyn protein levels between 1, 6, 10 and 19 months old rats (upper panel) and the corresponding densitometry analysis (lower panel). C) Western blot for the comparison of gSyn protein levels between 1, 6, 10 and 19 months old rats (upper panel) and the corresponding densitometry analysis (lower panel). D) Western blot for the comparison of aSyn protein levels between Sham and D-Gal rats (upper panel) and the corresponding densitometry analysis (lower panel). E) Western blot for the comparison of bSyn protein levels between Sham and D-Gal rats (upper panel) and the corresponding densitometry analysis (lower panel). F) Western blot for the comparison of gSyn protein levels between Sham and D-Gal rats (upper panel) and the corresponding densitometry analysis (lower panel). A representative image of the western blot is shown. All Western Blot data are presented as Mean ± SD.

Western blot analysis shows that aSyn seems not to be affected with ageing or accelerated ageing when comparing to 1 month old rats or Sham rats, respectively. Furthermore, pS129-aSyn protein levels were not detected both in ageing and accelerated ageing rats in the tested conditions (Fig. 3.4.A and D). Regarding bSyn there is no significant difference either with ageing when comparing to 1 month old rats or upon D-Gal treatment (Fig. 3.4.B and .E). Likewise, gSyn shows no difference with ageing nor with D-Gal administration, despite two decreasing tendencies of gSyn levels at the ages of 6 and 10 months old rats when comparing with 1 month old rats (Fig. 3.4.C and F).

In summary, none of the synucleins exhibited significant alterations in ageing rats and in D-Gal rats. However, some tendencies could become significant if the number of animals used for the western blot experiments could be increased.

3.5.2. Synucleins distribution profile in the retina of ageing and D-Gal rats

Making a whole retina protein extract accounts with the fact that the extract contains protein from the several existing retinal populations, and consequently numerous subpopulations (Kolb H. 2003). However, synucleins are not equally distributed by the several retinal layers, nor are they present in every retinal population (Surguchov A et al., 2001), which means that subtle changes could be occurring in specific retinal neurons that when making a whole retina protein extract become diluted.

Therefore, our aim was to check in the retina of the 1, 6, 10 and 19 months old rats, each synuclein distribution profile along the retinal layers by confocal microscopy, but also in Sham and D-Gal rats (Fig. 3.5.).

In addition, taking into account that different outcomes of the interaction between these proteins have been reported (Hashimoto M et al., 2001), (Tenreiro S et al., 2016), (Uversky VN et al., 2002), we assessed the colocalization between aSyn and bSyn and between aSyn and gSyn by confocal microscopy along the several retinal layers (Fig. 3.6. and 3.7.).

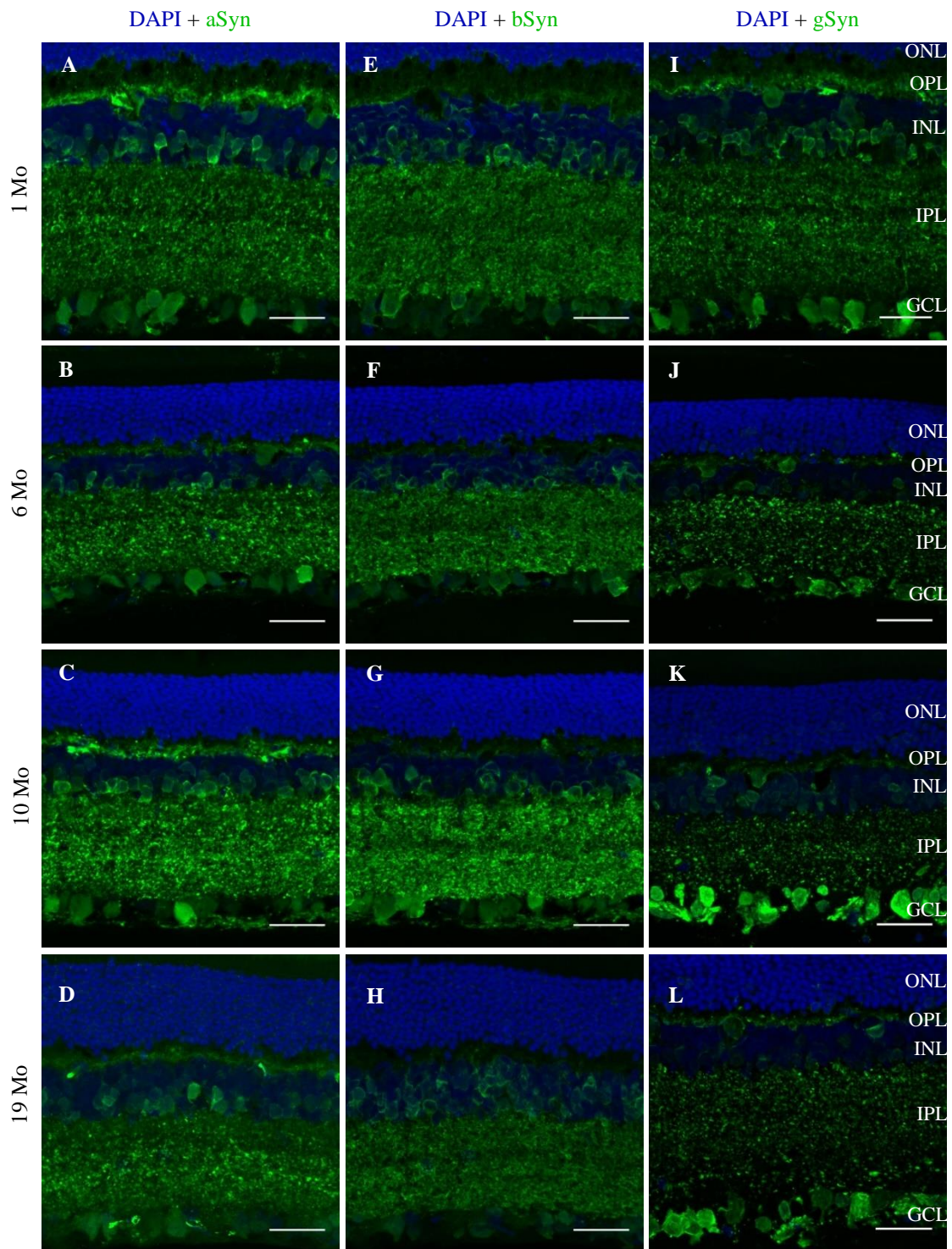


Figure 3.5. – Immunohistochemistry of the synuclein family distribution profile in the retina of 1, 6, 10 and 19 months old rats. A, B, C and D) aSyn distribution in the retina of 1, 6,10 and 19 months old rats, respectively. E, F, G and H) bSyn distribution in the retina of 1, 6,10 and 19 months old rats, respectively. I, J, K and L) gSyn distribution in the retina of 1, 6, 10 and 19 months old rats, respectively. N=3 for all ages. A representative image of central area of the retina is shown. Nucleus are stained with DAPI (blue) and aSyn, bSyn and gSyn stained with Alexa Fluor 488 GAR (Green). ONL, outer nuclear layer, OPL, outer plexiform layer, INL, inner nuclear layer, IPL, inner plexiform layer, GCL, ganglion cell layer. Maximum intensity projections obtained from confocal images obtained with a 40x objective. Scale bar = 30 μ m.

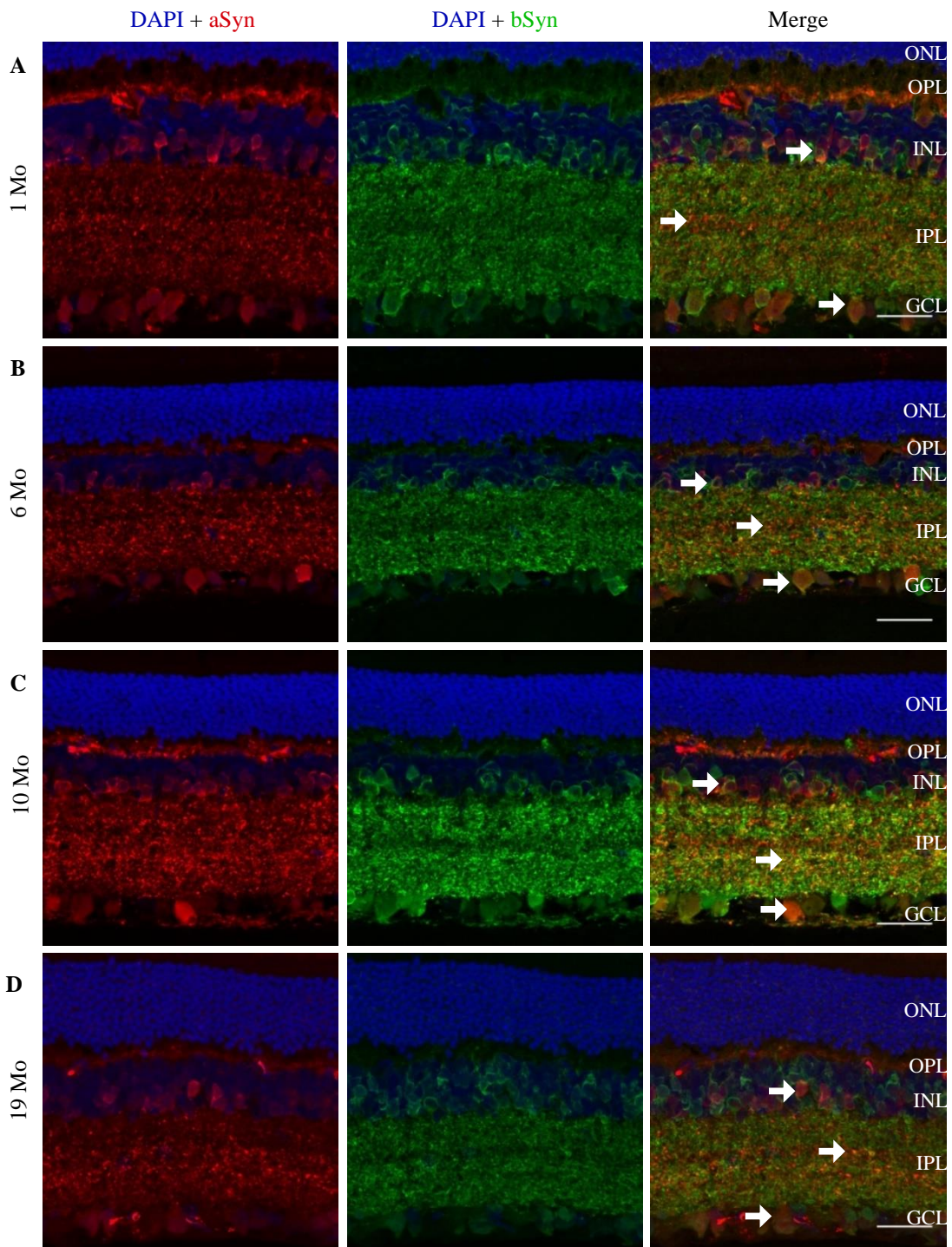


Figure 3.6. – Immunohistochemistry of the colocalization between aSyn and bSyn in the retina of 1, 6, 10 and 19 months old rats. A) Colocalization between aSyn and bSyn in 1 month old rats. B) Colocalization between aSyn and bSyn in 6 months old rats. C) Colocalization between aSyn and bSyn in 10 months old rats. D) Colocalization between aSyn and bSyn in 19 month old rats. N=3 for all ages. A representative image of central area of the retina is shown. Nucleus are stained with DAPI (blue), aSyn stained with Alexa Fluor 594 GAM (Red) and bSyn stained with Alexa Fluor 488 GAR (Green). ONL, outer nuclear layer, OPL, outer plexiform layer, INL, inner nuclear layer, IPL, inner plexiform layer, GCL, ganglion cell layer. Maximum intensity projections obtained from confocal images obtained with a 40x objective. Scale bar = 30 μ m.

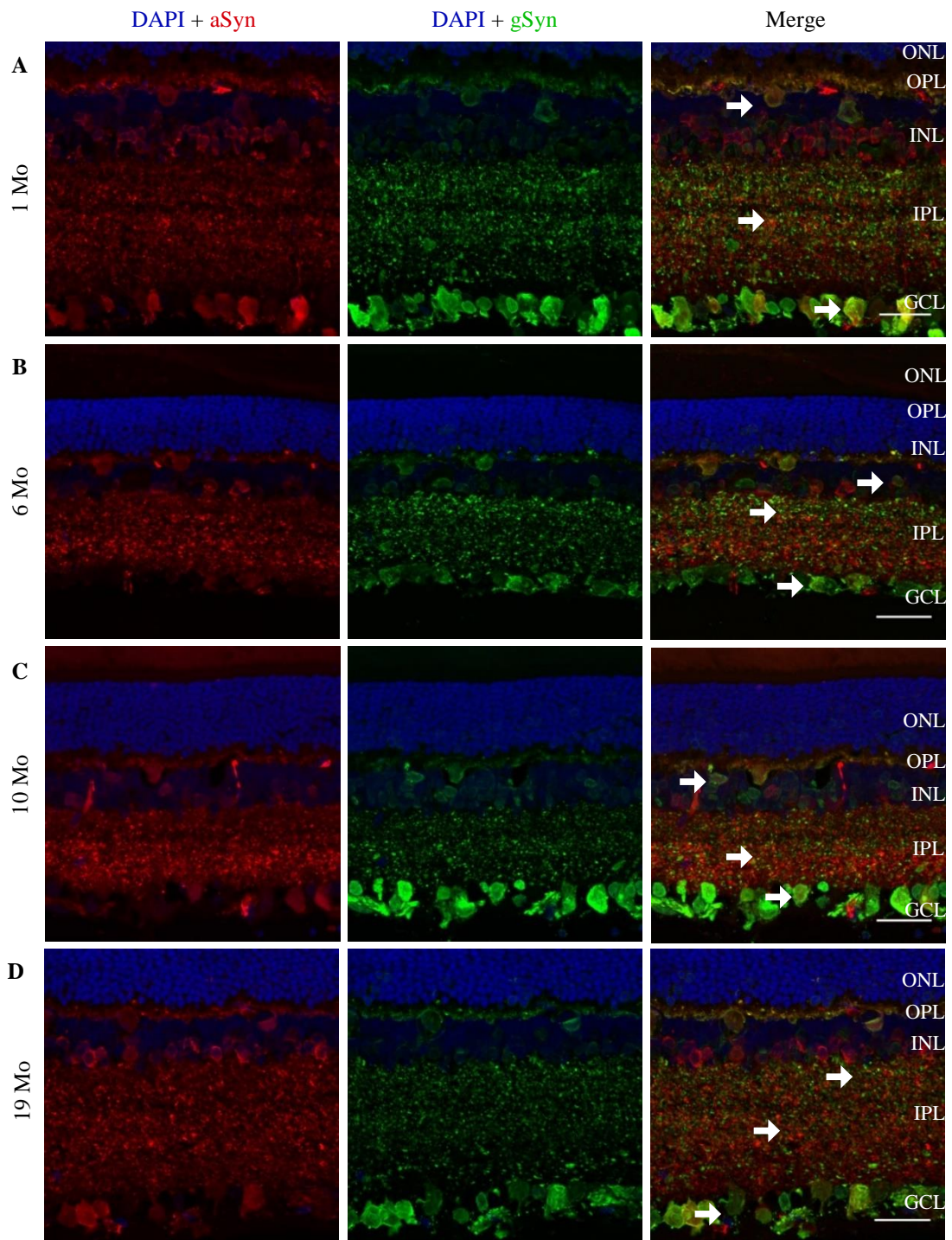


Figure 3.7. – Immunohistochemistry of the colocalization between aSyn and gSyn in the retina of 1, 6, 10 and 19 months old rats. A) Colocalization between aSyn and gSyn in 1 month old rats. B) Colocalization between aSyn and gSyn in 6 months old rats. C) Colocalization between aSyn and gSyn in 10 months old rats. D) Colocalization between aSyn and gSyn in 19 month old rats. N=3 for all ages. A representative image of central area of the retina is shown. Nucleus are stained with DAPI (blue), aSyn stained with Alexa Fluor 594 GAM (Red) and gSyn stained with Alexa Fluor 488 GAR (Green). ONL, outer nuclear layer, OPL, outer plexiform layer, INL, inner nuclear layer, IPL, inner plexiform layer, GCL, ganglion cell layer. Maximum intensity projections obtained from confocal images obtained with a 40x objective. Scale bar = 30 μ m.

Confocal microscopy revealed that aSyn is localized in the INL, IPL and GCL at all ages without any striking observable differences in comparison to 1 month old rats (Fig. 3.5.A, B, C and D). In the INL, aSyn seems to be preferentially present in the proximal region rather than in the distal, where horizontal cells usually rely (Kolb H, 2003).

Regarding bSyn, it is present in the INL, IPL and GCL of 1, 6, 10 and 19 months old rats retina, and no differences regarding their qualitative profile distribution was found when comparing to the younger rats (Fig. 3.5.E, F, G and H). In contrast to aSyn, the bSyn protein is widely present in the INL and does not stratify as aSyn.

Finally, gSyn is present in the same layers of the retina of these ageing rats as the other synucleins members and no striking differences were observed when comparing to 1 month old rats (Fig. 3.5.I, J, L and L). In the INL, gSyn has a scattered-like distribution similar to bSyn. Moreover, gSyn has the particularity of not being present in the IPL in the same proportion as the other synucleins.

Furthermore, there seems to be a mild stratification of the three synucleins in the IPL, evidenced by a lesser intensity in strata 3 (s3).

Concerning aSyn and bSyn colocalization, confocal microscopy revealed that these proteins colocalize in the INL, IPL and GCL at the ages of 1, 6, 10 and 19 months old, exhibiting no significant visual alterations in this profile upon ageing (Fig. 3.6.). The same observations were obtained for aSyn and gSyn colocalization in the retina of rats with the same age (Fig. 3.7.).

Afterwards, we addressed the synucleins distribution profile in the retina of Sham rats (rats with 6 months injected with Saline) and in age-match rats injected intraperitoneally with 250 mg/Kg of D-Gal for 6 weeks. Furthermore, we evaluated the colocalization between aSyn and bSyn and between aSyn and gSyn by confocal microscopy along the several retinal layers (Fig. 3.8., 3.9. and 3.10.).

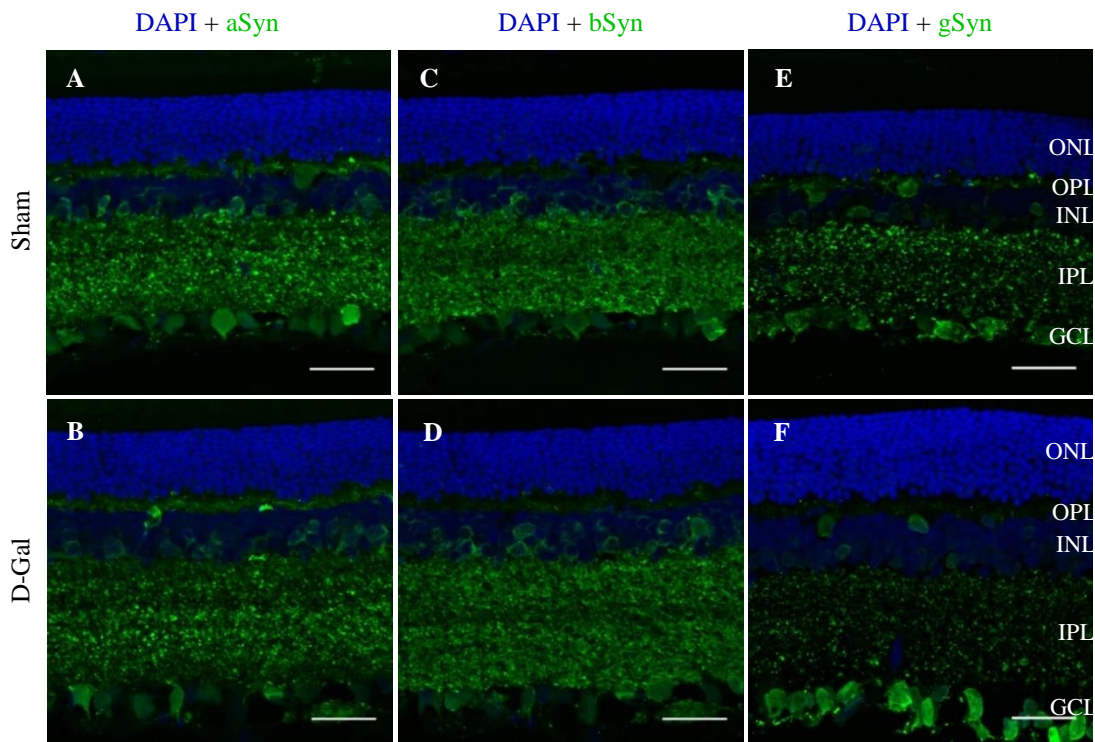


Figure 3.8. – Immunohistochemistry of the synuclein family distribution profile in the retina of Sham and D-Gal rats. A and B) aSyn distribution in the retina of Sham and D-Gal rats, respectively. C and D) bSyn distribution in the retina of Sham and D-Gal rats, respectively. E and F) gSyn distribution in the retina of 1, 6,10 and 19 months old rats, respectively. N=3 for all ages. A representative image of central area of the retina is shown. Nucleus are stained with DAPI (blue) and aSyn, bSyn and gSyn stained with Alexa Fluor 488 GAR (Green). ONL, outer nuclear layer, OPL, outer plexiform layer, INL, inner nuclear layer, IPL, inner plexiform layer, GCL, ganglion cell layer. Maximum intensity projections obtained from confocal images obtained with a 40x objective. Scale bar = 30 μ m.

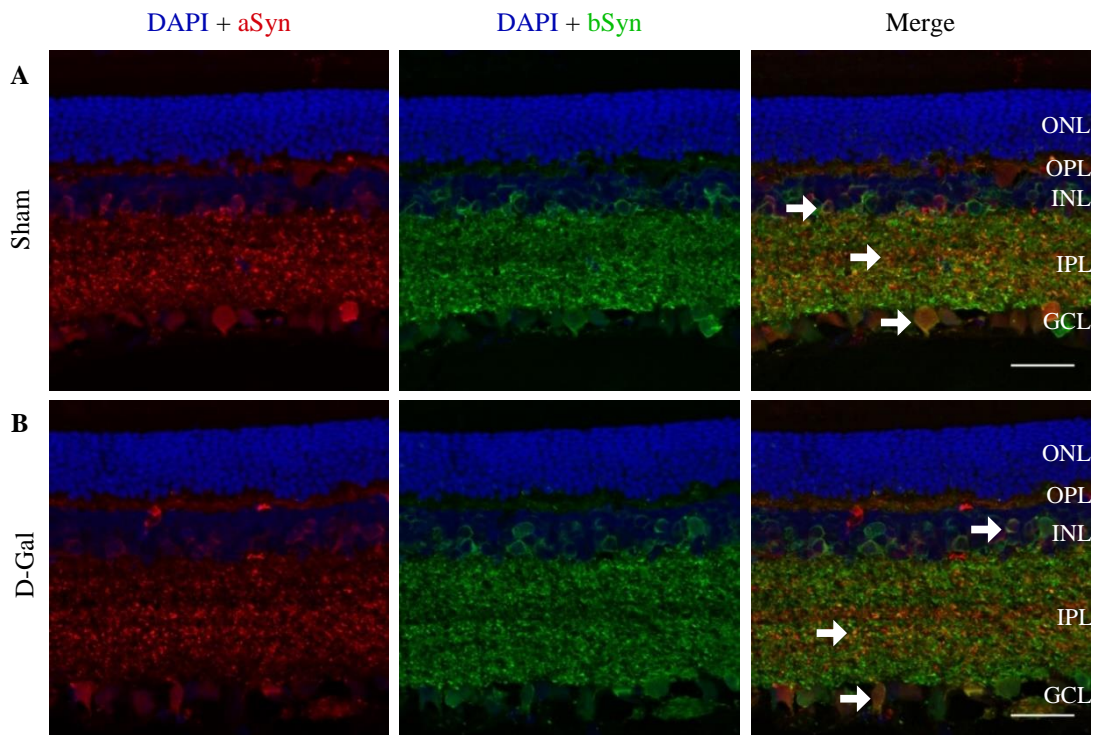


Figure 3.9. – Immunohistochemistry of the colocalization between aSyn and bSyn in the retina of Sham and D-Gal rats. A) Colocalization between aSyn and bSyn in Sham rats. B) Colocalization between aSyn and bSyn in D-Gal

rats. C) N=3 for all ages. A representative image of central area of the retina is shown. Nucleus are stained with DAPI (blue), aSyn stained with Alexa Fluor 594 GAM (Red) and bSyn stained with Alexa Fluor 488 GAR (Green). ONL, outer nuclear layer, OPL, outer plexiform layer, INL, inner nuclear layer, IPL, inner plexiform layer, GCL, ganglion cell layer. Maximum intensity projections obtained from confocal images obtained with a 40x objective. Scale bar = 30 μ m.

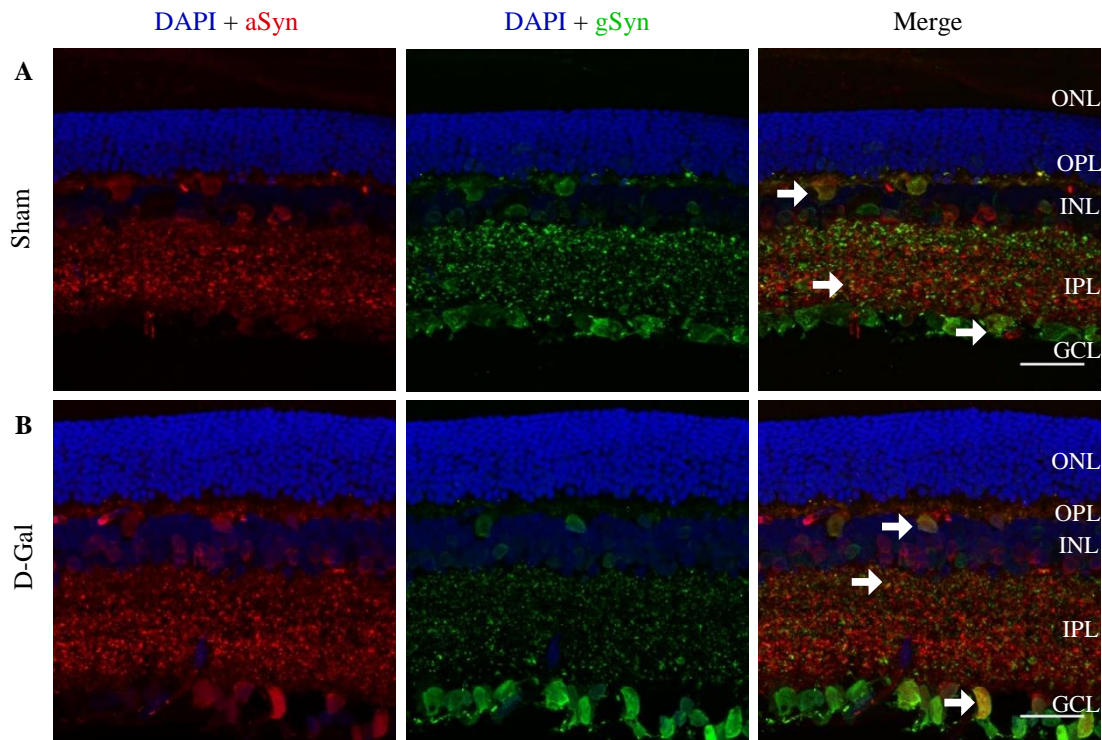


Figure 3.10. – Immunohistochemistry of the colocalization between aSyn and gSyn in the retina of Sham and D-Gal rats. A) Colocalization between aSyn and gSyn in Sham rats. B) Colocalization between aSyn and gSyn in D-Gal rats. N=3 for all ages. A representative image of central area of the retina is shown. Nucleus are stained with DAPI (blue), aSyn stained with Alexa Fluor 594 GAM (Red) and gSyn stained with Alexa Fluor 488 GAR (Green). ONL, outer nuclear layer, OPL, outer plexiform layer, INL, inner nuclear layer, IPL, inner plexiform layer, GCL, ganglion cell layer. Maximum intensity projections obtained from confocal images obtained with a 40x objective. Scale bar = 30 μ m.

Confocal microscopy revealed that aSyn is localized in the INL, IPL and GCL of Sham and D-Gal rats without any striking observable differences between the animals (Fig. 3.8.A and B). In the INL, aSyn seems to be preferentially present in the proximal region rather than the distal where horizontal cells usually rely (Kolb H, 2003).

Regarding bSyn, it is present in the INL, IPL and GCL of Sham and D-Gal rats and no differences regarding their qualitative profile distribution were found upon D-Gal administration. (Fig. 3.8.C and D). In contrast to aSyn, the bSyn protein is widely present in the INL and does not stratify as aSyn.

Finally, gSyn is present in the same layers of the retina of Sham and D-Gal rats and no striking differences were observed when comparing them (Fig. 3.8.E and F). In

the INL has a scattered-like distribution similar to bSyn. Moreover, gSyn has the particularity of not being in the present in the IPL in the same proportion as the other synucleins.

Furthermore, there seems to be a mild stratification of the three synucleins in the IPL, evidenced by a lesser intensity in strata 3 (s3).

Concerning aSyn and bSyn colocalization, confocal microscopy revealed that these proteins colocalize in the INL, IPL and GCL in Sham and D-Gal rats retina, exhibiting no significant visual alterations in this profile upon an accelerating ageing insult (Fig. 3.9.). The same observations were obtained for aSyn and gSyn colocalization in the retina of these rats (Fig. 3.10.).

Proceeding to quantitative analysis of the confocal images, synucleins counting in the GCL, colocalization quantifications in the IPL and GCL, and intensity measurements in the IPL were performed in the retina of ageing rats and accelerated ageing rats (Fig. 3.11.).

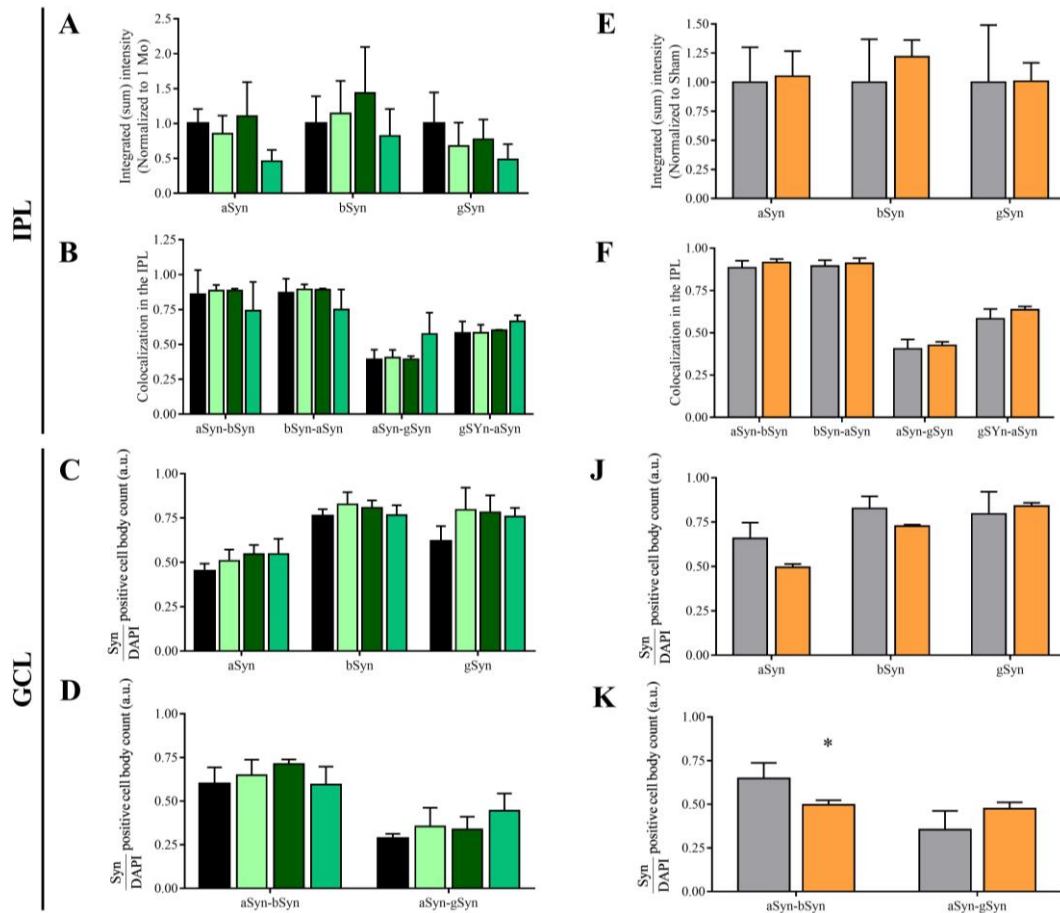


Figure 3.11. – Quantification of the synucleins distribution in the IPL and GCL in ageing and accelerated ageing rats. N=3 for 1, 6, 10 and 19 months old rats and for Sham and D-Gal rats. A) Quantification of the integrated (sum) intensity of aSyn and bSyn in the IPL of 1, 6, 10 and 19 months old rats. B) Mander's split coefficient gives a measure of the colocalization between the synucleins in the IPL of 1, 6, 10 and 19 months old rats. C) Quantification of aSyn-, bSyn- and gSyn-positive cell body per DAPI-positive cell body in the GCL of 1, 6, 10 and 19 months old rats. D) Evaluation of aSyn-bSyn and aSyn-gSyn colocalization levels per DAPI-positive cell body in the GCL of 1, 6, 10 and 19 months old rats. E) Quantification of the integrated (sum) intensity of aSyn, bSyn and gSyn in the IPL of Sham and D-Gal rats. F) Mander's split coefficient gives a measure of the colocalization between the synucleins in the IPL of Sham and D-Gal rats. G) Quantification of aSyn-, bSyn- and gSyn-positive cell body per DAPI-positive cell body in the GCL of Sham and D-Gal rats. H) Evaluation of aSyn-bSyn and aSyn-gSyn colocalization per DAPI-positive cell body in the GCL of Sham and D-Gal rats. All data are presented as Mean \pm SD. * $p < 0.05$ D-Gal compared to Sham; T-test.

In regard to the IPL, the integrated (sum) intensity of each synuclein in 6, 10 and 19 months old rats does not differ from rats with 1 month old, although at 19 months old there seems to be a decreasing tendency of aSyn (Fig. 3.11.A). Likewise, no difference was observed between Sham and D-Gal rats (Fig. 3.11.E). Afterwards, the colocalizations aSyn-bSyn, bSyn-aSyn, aSyn-gSyn and gSyn-aSyn in the IPL of 1, 6, 10, 19 months old rats were assessed and no significant differences were obtained when comparing to 1 month old rats (Fig. 3.11.B). However, it is possible to observe that throughout all ages

aSyn preferentially colocalizes with bSyn in the IPL rather than with gSyn. The same observations can be withdrawn in Sham and D-Gal rats retina (Fig. 3.11.F).

Concerning the GCL, synuclein-positive cell bodies were counted per number of stained nuclei, and no striking variations were found between 6, 10, and 19 months old rats and 1 month old rats (Fig. 3.11.C). In addition, it seems that throughout all ages aSyn is the synuclein least present in this layer, while bSyn and gSyn are at higher but similar levels. The same observations can be made for the comparison between Sham and D-Gal rats (Fig. 3.11.G). Furthermore, the colocalizations aSyn-bSyn and aSyn-gSyn were examined in the GCL and no differences were obtained between 6, 10 and 19 months old rats and 1 month old rats (Fig 3.11.D). In contrast, the same colocalizations were tested between D-Gal and Sham rats and a reduced colocalization between aSyn and bSyn in the GCL of D-Gal rats was obtained (0.497 ± 0.0258 vs 0.6483 ± 0.08852) (Fig. 3.11.H).

The present results are in agreement with the obtained unaltered synuclein protein levels in the retina of ageing and accelerated ageing rats (Fig. 3.4.). In fact, this data further discriminates a decreased colocalization between aSyn and bSyn in the GCL of D-Gal rats, which could be a consequence of the mild decreasing tendency in bSyn-positive cell bodies in this retinal layer of D-Gal rats. However, once more is important to mention that some tendencies could become significant if the number of animals used in the experiments could be increased.

3.6. Synaptic markers in the retina of ageing rat models

As electroretinographic studies in ageing animals reveal decreased amplitudes of a- and b-waves (Birch DG and Anderson JL 1992), it is possible that this is correlated with an impaired integrity of synaptic function. Thus, our approach was to assess by western blot the levels of proteins whose role is related with synaptic function such as the v-SNAREs Synaptophysin and Rab3a, the t-SNAREs SNAP-25 and Syntaxin 1A, PSD95 and TH in the retina of 1, 6, 10 and 19 months old rats and Sham and D-gal rats (Fig. 3.12.).

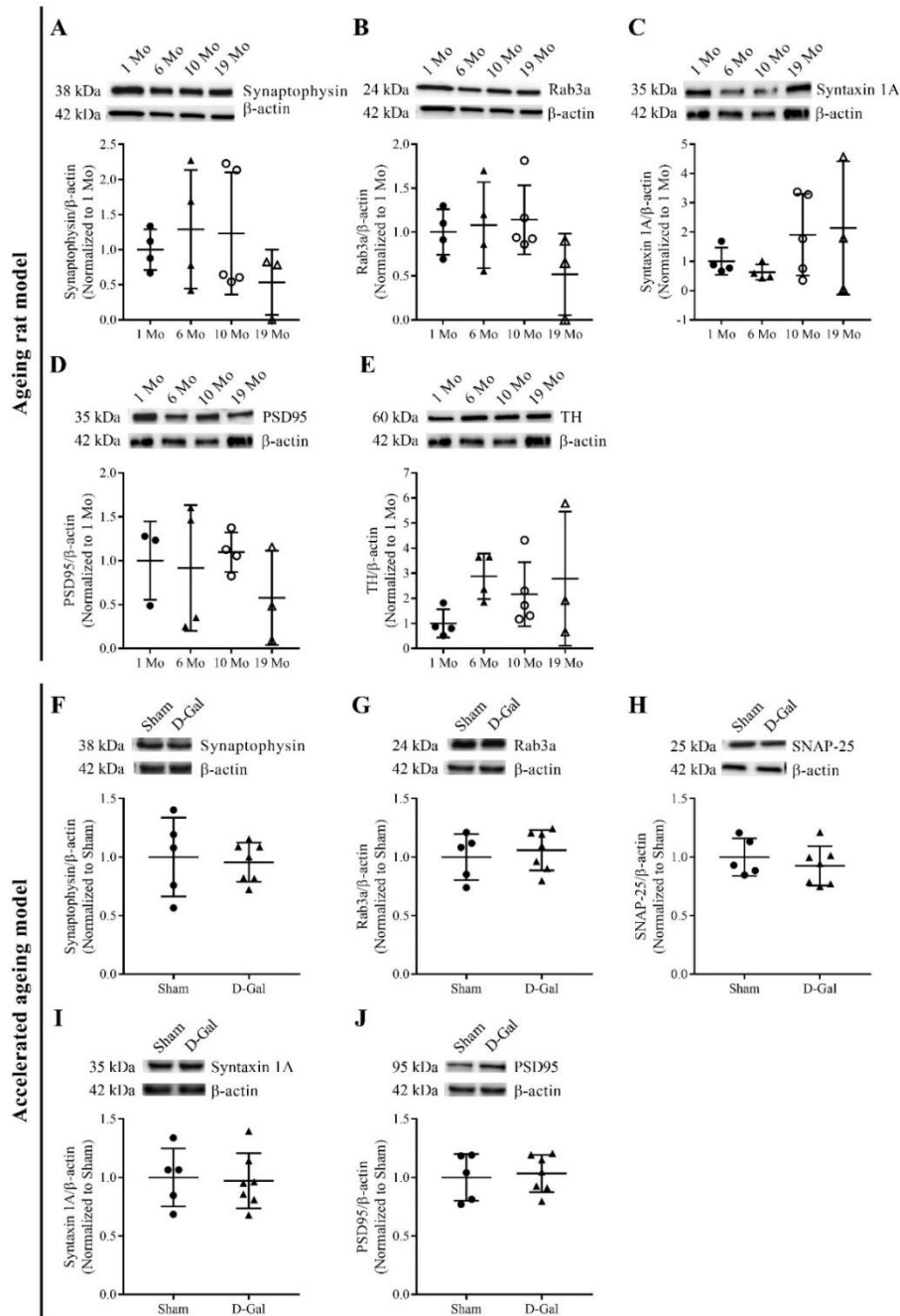


Figure 3.12. – Assessment of synaptic markers protein in ageing and accelerated ageing rats whole retina protein extracts. A) Western blot for the comparison of Synaptophysin protein levels between 1, 6, 10 and 19 months old rats (upper panel) and the corresponding densitometry analysis (lower panel). B) Western blot for the comparison of Rab3a protein levels between 1, 6, 10 and 19 months old rats (upper panel) and the corresponding densitometry analysis (lower panel). C) Western blot for the comparison of Syntaxin 1A protein levels between 1, 6, 10 and 19 months old rats (upper panel) and the corresponding densitometry analysis (lower panel). D) Western blot for the comparison of PSD95 protein levels between 1, 6, 10 and 19 months old rats (upper panel) and the corresponding densitometry analysis (lower panel). E) Western blot for the comparison of TH protein levels between 1, 6, 10 and 19 months old rats (upper panel) and the corresponding densitometry analysis (lower panel). F) Western blot for the comparison of Synaptophysin protein levels between Sham and D-Gal rats (upper panel) and the corresponding densitometry analysis (lower panel). G) Western blot for the comparison of Rab3a protein levels between Sham and D-Gal rats (upper panel) and the corresponding densitometry analysis (lower panel). H) Western blot for the comparison of SNAP-25 protein levels between Sham and D-Gal rats. I) Western blot for the comparison of Syntaxin 1A protein levels between Sham and D-Gal rats (upper panel) and the corresponding densitometry analysis (lower panel). J) Western blot for the comparison of PSD95 protein levels between Sham and D-Gal rats (upper panel) and the corresponding densitometry analysis (lower panel). A representative image of the western blot is shown. All Western Blot data are presented as Mean \pm SD.

Regarding the v-SNAREs Synaptophysin (Fig. 3.12.A and F) and Rab3a proteins (Fig. 3.12.B and G) there is no significant difference neither throughout all the ages of 6, 10 and 19 months old when comparing to 1 month old rats, neither between Sham and D-Gal rats. Likewise the t-SNARE Syntaxin 1A protein levels show no statistical difference between 6, 10 and 19 months old rats and 1 month old, nor do Sham and D-Gal rats (Fig. 3.12.C and I). SNAP-25, another v-SNARE, was only tested for Sham and D-Gal rats and similarly there are no striking differences between Sham and D-Gal rats (Fig. 3.12.H).

Concerning the protein levels of PSD95, the results obtained do not exhibit any variation in the protein levels in all ages when comparing to 1 month old rats and between Sham and D-Gal rats (Fig. 3.12.D and J).

Lastly, TH protein levels were only tested for ageing rats and there seems to be no evident alterations when comparing 6, 10 and 19 months old rats with 1 month old rats, although there could be an increasing tendency in 6 months old rats (Fig. 3.12.E).

On the whole, the levels of synaptic markers seem not to be affected with ageing neither with D-Gal administration. Furthermore, decreased dopamine activity was reported in the ageing retina (Hankins MW, 2000), however, the obtained results, aside from not showing any significant difference, only exhibit a mild increasing tendency and not any decreasing effect.

3.7. Cell survival markers in the retina of ageing rat models

3.7.1. Cell survival marker levels in the retina of ageing and D-Gal rats

Previous reports demonstrated the loss of thickness in the INL and neurodegeneration in the ONL (Nadal-Nicolás F et al., 2018). Hence, it was assessed by western blot the levels of cell survival markers such as the transcription factor NF- κ B, MLKL and pMLKL in the retina of 1, 6, 10 and 19 months old rats and Sham and D-Gal rats. STAT3 and its activated form pY705-STAT3, which are markers for cell proliferation, GFAP, a marker of inflammation, and caspase 3 protein levels were also assessed by western blot for the accelerated ageing rat model (Fig. 3.13.).

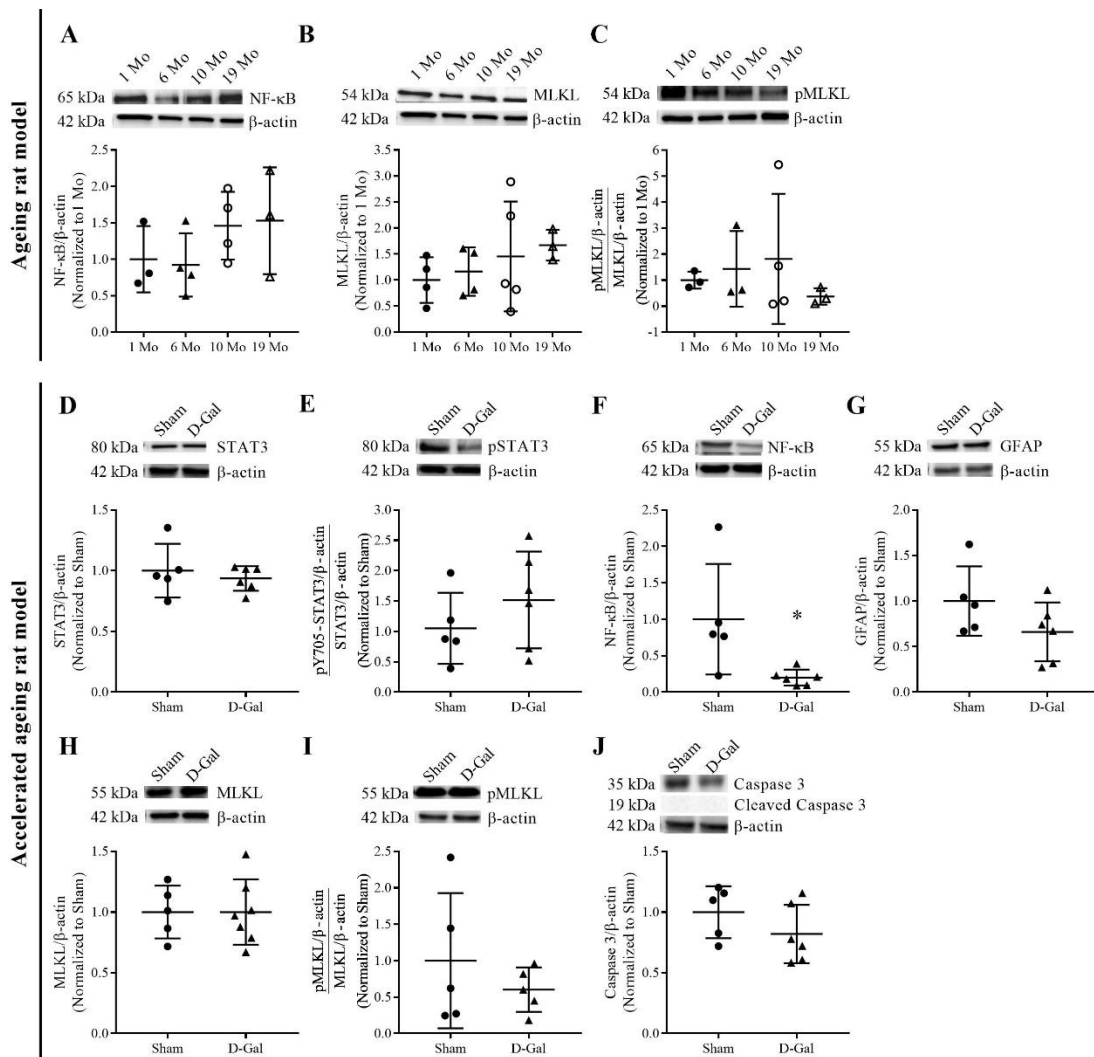


Figure 3.13. – Assessment of cell survival and inflammation markers levels in ageing and accelerated ageing rats whole retina protein extracts. A) Western blot for the comparison of NF-κB levels between 1, 6, 10 and 19 months old rats (upper panel) and the corresponding densitometry analysis (lower panel). B) Western blot for the comparison of MLKL protein levels between 1, 6, 10 and 19 months old rats (upper panel) and the corresponding densitometry analysis (lower panel). C) Western blot for the comparison of the ratio pMLKL/MLKL between 1, 6, 10 and 19 months old rats (upper panel) and the corresponding densitometry analysis (lower panel). D) Western blot for the comparison of STAT3 protein levels between Sham and D-Gal rats (upper panel) and the corresponding densitometry analysis (lower panel). E) Western blot for the comparison of the ratio pY705-STAT3/STAT3 between Sham and D-Gal rats (upper panel) and the corresponding densitometry analysis (lower panel). F) Western blot for the comparison of NF-κB protein levels between Sham and D-Gal rats (upper panel) and the corresponding densitometry analysis (lower panel). G) Western blot for the comparison of GFAP protein levels between Sham and D-Gal rats (upper panel) and the corresponding densitometry analysis (lower panel). H) Western blot for the comparison of MLKL protein levels between Sham and D-Gal rats (upper panel) and the corresponding densitometry analysis (lower panel). I) Western blot for the comparison of the ratio pMLKL/MLKL between Sham and D-Gal rats (upper panel) and the corresponding densitometry analysis (lower panel). J) Western blot for the comparison of Caspase 3 protein levels between Sham and D-Gal rats and detection of cleaved Caspase 3 (upper panel) and the corresponding densitometry analysis (lower panel). A representative image of the western blot is shown. All Western Blot data are presented as Mean ± SD. * $p < 0.05$ D-Gal compared to Sham; T-test.

Regarding NF-κB protein levels, the western blot quantification results show no difference between 6, 10 and 19 months old rats and 1 months old rats (Fig. 3.13.A). In contrast, D-Gal rats retina exhibit decreased NF-κB protein levels when comparing with

Sham rats (0.1988 ± 0.1095 vs 1.000 ± 0.7583) (Fig. 3.13.F). This result does not necessarily point to a decreased cell death or inflammation because only the confirmation of the subcellular localization of NF- κ B inside the nucleus would point to the activation of several pathways related with cell death and inflammation (Lawrence T, 2009). These reduced protein levels could be merely due to turnover aspects such as gene downregulation or increased clearance and cannot be correlated with protein activity.

Concerning MLKL protein levels, there are no striking differences between all the ages of 1, 6, 10 and 19 months neither between Sham and D-Gal rats (Fig. 3.13.B and H). Conversely, statistics reveal that the proportion of pMLKL over total MLKL protein levels does not vary with ageing neither with D-Gal administration in rats (Fig. 3.13.C and I).

In relation to STAT3 protein levels and to the ratio pY705-STAT3/STAT3, there are no differences when comparing D-Gal to Sham rats (Fig. 3.13.D and E).

The protein levels of GFAP, an astrogliosis marker, seem not to be affected by D-Gal administration (Fig. 3.13.G). Likewise, Caspase 3 levels did not suffer any change between Sham and D-Gal rats, nor cleaved caspase 3 levels were detected in the tested conditions (Fig. 3.13.J).

Altogether, the only observed difference in the tested conditions was a reduction in the NF- κ B levels in D-Gal rats retina.

3.7.2. Retinal layers integrity in ageing and D-Gal rats

Previous reports demonstrated that thinning of the retinal layers may indicate neurodegeneration (Alamouti BF et al., 2003). Therefore, by measuring the thickness of the OPL, INL and IPL in maximum intensity projections from confocal images one can understand whether the integrity of the retina of ageing animals and accelerated ageing animals is being compromised or not. It was not possible to measure the GCL thickness as there are no key visual indicators that would help limit the area of this layer. Therefore, the number of cell bodies per length of GCL was chosen as a solution, since it can give a hint of the existence of neurotoxic or neuroprotective events, depending on the outcome (Fig. 3.14.).

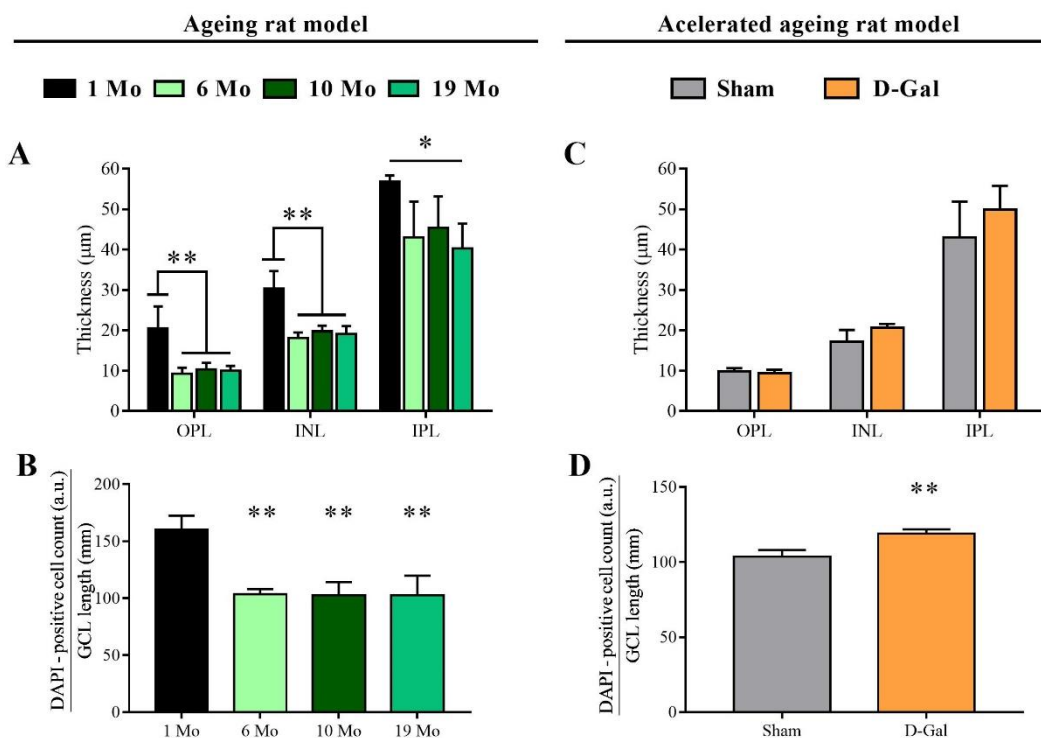


Figure 3.14. – Quantification of retinal layers' thickness and GCL cell density in ageing and accelerated ageing. A) Comparison of the thickness of the OPL, INL and IPL between 1, 6, 10 and 19 months old rats. B) GCL cell density comparison between 1, 6, 10 and 19 months old rats. C) Evaluation of the thickness of the OPL, INL and IPL between Sham and D-Gal rats. D) GCL cell density comparison between Sham and D-Gal rats. All Western Blot data are presented as Mean \pm SD. Rats with 6, 10 and 19 months old are compared with 1 month old rats with a one-way ANOVA followed by a Dunnett's Test. D-Gal rats are compared with Sham rats with T-test. * $p < 0.05$ 19 Mo compared to 1 Mo, ** $p < 0.01$ 6 Mo, 10 Mo and 19 Mo compared to 1 Mo, ** $p < 0.01$ D-Gal compared to Sham.

The results obtained for the OPL and INL show that in rats at the ages of 6 months (9.216 ± 1.53 vs 20.43 ± 5.524 ; 18.14 ± 1.363 vs 30.28 ± 4.405), 10 months (10.37 ± 1.614 vs 20.43 ± 5.524 ; 19.72 ± 1.46 vs 30.28 ± 4.405) and 19 months (9.918 ± 1.286 vs 20.43 ± 5.524 ; 19.01 ± 2.022 vs 30.28 ± 4.405) in comparison to 1 month old rats there is a decreased thickness of these two layers (Fig. 3.14.A). In the IPL, there is only a significant reduction of the thickness at 19 months old in rats when comparing with 1 month old rats (40.33 ± 6.057 vs 56.71 ± 1.653) (Fig. 3.14.A). In addition, cell density in the GCL also is significantly reduced in 6 months (103.6 ± 4.362 vs 159.8 ± 12.61), 10 months (102.7 ± 11.45 vs 159.8 ± 12.61) and 19 months old rats (102.5 ± 17.34 vs 159.8 ± 12.61) when compared to 1 month old rats (Fig. 3.14.B).

All these retinal layers are differently affected when comparing 6, 10 and 19 months old rats with 1 month old rats. These changes may be in accordance with previous reports on INL and GCL lack of integrity upon ageing (Nadal-Nicolás F et al., 2018), (Cano J et al., 1986). On the other hand, the size of the retina increases linearly with age

and body weight. This continuous growth leads to a proportional retinal thinning and cell density reduction, as previously reported for albino rats (Braekevelt CR and Hollenberg MJ, 1970). Indeed, after the 6 months of age no variation occurs in these layers, which could resemble more a maturing effect on the retina rather than an ageing effect. Another aspect to highlight, is the fact that only at 19 months old there is a significant reduction in the thickness of the IPL when comparing with 1 month old rats. If one considers that the alterations observed in the INL and GCL are result of neurodegeneration events, then this reduction in the thickness of this neuropil that only happens at 19 months old is not preceding the cell body loss and is not in agreement with the higher susceptibility of synapses (Wishart TM et al., 2018). However, if we consider that there is a maturing effect in the INL and GCL, then the thickness reduction in the IPL of 19 month rats may possibly be anticipating cell body loss in the retina of older albino rats.

The same quantifications were done in Sham and D-Gal rats and it seems that the OPL, INL and IPL are not affected upon D-Gal treatment regarding Sham rats (Fig. 3.14.C). However, D-Gal rats seem to have a greater cell density in the GCL when comparing with Sham rats (119 ± 2.887 vs 103.6 ± 4.362) (Fig. 3.14.D). This result fails to be in accordance with the reported accelerated ageing in this model, as the ageing retina has been described to have fewer RGCs (Cano J et al., 1986), therefore perhaps D-Gal administration prevents the loss of RGCs.

Summing up, most of the alterations are decreased thickness or cell density of the retinal layers in the ageing rat model, which the D-Gal administration was not able to reproduce, but instead exhibited increased GCL cell density.

3.8. Body weight and glycaemic characterization of T2DM animal models

Before one can proceed with any evaluations in the diabetic animal models used in the present work, the NCD and HFD mice and Lean and ZDF rats, it was important to ensure that these animals exhibit the overweight and hyperglycaemic features that are characteristic of these T2DM animal models (Winzell MS and, Ahre B, 2044), (Peterson RG et al., 1990).

Body weight and blood glucose measurements revealed to be increased in HFD mice in comparison to NCD mice (41.38 ± 3.301 g vs 28.37 ± 1.759 g; 136 ± 30.15 mg/dL vs 93.17 ± 19.72 mg/dL) (See Sup. Fig. 2). Likewise, the same measurements are increased in ZDF rats in comparison to Lean rats (487.3 ± 35.68 g vs 347.7 ± 27.53 g; 203.8 ± 102.1 mg/dL vs 81 ± 6.633 mg/dL) (See Sup. Fig. 3).

Although, the NCD and HFD mouse model were initially reported to respectively reach blood glucose levels of 169 mg/dL and 240 mg/dL (Surwit RD et al., 1988), this mice population does not show the same values. This difference may well be due to genetic background influence, the duration of the diet, the diet content and other factors. Nevertheless, this mice population reveals clear obesity and higher glycaemia, which potentially point to T2DM.

Regarding the ZDF rat model, these animals are reported to have 400 to 500 mg/dL of glucose in the blood (Schmidt RE et al., 2003), which are not in agreement with the present ZDF rat population (203.8 ± 102.1 mg/dL). This discrepancy may result as well from genetic background and microbiota influence. However, the ZDF rat population shows overweight and a higher glycaemia that, altogether, point to T2DM.

3.9. The synucleins family in the retina of T2DM animal models

3.9.1. Synucleins levels in whole retina extracts of HFD mice and ZDF rats

In the diabetic cellular environment there is mitochondrial dysfunction, oxidative stress, ER stress and others. These are some of the several molecular mechanisms by which synucleins toxicity may be triggered (Wales P et al, 2013). Furthermore, the typical hyperglycaemia in diabetes is accompanied by increased AGEs levels that promote synucleins glycation, hence enhancing their ability to aggregate and have neurotoxic effects (Miranda MV and Outeiro TF, 2010). Therefore, we next assessed the synucleins levels, including pS129-aSyn, by western blot in whole retina proteins extracts in NCD and HFD mice and in Lean and ZDF rats (Fig. 3.15.).

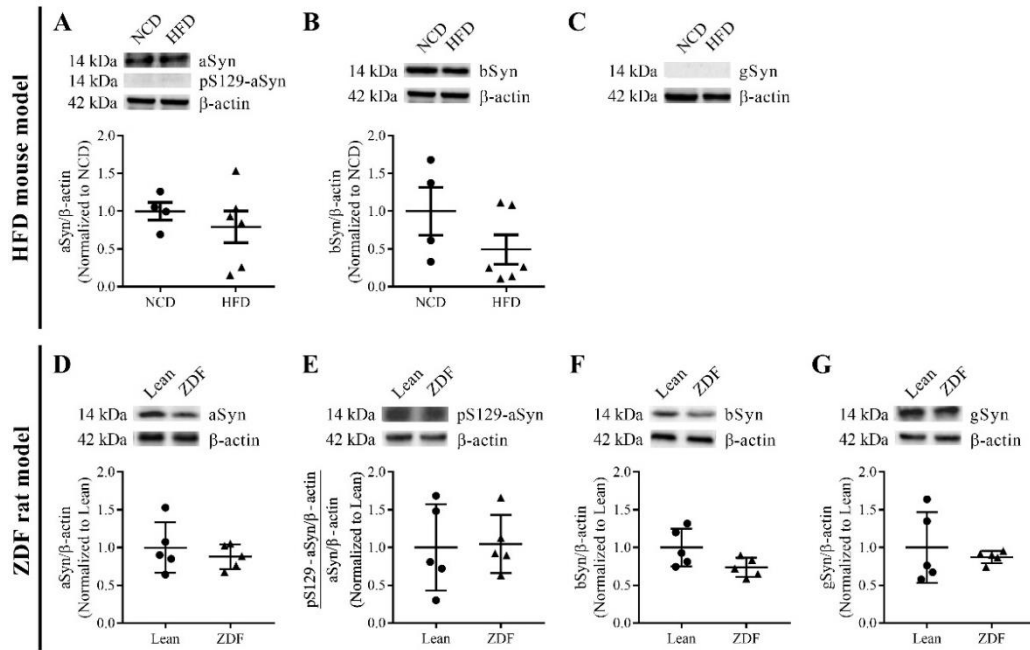


Figure 3.15. – Assessment of synucleins levels in HFD mice and ZDF rats whole retina protein extracts. A) Western blot for the comparison of aSyn protein levels between NCD and HFD mice and detection of pS129-aSyn (upper panel) and the corresponding densitometry analysis (lower panel). B) Western blot for the comparison of bSyn protein levels between NCD and HFD mice (upper panel) and the corresponding densitometry analysis (lower panel). C) Western blot for the detection of gSyn protein levels in NCD and HFD mice (upper panel) and the corresponding densitometry analysis (lower panel). D) Western blot for the comparison of aSyn protein levels between Lean and ZDF rats (upper panel) and the corresponding densitometry analysis (lower panel). E) Western blot for the comparison of the ratio pS129-aSyn over total aSyn protein levels between Lean and ZDF rats (upper panel) and the corresponding densitometry analysis (lower panel). F) Western blot for the comparison of bSyn protein levels between Lean and ZDF rats (upper panel) and the corresponding densitometry analysis (lower panel). G) Western blot for the comparison of gSyn protein levels between Lean and ZDF rats (upper panel) and the corresponding densitometry analysis (lower panel). A representative image of the western blot is shown. All Western Blot data are presented as Mean \pm SD.

The results obtained show that aSyn protein levels are not affected neither in HFD mice and ZDF rats when comparing to NCD mice and Lean rats, respectively (Fig. 3.15.A and D). In regard to pS129-aSyn protein levels, no detection in the tested conditions was obtained in NCD and HFD mice. In the T2DM rat model, pS129-aSyn was detected and the proportion of pS129-aSyn over total aSyn protein levels is not affected in T2DM (Fig. 3.15.E).

Concerning bSyn there is no significant difference either in HFD mice and ZDF rats when comparing to HFD mice and Lean rats, respectively (Fig. 3.15.B and F). Although, there seems to be a mild decreasing tendency in both T2DM animal models.

In regard to gSyn, it was not detected in the tested conditions in the retina of NCD and HFD mice (Fig. 3.15.C). In contrast, in Lean and ZDF rats gSyn was detected but western blot analysis showed no significant differences in the protein levels between them (Fig. 3.15.G).

In summary, none of the synucleins protein levels were affected by T2DM. This result is contrasting with an another study that demonstrated that in the retina of 12 months old *Ins2^{Akita}* mice, an animal model of T1DM, there is higher levels of aSyn when comparing with age-matched wild type mice (Santos G., 2017). On the other hand, bSyn exhibited mild decreasing tendencies in both T2DM animal models, which may be related to the reported reduced bSyn levels in 9 months old *Ins2^{Akita}* mice when compared with age-matched wild type mice (Santos G, 2017). Therefore, perhaps only a more severe diabetic environment can trigger these alterations.

3.9.2. Synucleins distribution profile in the retina of HFD mice and ZDF rats

Regarding the previously pointed inconveniences of making a whole retina protein, we aimed to check in the retina of the HFD mouse model and ZDF rat model, each synuclein distribution profile along the retinal layers by confocal microscopy (Fig. 3.16.). Furthermore, we also assessed the colocalization between aSyn and bSyn and between aSyn and gSyn by confocal microscopy along the several retinal layers in both models (Fig. 3.17. and 3.18.).

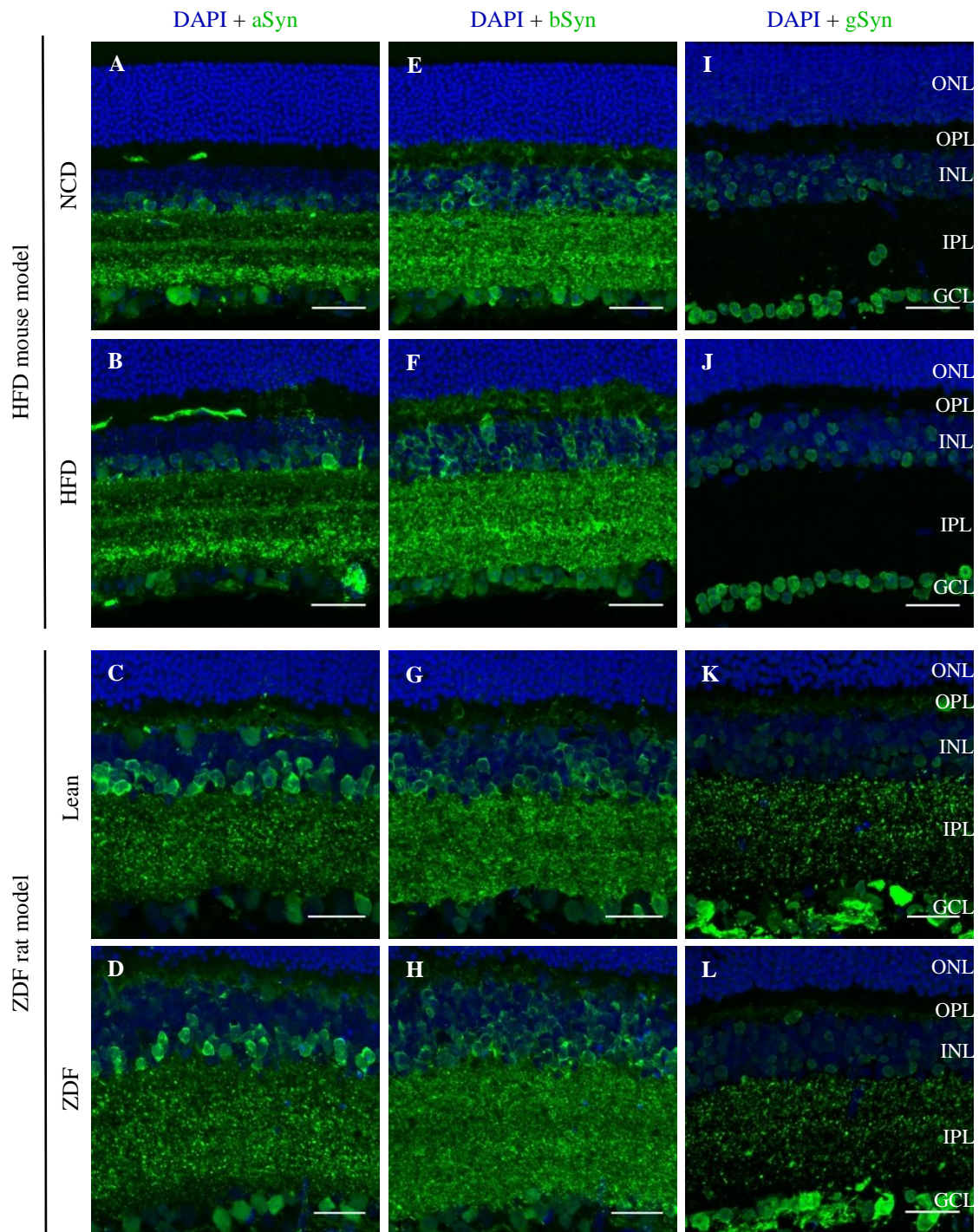


Figure 3.16. – Synuclein family distribution profile in the retina of NCD and HFD mice and Lean and ZDF rats. A and B) aSyn distribution in the retina of NCD and HFD mice, respectively. C and D) aSyn distribution in the retina of Lean and ZDF rats, respectively. E and F) bSyn distribution in the retina of NCD and HFD mice, respectively. G and H) bSyn distribution in the retina of Lean and ZDF rats, respectively. I and J) gSyn distribution in the retina of NCD and HFD mice, respectively. K and L) gSyn distribution in the retina of Lean and ZDF rats, respectively. N=3 for both T2DM animal models. A representative image of central area of the retina is shown. Nucleus are stained with DAPI (blue) and aSyn, bSyn and gSyn stained with Alexa Fluor 488 GAR (Green). ONL, outer nuclear layer, OPL, outer plexiform layer, INL, inner nuclear layer, IPL, inner plexiform layer, GCL, ganglion cell layer. Maximum intensity projections obtained from confocal images obtained with a 40x objective. Scale bar = 30 μ m.

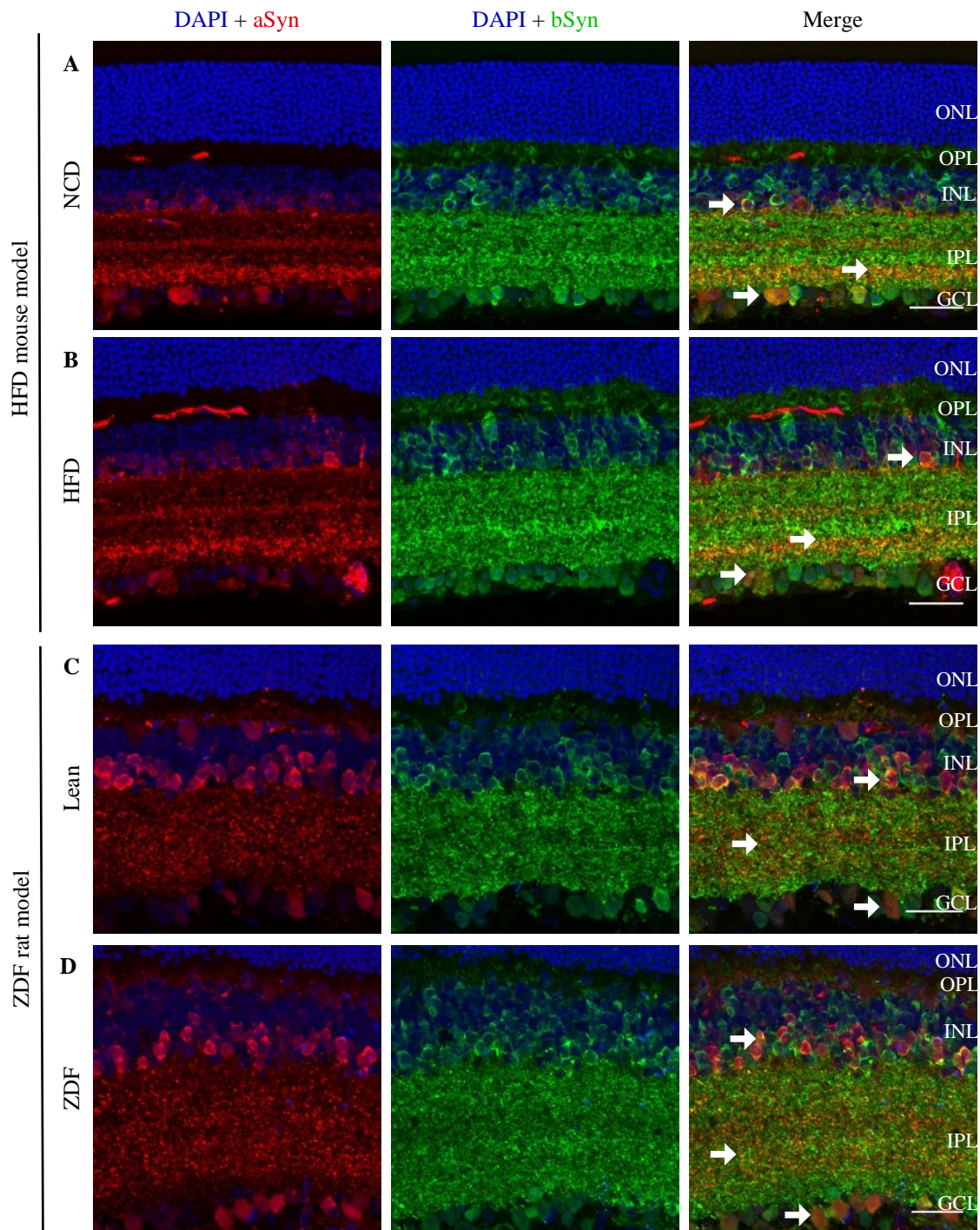


Figure 3.17. – Immunohistochemistry of the colocalization between aSyn and bSyn in the retina of NDC and HFD mice and also Lean and ZDF rats A and B) Colocalization between aSyn and bSyn in NCD and HFD mice, respectively. C and D) Colocalization between aSyn and bSyn in Lean and ZDF rats, respectively. N=3 for both T2DM animal models. A representative image of central area of the retina is shown. Nucleus are stained with DAPI (blue), aSyn stained with Alexa Fluor 594 GAM (Red) and bSyn stained with Alexa Fluor 488 GAR (Green). ONL, outer nuclear layer, OPL, outer plexiform layer, INL, inner nuclear layer, IPL, inner plexiform layer, GCL, ganglion cell layer. Maximum intensity projections obtained from confocal images obtained with a 40x objective. Scale bar = 30 μ m.

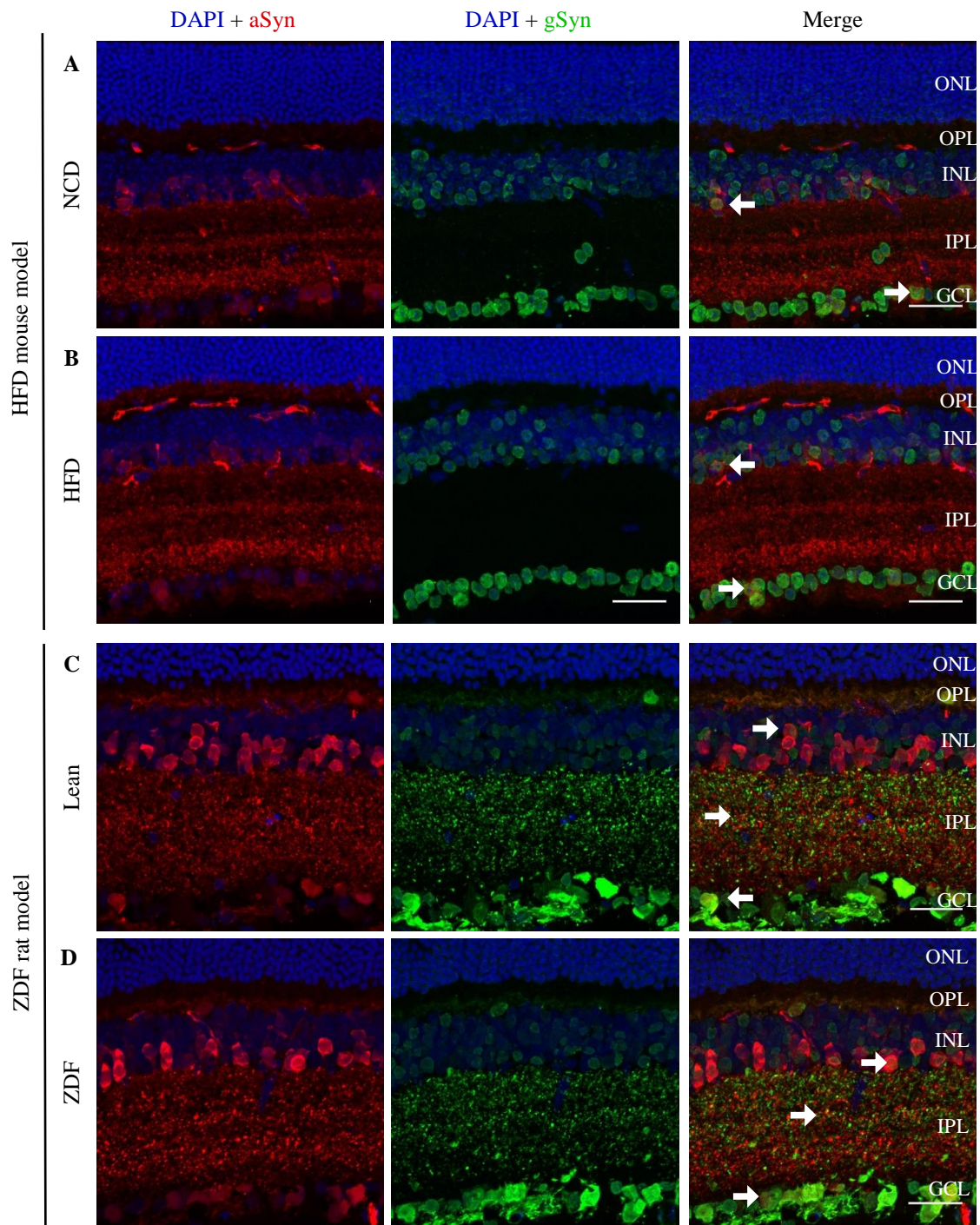


Figure 3.18. – Immunohistochemistry of the colocalization between aSyn and gSyn in the retina of NDC and HFD mice and also Lean and ZDF rats. A and B) Colocalization between aSyn and gSyn in NDC and HFD mice, respectively. C and D) Colocalization between aSyn and gSyn in Lean and ZDF rats, respectively. N=3 for both T2DM animal models. A representative image of central area of the retina is shown. Nucleus are stained with DAPI (blue), aSyn stained with Alexa Fluor 594 GAM (Red) and gSyn stained with Alexa Fluor 488 GAR (Green). ONL, outer nuclear layer, OPL, outer plexiform layer, INL, inner nuclear layer, IPL, inner plexiform layer, GCL, ganglion cell layer. Maximum intensity projections obtained from confocal images obtained with a 40x objective. Scale bar = 30 μ m.

In both T2DM animal models, aSyn is localized in the INL, IPL and GCL and there are no striking observable differences in comparison with the respective controls (Fig. 3.16.A, B, C and D). However, aSyn distribution profile is slightly different between mice and rats. In the INL of mice, aSyn is almost only present in the proximal region and rarely in the distal area where horizontal cells usually are located (Kolb H, 2003). In contrast, in the INL of rats, aSyn-positive cell bodies are more easily found in the distal INL than in mice, however they are still in fewer amounts than in the proximal area. In addition, in the IPL of mice, aSyn appears to be stratified in strata 1, 3 and 5 (s1, s3 and s5), revealing higher intensities in the s5 which is where ON bipolar and ON ganglion cells as well as amacrine cells communicate (Kolb H, 2003). This contrasts with the absence of the stratification pattern in the rats.

Regarding bSyn, in the retina of NCD and HFD mice and Lean and ZDF rats, bSyn is present in the INL, IPL and GCL and no differences regarding their qualitative profile distribution were found (Fig. 3.16.E, F, G and H).

Finally, gSyn is present in the retina of NCD and HFD mice and Lean and ZDF rats, and no striking differences were observed (Fig. 3.16.I, J, L and L). However, gSyn has the particularity of not being present in the IPL of mice retina as opposing to aSyn and bSyn. However, in rats gSyn is present in the IPL, although in far less amounts than the other members of the synuclein family. The gSyn protein is in both T2DM animal models, and respective controls, localized as well in INL, with a scattered-like distribution similar to bSyn, and also localized in the GCL.

Concerning aSyn and bSyn colocalization, confocal microscopy revealed that these proteins colocalize in the INL, IPL and GCL in NCD and HFD mice retina, exhibiting no significant visual alterations in this profile upon T2DM (Fig. 3.17.A and B). The same observations were obtained in the retina of Lean and ZDF rats and no substantial visual changes were observed in their colocalization in this T2DM rat model (Fig. 3.17 C and D). The same observations were obtained in both T2DM animal models for the colocalization between aSyn and gSyn in the retina (Fig. 3.18.).

Proceeding to quantitative analysis of the confocal images, synucleins counting in the INL and GCL, colocalization quantification in the INL, IPL and GCL, and intensity measurements in the IPL were performed in the retina of NCD and HFD mice and Lean and ZDF rats (Fig. 3.19.).

As aSyn has a characteristic pattern in the INL, this layer was split into proximal and distal regions and aSyn-positive cell body counts were made in accordance to this analysis criteria for both T2DM animal models and respective controls. In contrast, bSyn and gSyn counting did not follow any strict guidelines (Fig. 3.19).

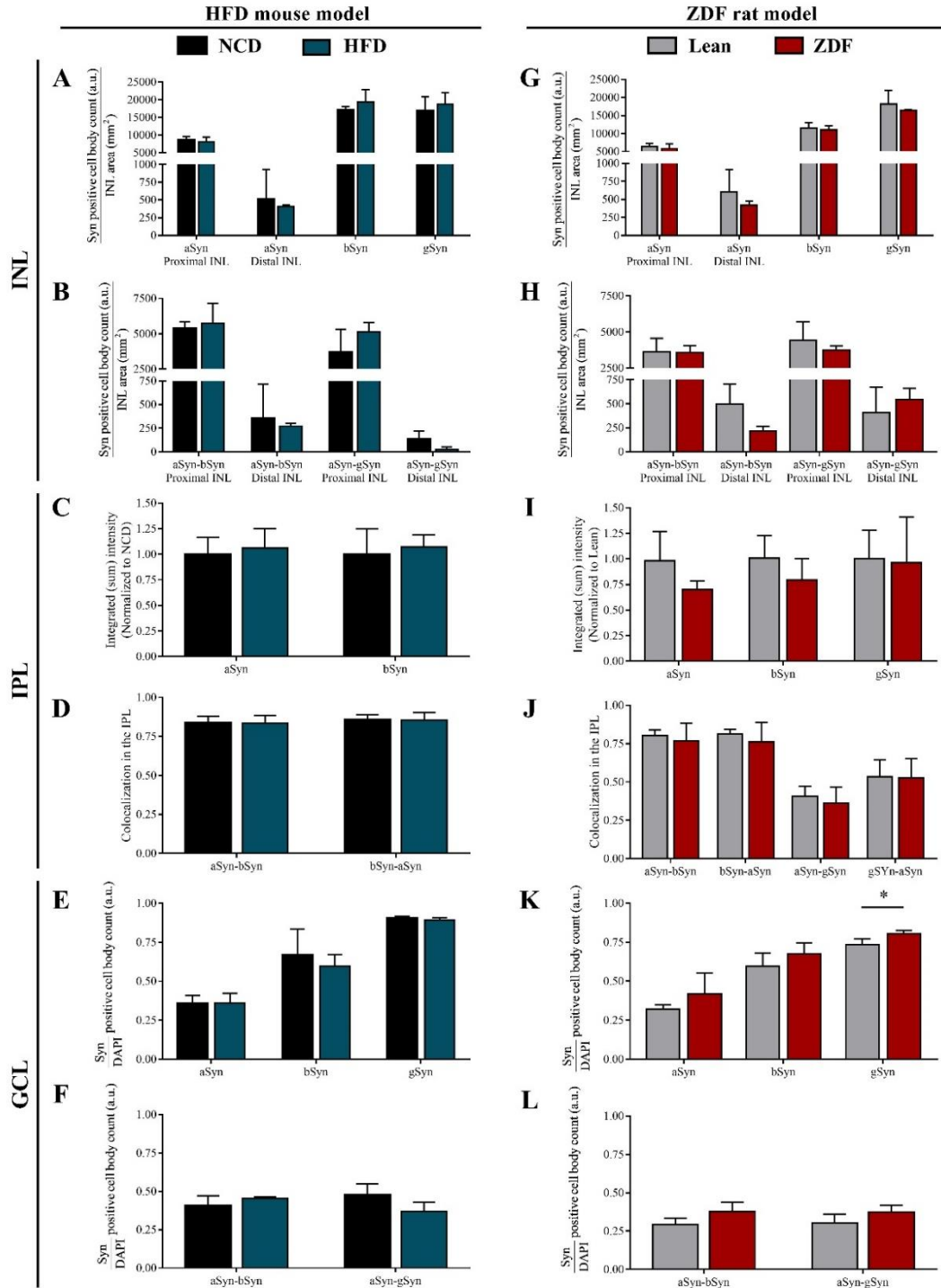


Figure 3.19. - Quantification of the synucleins distribution in the INL, IPL and GCL in HFD mice and ZDF rats. N=3 for NCD and HFD mice and for Lean and ZDF rats. A) Quantification of aSyn-,bSyn- and gSyn-positive cell

body density in the INL for comparison between NCD and HFD mice. B) Assessment of the levels of the colocalizations aSyn-bSyn and aSyn-gSyn in the INL of NCD and HFD mice. C) Quantification of the integrated (sum) intensity of the aSyn and bSyn in the IPL of HFD mice normalized to NCD mice. D) Mander's split coefficient gives a measure of the colocalization between aSyn and bSyn in the IPL of NCD and HFD mice. E) Quantification of aSyn-, bSyn- and gSyn-positive cell body per DAPI-positive cell body in the GCL of NCD and HFD mice. F) Evaluation of synucleins colocalization levels per DAPI-positive cell body in the GCL of NCD and HFD mice. G) Quantification of aSyn-, bSyn- and gSyn-positive cell body density in the INL for comparison between Lean and ZDF rats. H) Assessment of the levels of the colocalizations aSyn-bSyn and aSyn-gSyn in the INL of Lean and ZDF rats. I) Quantification of the integrated (sum) intensity of the aSyn, bSyn and gSyn in the IPL of ZDF rats normalized to Lean mice. J) Mander's split coefficient gives a measure of the colocalization between the synucleins in the IPL of Lean and ZDF rats. K) Quantification of aSyn-, bSyn- and gSyn-positive cell body per DAPI-positive cell body in the GCL of Lean and ZDF rats. L) Evaluation of synucleins colocalization per DAPI-positive cell body in the GCL of Lean and ZDF rats. All Western Blot data are presented as Mean \pm SD. * $p < 0.05$ ZDF compared to Lean; T-test.

Counting for each synuclein in the INL of NCD and HFD mice and Lean and ZDF rats were performed following the previously mentioned criteria (Fig. 3.19.A and G). No differences were observed for both diabetic animal models, however one can observe that in ZDF rats gSyn is more abundant, followed by bSyn and lastly by aSyn, whereas in HFD mice bSyn and gSyn are at the same levels and afterwards followed by aSyn. Moreover, the colocalizations aSyn-bSyn and aSyn-gSyn were also assessed, while still taking into account the proximal and distal criteria for both diabetic animal models (Fig. 3.19.B and H). The results show no statistical difference between NCD and HFD mice nor between Lean and ZDF rats. Nevertheless, it is still apparent for both animal models that aSyn preferentially localizes in the proximal area rather than in the distal INL and that aSyn equally colocalizes with bSyn and gSyn.

In regard to the IPL, quantifications of the integrated (sum) intensity of each synuclein between NCD and HFD mice and between Lean and ZDF rats does not differ (Fig. 3.19.C and I).

Afterwards, the colocalization levels of aSyn-bSyn and bSyn-aSyn, in the IPL of NCD and HFD mice and Lean and ZDF rats were assessed (Fig. 3.19.D and J). The results show no significant differences when comparing HFD mice to NCD mice or Lean to ZDF rats. Moreover, one can observe that in both Lean and ZDF rats, aSyn has a higher colocalization with bSyn than with gSyn in the IPL of these rats, whereas in mice aSyn equally colocalizes with bSyn and gSyn.

Concerning the GCL, synuclein-positive cell bodies were counted per number of stained nuclei, and no striking variations were found between NCD and HFD mice (Fig. 3.19.E). The same observations cannot be withdrawn for ZDF rats as there is an increased number of cell bodies containing gSyn in the GCL of ZDF rats retina in comparison to Lean rats (0.8403 ± 0.1834 vs 0.7962 ± 0.1249) (Fig. 3.19.K). This result is not in

agreement with the western blot analysis for gSyn protein levels in Lean and ZDF rats, as there no substantial alterations between them, thus proving the point of the dilution effect in western blot of whole retina extracts.

Furthermore, it seems that gSyn is the most abundant synuclein in the GCL, followed by bSyn and lastly by aSyn, in both T2DM animal models. Moreover, the colocalizations aSyn-bSyn and aSyn-gSyn were also examined in the GCL and no differences were obtained between NCD and HFD mice (Fig. 3.19.F). Likewise, the same colocalizations were tested between Lean and ZDF rats and no differences were obtained as well (Fig. 3.19.L). In both diabetic animal models aSyn does not preferentially colocalize with bSyn or gSyn.

In summary, both in the INL and GCL the number of cell bodies containing each aSyn or bSyn is not affected by the diabetic environment in both T2DM animal models, which correlates with the absence of differences observed in the western blot results (Fig. 3.15.A, B, D and F). However, gSyn is affected only in the GCL, revealing an increased number of cell bodies containing this protein, which is a subtle alteration that could not be detected by western blot. In the IPL, no striking alterations of the synucleins intensity were observed for both T2DM animal models, as well as in colocalization levels between the synucleins in all the three tested layers.

3.10. Synaptic markers in the retina of T2DM animal models

It was previously reported alterations in the synaptic content of retinal terminal nerves (Gaspar JM et al., 2010), (Batista FI et al., 2011), (Vanguilder HD et al., 2008). Hence, our goal was to assess by western blot the level of synaptic markers such as the v-SNAREs Synaptophysin and Rab3a, the t-SNAREs SNAP-25 and Syntaxin 1A, PSD95 and TH in whole retina protein extracts of NCD and HFD mice and Lean and ZDF rats (Fig. 3.20.).

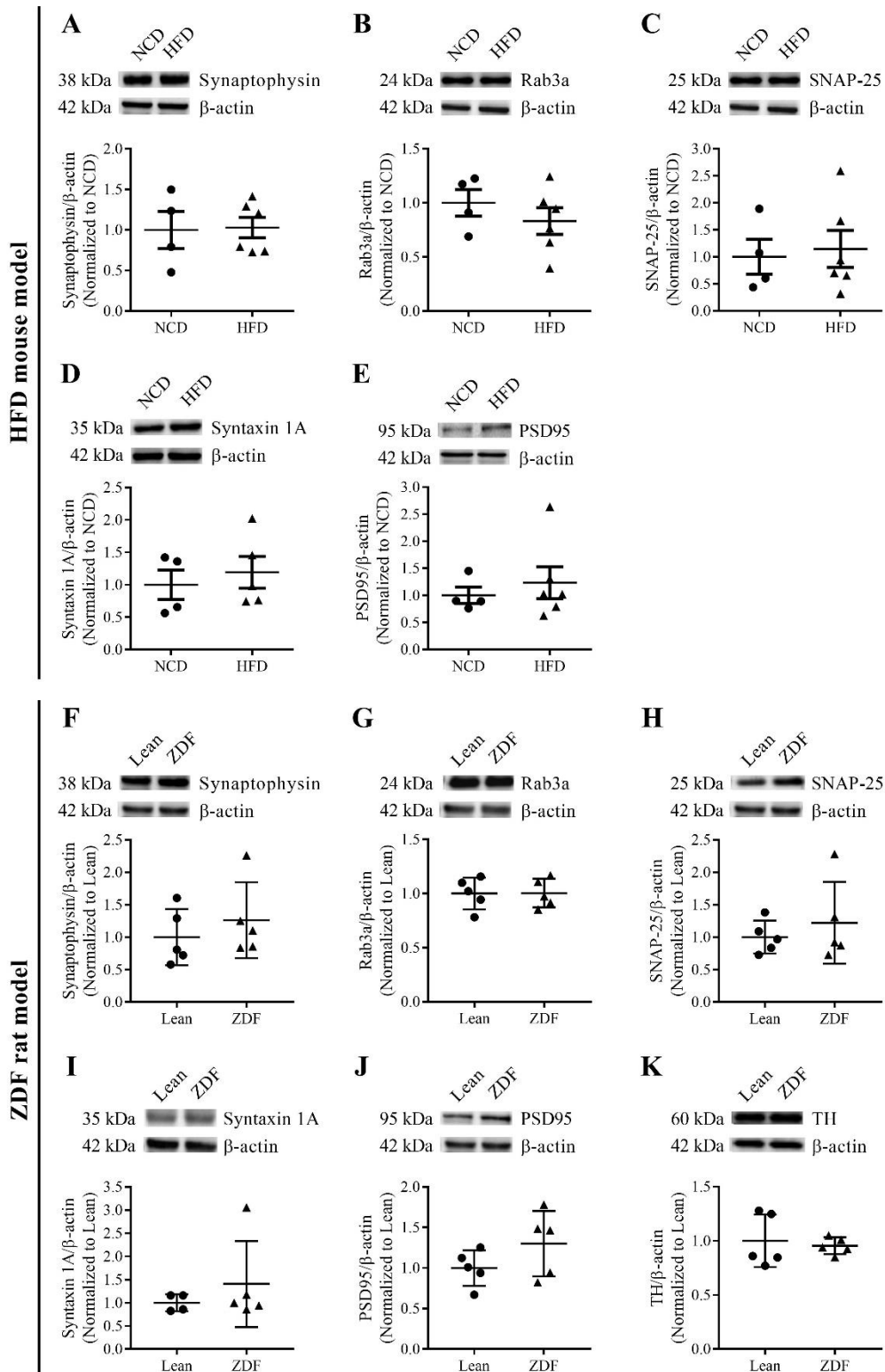


Figure 3.20. – Assessment of synucleins levels in HFD mice and ZDF rats whole retina protein extracts. A) Western blot for the comparison of Synaptophysin protein levels between NCD and HFD (upper panel) and the corresponding densitometry analysis (lower panel). B) Western blot for the comparison of Rab3a protein levels between NCD and HFD mice (upper panel) and the corresponding densitometry analysis (lower panel). C) Western blot for the comparison of SNAP-25 protein levels in NCD and HFD mice (upper panel) and the corresponding densitometry analysis (lower panel). D) Western blot for the comparison of Syntaxin 1A protein levels in NCD and HFD mice (upper panel) and the corresponding densitometry analysis (lower panel). E) Western blot for the comparison of PSD95 protein levels in NCD and HFD mice (upper panel) and the corresponding densitometry analysis (lower panel). F) Western

blot for the comparison of synaptophysin protein levels between Lean and ZDF rats (upper panel) and the corresponding densitometry analysis (lower panel). G) Western blot for the comparison of Rab3a protein levels between Lean and ZDF rats (upper panel) and the corresponding densitometry analysis (lower panel). H) Western blot for the comparison of SNAP-25 protein levels between Lean and ZDF rats (upper panel) and the corresponding densitometry analysis (lower panel). I) Western blot for the comparison of PSD95 protein levels between Lean and ZDF rats (upper panel) and the corresponding densitometry analysis (lower panel). J) Western blot for the comparison of TH protein levels between Lean and ZDF rats (upper panel) and the corresponding densitometry analysis (lower panel). A representative image of the western blot is shown. All Western Blot data are presented as Mean \pm SD

Western blot analysis of the results show that in the levels of the v-SNAREs Synaptophysin (Fig. 3.20.A and F) and Rab3a proteins (Fig. 3.20.B and G) there is no significant difference between NCD and HFD mice nor between Lean and ZDF rats retina. Likewise, the t-SNAREs Syntaxin 1A protein (Fig. 3.20.C and H) and SNAP-25 (Fig. 3.20.D and I) do not show any statistical difference between NCD and HFD mice or Lean and ZDF rats.

Regarding the protein levels of PSD95, no striking changes were observed either between NCD and HFD mice or between Lean and ZDF rats (Fig. 3.20.E and J).

Lastly, TH protein levels were only tested for the ZDF rats and it seems that T2DM does not lead to evident alterations in ZDF rats when comparing to Lean rats (Fig. 3.20.K). This potentially means that DA cell loss is not occurring, which contrasts with the reported neurodegeneration of these neurons in the T1DM rat model STZ and mouse model *Ins2^{Akita}* (Gastinger MJ et al., 2006).

Altogether, these results suggest that in the tested models of T2DM, the HFD mice and ZDF rats, no effect on the levels of markers important for synaptic function are observed, which contrasts with previous evidences demonstrating altered retinal nerve content (Gaspar JM et al., 2010), (Batista FI et al., 2011), (Vanguilder HD et al., 2008). Furthermore, the unaffected TH protein levels in the ZDF rat possibly point to the fact that the diabetic environment in these animals was not able to induce dopaminergic loss.

3.11. Cell survival markers in the retina T2DM animal models

3.11.1. Cell survival markers levels in the retina of HFD mice and ZDF rats

As neurodegeneration in the retina of diabetic animals with DR is an event that precedes vascular changes (Duh EJ et al., 2017), it was evaluated by western blot the levels of cell survival markers such as the transcription factor NF- κ B, MLKL and pMLKL

in the retina of NCD and HFD mice and Lean and ZDF rats. STAT3 and its activated form pY705-STAT3, which are markers for cell proliferation, GFAP, a marker of inflammation, and caspase 3 protein levels were also assessed by western blot for both T2DM animal models (Fig. 3.21.).

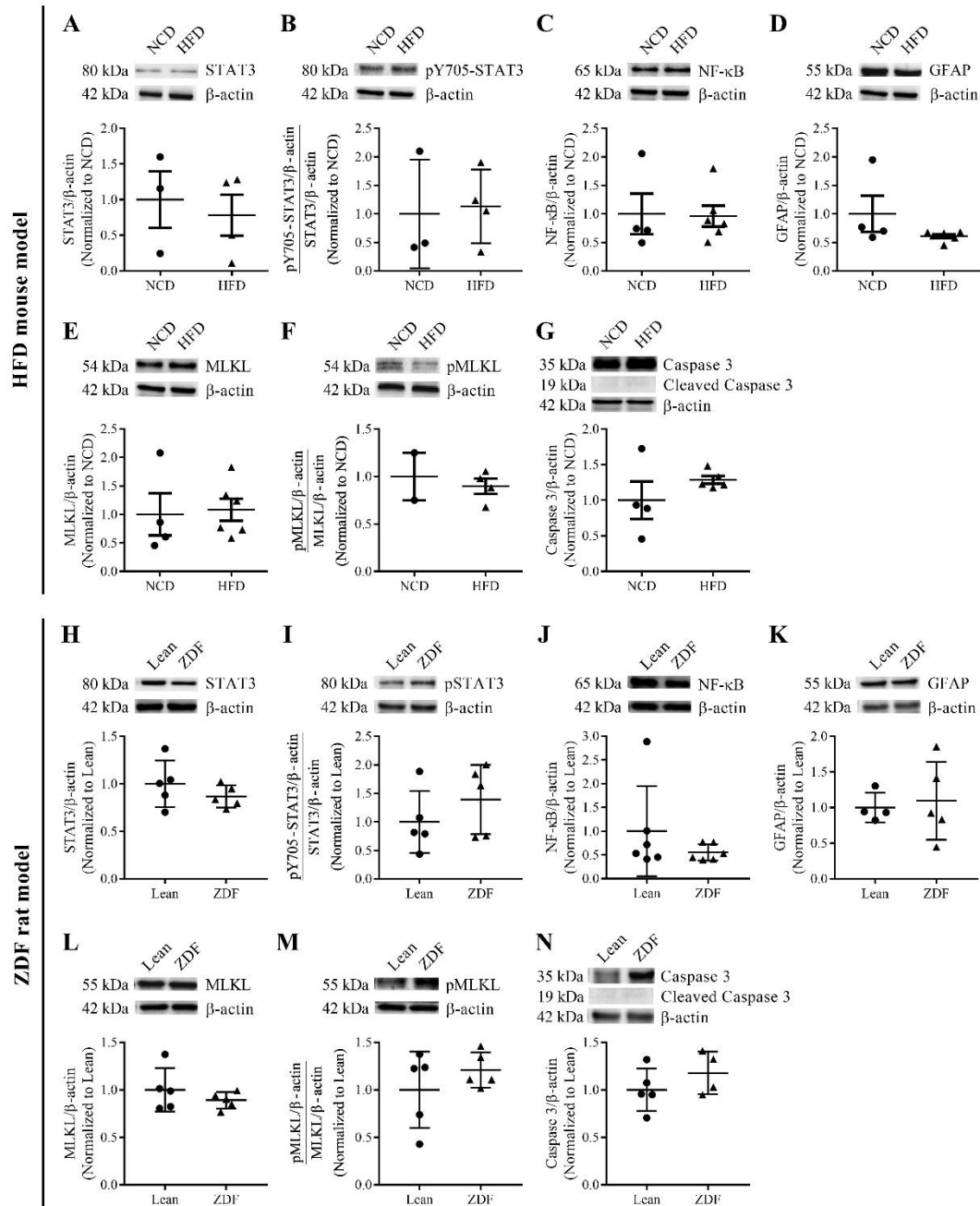


Figure 3.21. – Assessment of cell survival and inflammation markers levels in HFD mice and ZDF rats whole retina protein extracts. A) Western blot for the comparison of STAT3 protein levels between NCD and HFD mice (upper panel) and the corresponding densitometry analysis (lower panel). B) Western blot for the ratio pY705-STAT3/STAT3 between NCD and HFD mice (upper panel) and the corresponding densitometry analysis (lower panel). C) Western blot for the comparison of NF- κ B protein levels between NCD and HFD mice (upper panel) and the corresponding densitometry analysis (lower panel). D) Western blot for the comparison of the ratio GFAP protein levels

between NCD and HFD mice (upper panel) and the corresponding densitometry analysis (lower panel). E) Western blot for the comparison of the ratio pMLKL/MLKL protein levels between NCD and HFD mice(upper panel) and the corresponding densitometry analysis (lower panel). F) Western blot for the comparison of the ratio pMLKL/MLKL between NCD and HFD mice (upper panel) and the corresponding densitometry analysis (lower panel). G) Western blot for the comparison of caspase 3 protein levels between NCD and HFD and detection of cleaved caspase 3 (upper panel) and the corresponding densitometry analysis (lower panel). H) Western blot for the comparison of STAT3 protein levels between Lean and ZDF rats (upper panel) and the corresponding densitometry analysis (lower panel). I) Western blot for the ratio pY705-STAT3/STAT3 between Lean and ZDF rats (upper panel) and the corresponding densitometry analysis (lower panel). J) Western blot for the comparison of NF- κ B protein levels between Lean and ZDF rats (upper panel) and the corresponding densitometry analysis (lower panel). K) Western blot for the comparison of the ratio GFAP protein levels between Lean and ZDF rats (upper panel) and the corresponding densitometry analysis (lower panel). L) Western blot for the comparison of the ratio pMLKL/MLKL protein levels between Lean and ZDF rats (upper panel) and the corresponding densitometry analysis (lower panel). M) Western blot for the comparison of the ratio pMLKL/MLKL between Lean and ZDF rats (upper panel) and the corresponding densitometry analysis (lower panel). N) Western blot for the comparison of caspase 3 protein levels between Lean and ZDF rats and detection of cleaved caspase 3(upper panel) and the corresponding densitometry analysis (lower panel). A representative image of the western blot is shown. All Western Blot data are presented as Mean \pm SD.

Western blot analysis of the STAT3 protein levels show that there is no difference between NCD and HFD mice and between Lean and ZDF rats (Fig. 3.21.A and H). Conversely, there is no significant difference in the ratio pY705-STAT3/ STAT3 in HFD when comparing to NCD mice or ZDF when comparing to Lean rats (Fig. 3.21.B and I).

Likewise, both the NF- κ B (Fig. 3.21.C and J) and GFAP protein levels (Fig. 3.21.D and K) do not show striking alterations between NCD and HFD mice or Lean and ZDF rats.

Regarding the necroptosis marker MLKL it seems there is no changes between NCD and HFD mice or Lean and ZDF rats (Fig. 3.21.E and L). Similarly, the ratio pMLKL/MLKL does not vary in both T2DM animal models (Fig. 3.21.F and M).

Lastly, caspase 3 protein levels seem also not to be affected by T2DM when comparing NCD with HFD mice or Lean with ZDF rats. Moreover, cleaved caspase 3 levels were not detected in both diabetic animal models in the tested conditions (Fig. 3.21.G and N).

Altogether, the results here obtained do not show any difference in the necroptotic events in both tested T2DM animal models. However, this does not mean that there are not any cell death events occurring as the activated form Caspase 3, indicator of intrinsic apoptotic pathway induction, was not detected in tested conditions. In addition, cell proliferation is also not affected as seen by the pY705-STAT3/STAT3 ratio readout, nor there is the increased and characteristic inflammation in DR confirmed by the unaltered NF- κ B protein levels (Wong TY et al., 2016). It is even possible that only a few neuronal subpopulations could be dying, but that cannot be detected due to a dilution effect in the western blot.

3.11.2. Retinal layers integrity in HFD mice and ZDF rats

In DR the retina undergoes different structural changes. It can either become thinner, a sign of neurodegeneration (Carpineto P et al., 2016), (Barber AJ et al., 1988), or swell, an indicator of inflammation (Alamouti BF et al., 2003). Hence, by measuring the thickness of the OPL, INL and IPL in maximum intensity projections from confocal images, one can understand if the integrity of the retina in HFD mice and ZDF rats is being compromised. The GCL thickness was not possible to be measured as there are no key visual indicators that would help limit the area of this layer, therefore the number of cell bodies per length of the GCL was chosen as a solution, since it can give a hint of the existence of neurotoxic or neuroprotective events, depending on the outcome (Fig. 3.22.).

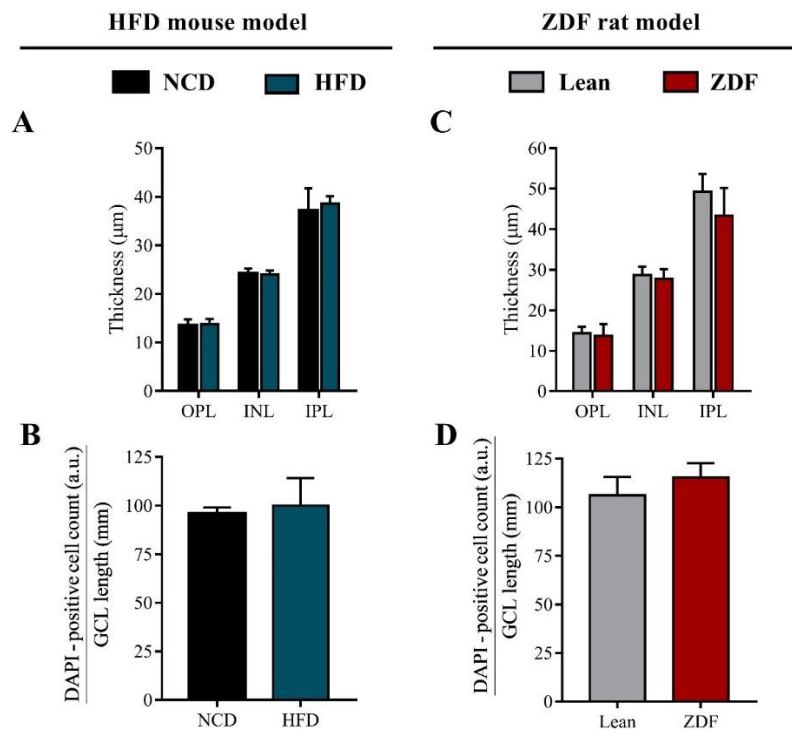


Figure 3.22. – Quantification of retinal layers' thickness and GCL cell density in HFD mice and ZDF rats. A) Comparison of the thickness of the OPL, INL and IPL between NCD and HFD mice. B) GCL cell density comparison between NCD and HFD mice. C) Evaluation of the thickness of the OPL, INL and IPL between Lean and ZDF rats. D) GCL cell density comparison between Lean and ZDF rats. All Western Blot data are presented as Mean \pm SD.

The results obtained show that both HFD mice, in comparison with NCD, and ZDF rats, comparing with Lean rats, do not have any thickness alterations in the OPL, INL and IPL thickness (Fig. 3.22.A and C). In addition, the cell density in the GCL of

both HDF mice, in comparison to NCD, and ZDF rats, comparing with Lean rats, is not affected by T2DM (Fig. 3.22.B and D).

On the whole, the structural integrity of the retina is not being compromised in both T2DM animals, which correlates with the stable levels of TH (Fig. 3. 20.K) and cell survival markers previously obtained (Fig. 3.21.).

4. Conclusion

Retinal neurodegeneration is an event known to happen in PD, DM and in aged individuals (Wong TY et al., 2016), (Inzelberg et al. 2004), (Hajee et al., 2009), (Nadal-Nicolás F et al., 2018). Indeed, the diabetic and ageing cellular environments share several molecular mechanisms that are also known to be present in PD (Tian T et al., 2015), (López-Otín C et al., 2013). Interestingly, synucleins, a family of proteins highly associated with the pathogenesis of PD in the brain (Wales P et al., 2013), are also expressed in the retina (Surguchov A et al., 2001). This further suggests that synucleins upon diabetes or ageing may be triggered to exert a neurotoxic role similar to what happens in PD, hence promoting synaptic dysfunction and, eventually, cell death (Wales P et al., 2013).

Therefore, we performed in the retina of PD, DM and ageing animal models, a characterization of the synucleins protein levels and localization in the retina, but also a quantification of synaptic and cell survival markers protein levels.

The MPTP and rotenone mouse models are animal models of PD very similar to the MitoPark mouse model, as they reproduce the same fundamental principle, which is mitochondrial dysfunction in dopaminergic neurons in the brain, that ultimately leads to cell death events. One of the consequences of mitochondrial impairment in the MPTP and rotenone model results in aSyn-positive inclusions in the brain (Meredith G and Rademacher D, 2012). Although in a different tissue – the retina – our results point to alterations in the protein levels of another synuclein, rather than the usual central player aSyn, since we observed in MitoPark mice retina increased protein levels of bSyn when comparing to control mice (Fig. 3.1.C).

Concerning the two ageing rat models used, the naturally ageing and the accelerated ageing (D-Gal treated rats) models, none of the synucleins suffered variations in the protein levels (Fig. 3.4.). As synucleins accumulate PTMs throughout time (Wales P et al., 2013), and since aSyn could be a target of glycation in the D-Gal rat model (Wu DM et al., 2008), (Miranda MV et al., 2017), it could be expected increased protein levels due to an impaired clearance mechanism, however this was not observed. Nevertheless, gSyn still seems to show a decreasing tendency in 6 months old rats, only increasing at 19 months to levels similar to 1 month old rats (Fig. 3.4.C), which was not obtained in D-

Gal rats retina. Furthermore, we next quantified the differential distribution of each synuclein in the retina, as well as colocalizations in the IPL and GCL in both rat models. Only one significant difference was observed, which was a reduced colocalization between aSyn and bSyn in the GCL of D-Gal rats when comparing to Sham rats (Fig. 3.11.L).

Regarding the T2DM animal models used, the HFD mouse model and the ZDF rat model, none of the synucleins protein levels was affected (Fig. 3.15.). Taking into account the similarities between PD and DM cellular environment, it would be likely to find alterations in the synucleins levels that are described in this neurodegenerative disorder. However, results do not point to any alteration, albeit there is a common decreasing tendency in the protein levels of bSyn both in the HFD mice and in the ZDF rats (Fig. 3.15.B and F). This tendency could potentially be in accordance to the reported decreased bSyn protein levels in the retina of 9 months old *Ins2^{Akita}* mice, a T1DM model (Santos G, 2017), perhaps if under a more severe diabetic environment. On the other hand, this result contrasts with the increased bSyn protein levels obtained in MitoPark mice retina. Furthermore, we next quantified the differential distribution of each synuclein in the retina, as well as colocalizations in the INL, IPL and GCL in both T2DM animal models. Our results indicate that there is a significant increase in the number of cell bodies containing gSyn in the GCL of ZDF rats when comparing with Lean rats (Fig. 3.19.K). This result is not in accordance with the western blot analysis for gSyn, as no differences in the protein levels of this protein were obtained between Lean and ZDF rats retina, further strengthening the idea of a dilution effect when making a whole retina protein extract (Fig. 3.15.G).

Synaptic dysfunction was also observed in the brain of PD patients (Wales P et al., 2013). Of the several synaptic markers tested, only Synaptophysin protein levels significantly reduced in the retina of MitoPark mice (Fig. 3.2.A), which may suggest an impaired synaptic function. Whether bSyn levels are increased to prevent aSyn aggregation (Hashimoto M et al., 2001), (Hashimoto M et al., 2004) or to compensate Synaptophysin loss by promoting the SNARE-complex assembly (Burré J et al., 2010) it remains elusive. Moreover, MitoPark mice were also expected to have decreased levels of TH in the retina, due to possible loss of dopaminergic neurons in this tissue, as

dopaminergic neurons in the brain are reported to be progressively lost, starting at 12 weeks of age (Ekstrand MI and Galter D, 2009), which was not obtained (Fig. 3.2.C).

Ageing is also reported to interfere with synaptic integrity. However, the unaltered protein levels of several synaptic markers both in ageing rats and in D-Gal treated rats point to a stable and uncompromised neurotransmission process (Fig. 3.12.). Impaired retinal dopaminergic system was also previously demonstrated in the retina of rats (Djamgoz B et al., 1997), which theoretically would imply decreased TH protein levels. However, our assessment of TH protein levels in the retina of rats with 1, 6, 10 and 19 months old indicated no differences throughout ageing (Fig. 3.12.E). Nevertheless, there seems to be an increasing tendency at 6 months old when comparing to 1 month old rats.

Concerning the HFD mouse model and the ZDF rat model, the results demonstrate unaffected protein levels of proteins whose function is related with synaptic activity (Fig. 3.21), contrasting with previous evidence of altered retinal nerve content (Gaspar JM et al., 2010). Even TH protein levels remained similar to non-diabetic animals, despite previous evidence DA cell disruption (Fig. 3.20.) (Djamgoz B et al., 1997).

In regard to cell death events, one would in fact anticipate that there would be more cells dying than DA cells in the MitoPark mice retina, as there more cells expressing the DAT protein in the retina than solely DA cells (Cheng Z et al., 2006), in which the cre recombinase could excise the *TFAM* gene (Ekstrand MI and Galter D, 2009). However, our results demonstrate no variations in the protein levels of caspase-dependent and -independent cell death markers in the retina of this animal model of PD (Fig.3.4.).

All retinal layers are differently affected when comparing 6, 10 and 19 months old rats with 1 month old rats. These changes may be in accordance with previous reports on INL and GCL lack of integrity upon ageing (Nadal-Nicolás F et al., 2018), (Cano J et al., 1986). On the other hand, the size of the retina increases linearly with age and body weight. This continuous growth leads to a proportional retinal thinning and cell density reduction, as previously reported for albino rats (Braekevelt CR and Hollenberg MJ, 1970). Indeed, after the 6 months of age no variation occurs in these layers, which could resemble more a maturing effect on the retina rather than an ageing effect. Another aspect to highlight, is the fact that only at 19 months old there is a significant reduction in the thickness of the IPL when comparing with 1 month old rats. If one considers that the alterations observed in the INL and GCL are result of neurodegeneration events, then this

reduction in the thickness of this neuropil that only happens at 19 months old is not preceding the cell body loss and is not in agreement with the higher susceptibility of synapses (Wishart TM et al., 2018). However, if we consider that there is a maturing effect in the INL and GCL, then the thickness reduction in the IPL of 19 month rats may possibly be anticipating cell body loss in the retina of older albino rats.

Interestingly, only in the D-Gal rats retina was observed a significant difference in the western blot results, namely a reduction in the NF- κ B protein levels. This result does not necessarily point to a decreased cell death or inflammation, because only the confirmation of the subcellular localization of NF- κ B inside the nucleus could trigger several cell death-related pathways (Lawrence T, 2009). Alternatively, these reduced protein levels could be merely due to turnover aspects – either gene downregulation or increased clearance – and cannot be correlated with protein activity.

The same quantifications on the retinal thickness were also done in Sham and D-Gal rats, and it seems that the OPL, INL and IPL are not affected upon D-Gal treatment regarding Sham rats (Fig. 3.14.C). Nevertheless, D-Gal rats seem to have a greater cell density in the GCL when comparing with Sham rats (Fig. 3.14.D). This result fails to be in accordance with the reported accelerated ageing in this model, as the ageing retina was described to have fewer RGCs (Cano J et al., 1986), therefore D-Gal administration may be preventing the loss of RGCs or be related with a decreased colocalization between aSyn and bSyn in this layer.

In regard to the both T2DM animal models that were tested, despite the fact that neurodegeneration was demonstrated to occur in an early phase of DR (Duh EJ et al., 2017), protein levels of markers of cell survival and inflammation were not altered upon diabetes (Fig. 3.21.). Concerning the quantification of the OPL, INL and IPL thickness and GCL cell density in the retina of HFD mice and ZDF rats, no significant differences were observed, which is coherent with the absence of western blot positive results regarding cell death markers (Fig. 3.22.).

Although we did not perform all tests required to prove that MitoPark mice have in fact the cre-loxP system working, there are some differences obtained in the retina of these animals regarding bSyn and Synaptophysin, which might have mitochondrial dysfunction as being the first underlying cause in a cascade of events to trigger these alterations.

D-Gal treated rats are described as model of accelerated ageing in the brain (Hao L et al., 2014), however the retina of these rats does not exhibit the same observations as in ageing rats retina, which may indicate that the retina of D-Gal rats does not age upon the administration of this sugar. Maybe, increasing the dosage or a longer treatment period would cause a higher retinal damage and more effects similar to the ageing animals. Regarding ageing rats, no changes in the synucleins levels or distribution were obtained in the retina of 6, 10 and 19 months old rats when comparing with 1 month old rats. While one could argue that albino rat retinas environment should easily influence synucleins behaviour due to their retina's intrinsic higher susceptibility to neurodegeneration, the albino rat strain used, and consequently genetic background, may be having a great impact in the results obtained.

Concerning the T2DM animal models tested in this work, also very few changes were observed regarding synucleins levels and distribution, synaptic integrity, cell survival and inflammation status. It is likely that DR in these animals was still highly underdeveloped, hence not being able to compromise global retinal function. Alternatively, it is possible that T2DM cellular environment is not as hostile as in T1DM, in which molecular changes may be more easily triggered. One can also consider the fact that HFD mice had a short duration of feeding with high-fat content, which would not be enough to trigger any major alterations in the retina. However, these mice were shown to be obese and to have increased blood glucose levels, albeit not so augmented as in the original experiments first conducted with this mouse model (Surwit RD et al., 1988).

In summary, the synucleins role in retinal neurodegeneration in PD, DM and ageing still remains to be elucidated, however, some changes were still reported, mostly not involving the central player of the synuclein family, aSyn, but instead bSyn. Nevertheless, synucleins characterization in the retina is underexplored and with this work we provide new insights on a detailed description in mice and rats retina but also on 5 different animal models: MitoPark mouse model of PD, HFD mouse and ZDF rats models of T2DM, naturally ageing and accelerated ageing.

It is worth mentioning that there are no perfect animal models, as they only recapitulate a portion of the known molecular mechanisms associated with the disease and a part of the symptoms. Furthermore, despite being mammals they are not humans, which impairs any extrapolations from these animals to humans. However, the animal

models used still focus on several key points such as the characteristic mitochondrial dysfunction in dopaminergic neurons of PD, hyperglycaemia in diabetes and the loss of physiological integrity with ageing. In fact, these animal models are intertwined to the point that the MitoPark mice exhibit features of an age-related disorder (PD), as well as both the HFD mice and ZDF rats that have T2DM, another age-associated disease that is in fact a risk factor for PD development. One could argue that T1DM animal models would possibly help clarifying some results due a more severe diabetic environment, and although the underlying molecular mechanisms do contribute to PD pathogenesis, T1DM is not an age-related disorder.

As future work, all tests required to prove the activity of the Cre-loxP system in MitoPark mice retina should be assessed, as well as confocal microscopy to evaluate the synucleins differential distribution in the retina of these mice. Moreover, counting of the synucleins distribution in the INL in both ageing and accelerated ageing rat models used must be quantified to conclude the distribution profile studies. Furthermore, synucleins aggregated conformations are an important pathologic sign that can be tested in the retina of all animals, possibly through confocal microscopy, by evaluating the colocalization between synucleins and markers of the UPS and ALP, such as the ubiquitin and p62 proteins, respectively, or with the antibody 5G4 (Sigma, MABN389), which is described to recognize aSyn oligomeric species. In addition, colocalization between the synucleins and synaptic markers such as Synaptophysin and Synatxin 1A can be addresses as well, to indirectly evaluate the efficiency of assembly of the SNARE-complex. Finally, TH-positive cell bodies count in all animal models used should be quantified to provide a secondary approach for checking if in fact there is any DA cell loss.

5. References

- Abcouwer, Steven F., Gardner, Thomas W. - Diabetic retinopathy: Loss of neuroretinal adaptation to the diabetic metabolic environment. Annals of the New York Academy of Sciences. ISSN 17496632. 1311:1, (2014), 174–190.
- Ahmed, A.M. - History of diabetes mellitus. Saudi Med. J. 23 (2002), 373–378.
- Ahn, Jeeyun et al. - Retinal thinning associates with nigral dopaminergic loss in de novo Parkinson disease. Neurology. ISSN 0028-3878. (2018)
- Akopian, Armen N., Wood, John N. - Peripheral Nervous System-specific Genes Identified by Subtractive cDNA Cloning. Journal of Biologic Chemistry. 270:36, (1995), 21264–21270.
- Archibald, Neil K. et al. - The retina in Parkinsons disease. Brain. ISSN 14602156. 132:5, (2009), 1128–1145.
- Armstrong, Richard A. - Visual signs and symptoms of dementia with Lewy bodies. Clinical and Experimental Optometry. ISSN 08164622. 95:6, (2012), 621–630.
- Anwar, S. et al. - Functional Alterations to the Nigrostriatal System in Mice Lacking All Three Mem bers of the Synuclein Family. Journal of Neuroscience. ISSN 0270-6474. 31:20, (2011), 7264–7274.
- Barber, Alistair J. et al. - Neural apoptosis in the retina during experimental and human diabetes: Early onset and effect of insulin. Journal of Clinical Investigation. ISSN 00219738. 102:4, (1998), 783–791.
- Bartels, Tim et al. - α -Synuclein occurs physiologically as a helically folded tetramer that resists aggregation. Nature. ISSN 0028-0836. 477:7362, (2011), 107–110.
- Barzilai, Nir et al. - The critical role of metabolic pathways in aging. Diabetes. ISSN 00121797. 61:6, (2012), 1315–1322
- Alamouti, Bijan, Funk, J. - Retinal thickness decreases with age: An OCT study. British Journal of Ophthalmology. ISSN 00071161. 87:7, (2003), 899–901.
- Bandello, Francesco et al. - Retinal Layer Location of Increased Retinal Thickness in Eyes with Subclinical and Clinical Macular Edema in Diabetes Type 2. Ophthalmic Research. ISSN 14230259. 54:3, (2015), 112–117.
- Baptista, Filipa I. et al. - Diabetes induces early transient changes in the content of vesicular transporters and no major effects in neurotransmitter release in hippocampus and retina. Brain Research. ISSN 00068993. 1383 (2011), 257–269.
- Baynest, Habtamu Wondifraw - Classification, Pathophysiology, Diagnosis and Management of Diabetes Mellitus. Journal of Diabetes & Metabolism. ISSN 21556156. 6:5, (2015).

- Bertoncini, Carlos W. et al. - Structural Characterization of the Intrinsically Unfolded Protein β -Synuclein, a Natural Negative Regulator of α -Synuclein Aggregation. Journal of Molecular Biology. (2007), 708–722.
- Biousse, V. et al. - Ophthalmologic features of Parkinson's disease. Neurology. ISSN 00283878. 62:2, (2004), 177–180
- Blesa, Javier et al. - Animal Models of Parkinson's Disease. Challenges in Parkinson's disease. (2016).
- Bloomfield, Stewart A., Dacheux, Ramon F. - Rod vision: Pathways and processing in the mammalian retina. Progress in Retinal and Eye Research. ISSN 13509462. 20:3, (2001), 351–384.
- Bloomfield, Stewart A., Völgyi, Béla - The diverse functional roles and regulation of neuronal gap junctions in the retina. Nature Reviews Neuroscience. ISSN 1471003X. 10:7, (2009), 495–506.
- Bolam, J. Paul, Pissadaki, Eleftheria K. - Living on the edge with too many mouths to feed: Why dopamine neurons die. Movement Disorders. ISSN 08853185. 27:12, (2012), 1478–1483.
- Bodis-Wollner, Ivan et al. - A-Synuclein in the Inner Retina in Parkinson Disease. Annals of Neurology. ISSN 15318249. 75:6, (2014), 964–966.
- Braekevelt C.R. and Hollenberg M.J. - The Development of the retina of the albino rat. American Journal of Anatomy. 10:1, (1978).
- Bringmann, Andreas, Wiedemann, Peter - Müller Glial Cells in Retinal Disease. Ophthalmologica. (2012), 1–19.
- Bui, Bang V. et al. - Investigating structural and biochemical correlates of ganglion cell dysfunction in streptozotocin-induced diabetic rats. Experimental Eye Research. ISSN 00144835. 88:6, (2009), 1076–1083.
- Bulens, C. et al. - Effect of stimulus orientation on contrast sensitivity in Parkinson's disease. Neurology. 38:1, (1988), 76 LP-76.
- Burré, Jacqueline et al. - α -Synuclein Promotes SNARE-Complex Assembly in Vivo and in Vitro. Science. 329:5999, (2010), 1663 LP-1667.
- Butler, Brittany et al. - Alpha-synuclein modulates dopamine neurotransmission. Journal of Chemical Neuroanatomy. ISSN 0891-0618. (2016), 1–9.
- Cano, J. et al. - Morphological changes in the retina of ageing rats. Archives of Gerontology and Geriatrics. ISSN 01674943. 5:1, (1986), 41–50.

- Cárdenas, Ana María, Marengo, Fernando D. - How the stimulus defines the dynamics of vesicle pool recruitment, fusion mode, and vesicle recycling in neuroendocrine cells. Journal of Neurochemistry. ISSN 14714159. (2016), 867–879.
- Carpineto, P. et al. - Neuroretinal alterations in the early stages of diabetic retinopathy in patients with type 2 diabetes mellitus. Eye (Basingstoke). ISSN 14765454. 30:5, (2016), 673–679.
- Chang, Richard Cheng-An et al. - High-Fat Diet–Induced Retinal Dysfunction. Investigative Ophthalmology & Visual Science. ISSN 1552-5783. 56:4, (2015), 2367.
- Cheng, Zhe et al. - Expression of the dopamine transporter in rat and bullfrog retinas. NeuroReport. ISSN 0959-4965. 17:8, (2006), 773–777.
- Chinta, Shankar J. et al. - Mitochondrial alpha-synuclein accumulation impairs complex I function in dopaminergic neurons and results in increased mitophagy in vivo. Neuroscience Letters. ISSN 03043940. 486:3, (2010), 235–239.
- Clayton, David F., George, Julia M. - The synucleins: A family of proteins involved in synaptic function, plasticity, neurodegeneration and disease. Trends in Neurosciences. ISSN 01662236. 21:6, (1998), 249–254.
- Cooper, Antony A. et al. - α -Synuclein Blocks ER-Golgi Traffic and Rab1 Rescues Neuron Loss in Parkinson's Models. Science. 313:5785, (2006), 324 LP-328.
- Chu, Yaping and Kordower, Jeffrey H. - Age-associated increases of α -synuclein in monkeys and humans are associated with nigrostriatal dopamine depletion : Is this the target for Parkinson's disease ?. Neurobiology of Disease. 25 (2007), 134–149.
- Das, Arup - Diabetic Retinopathy : Battling the Global Epidemic. Investigating Ophthalmology & Visual Sciences. ISSN: 1552-5783, 57:15, (2016).
- Dauer, William, Przedborski, Serge - Parkinson's disease: Mechanisms and models. Neuron. ISSN 08966273. 39:6, (2003), 889–909.
- Dehay B et al. - Targeting α -synuclein for treating Parkinson's disease: mechanistic and therapeutic considerations. Lancet Neurology. 14:8, (2017), 855–866.
- Dickson, Dennis W. et al. - Neuropathological assessment of Parkinson's disease: refining the diagnostic criteria. The Lancet Neurology. ISSN 1474-4422. 8:12, (2009), 1150–1157.
- Dijk, Hille W. Van et al. - Selective Loss of Inner Retinal Layer Thickness in Type 1 Diabetic Patients with Minimal Diabetic Retinopathy. Investigative Ophthalmology & Visual Science. ISSN 1552-5783. 50:7, (2009), 3404.
- Djamgoz, M. B. A. et al. - Neurobiology of retinal dopamine in relation to degenerative states of the tissue. Vision Research. ISSN 00426989. 37:24, (1997), 3509–3529.

- Doherty, Karen M. et al. – Parkinson’s Disease: A Clinicopathologic Entity? JAMA neurology. 70:5, (2014), 571–579.
- Dorsey, Er et al. - Projected number of people with Parkinson disease in the most populous nations, 2005 through 2030. Neurology. ISSN 0028-3878. 68 (2007), 384–386.
- Duh, Elia J. et al. - Diabetic retinopathy: current understanding, mechanisms, and treatment strategies. JCI Insight. ISSN 2379-3708. 2:14, (2017).
- Eeden, S. K. Van Den - Incidence of Parkinson’s Disease: Variation by Age, Gender, and Race/Ethnicity. American Journal of Epidemiology. ISSN 0002-9262. 157:>11, (2003), 1015–1022.
- Ekstrand, M. I. et al. - Progressive parkinsonism in mice with respiratory-chain-deficient dopamine neurons. Proceedings of the National Academy of Sciences. ISSN 0027-8424. 104:4, (2007), 1325–1330.
- Ekstrand, Mats I., Galter, Dagmar - The MitoPark Mouse - An animal model of Parkinson’s disease with impaired respiratory chain function in dopamine neurons. Parkinsonism and Related Disorders. ISSN 13538020. 15:SUPPL. 3, (2009), S185–S188.
- Emamzadeh, Fatemeh Nouri - Alpha-synuclein structure, functions, and interactions. Journal of Research in Medical Sciences. ISSN 17357136. 21:2, (2016).
- El-Sayyad, Hassan I. H. et al. - Analysis of fine structure and biochemical changes of retina during aging of Wistar albino rats. Clinical & experimental ophthalmology. ISSN 1442-9071. 42:2, (2014), 169–81.
- Fahn, Stanley, Sulzer, David - Neurodegeneration and Neuroprotection in Parkinson Disease. NeuroRx. ISSN 15455343. 1:1, (2004), 139–154.
- Fox, Susan H. et al. - The Movement Disorder Society Evidence-Based Medicine Review Update: Treatments for the motor symptoms of Parkinson’s disease. Movement Disorders. ISSN 08853185. 26:S3, (2011), S2–S41.
- Frank, Robert N. - Diabetic Retinopathy. New England Journal of Medicine. 350:1, (2004), 48–58.
- Fujiwara, Hideo et al. - A-Synuclein Is Phosphorylated in Synucleinopathy Lesions. Nature Cell Biology. ISSN 14657392. 4:2, (2002), 160–164.
- Fusco, Giuliana et al. - Structural basis of synaptic vesicle assembly promoted by a -synuclein. Nature Communications. 7 (2016), 1–11.
- Galvin, J. E. et al. - Axon pathology in Parkinson’s disease and Lewy body dementia hippocampus contains alpha -, beta -, and gamma -synuclein. Proceedings of the National Academy of Sciences. ISSN 0027-8424. 96:23, (1999), 13450–13455.

- Gao, Hui Ming, Hong, Jau Shyong - Why neurodegenerative diseases are progressive: uncontrolled inflammation drives disease progression. Trends in Immunology. ISSN 14714906. 29:8, (2008), 357–365.
- Gaspar, J. M. et al. - Diabetes differentially affects the content of exocytotic proteins in hippocampal and retinal nerve terminals. Neuroscience. ISSN 03064522. 169:4, (2010), 1589–1600.
- Gastinger, Matthew J. et al. - Loss of cholinergic and dopaminergic amacrine cells in streptozotocin- diabetic rat and Ins2Akita-diabetic mouse retinas. Investigative Ophthalmology and Visual Science. ISSN 01460404. 47:7, (2006), 3143–3150.
- George, Julia M. - The synucleins. Genome Biology. ISSN 1465-6914. (2001), 1–6.
- Giasson, Benoit I. et al. - A Hydrophobic Stretch of 12 Amino Acid Residues in the Middle of α -Synuclein Is Essential for Filament Assembly. Journal of Biological Chemistry. ISSN 00219258. 276:4, (2001), 2380–2386.
- Green, Douglas R. et al. - Mitochondria and the autophagy-inflammation-cell death axis in organismal aging. Science. ISSN 00368075. 333:6046, (2011), 1109–1112.
- Greten-Harrison, B. et al. – α -Synuclein triple knockout mice reveal age-dependent neuronal dysfunction. Proceedings of the National Academy of Sciences. ISSN 0027-8424. 107:45, (2010), 19573–19578.
- Gropper, Sareen Stepnick et al. - Free galactose content of fresh fruits and strained fruit and vegetable baby foods: More foods to consider for the galactose-restricted diet. Journal of the American Dietetic Association. ISSN 00028223. 100:5, (2000), 573–575.
- Gubellini, P., Kachidian, P. - Animal models of Parkinson's disease: An updated overview. Revue neurologique. ISSN 0035-3787. 171:11, (2015), 750—761.
- Gustincich, Stefano et al. - Control of dopamine release in the retina: A transgenic approach to neural networks. Neuron. ISSN 08966273. 18:5, (1997), 723–736.
- Haider, Saida et al. - Age-related learning and memory deficits in rats : role of altered brain neurotransmitters , acetylcholinesterase activity and changes in antioxidant defense system. (2014).
- Hajee, M. E. et al. - Inner retinal layer in Parkinson disease. Archives of Ophthalmology. 127:6, (2009), 737–741.
- Halban, Philippe A. et al. - β -Cell failure in type 2 diabetes: Postulated mechanisms and prospects for prevention and treatment. Journal of Clinical Endocrinology and Metabolism. ISSN 19457197. 99:6, (2014), 1983–1992.
- Hankins, M. W. - Functional dopamine deficits in the senile rat retina. Visual Neuroscience. 17:6, (2000), 839–845.

- Hansen, Christian et al. - α -Synuclein Propagates From Mouse Brain To Grafted Dopaminergic Neurons and Seeds Aggregation in Cultured Human Cells. The Journal of Clinical Investigation. ISSN 00219738. 121:2, (2011), 715–725.
- Hao, Ling et al. - The influence of gender, age and treatment time on brain oxidative stress and memory impairment induced by D-galactose in mice. Neuroscience Letters. ISSN 18727972. (2014).
- Harwerth, Ronald S. et al. - Age-related losses of retinal ganglion cells and axons. Investigative Ophthalmology and Visual Science. ISSN 01460404. 49:10, (2008), 4437–4443.
- Hashimoto, M. et al. - β -Synuclein inhibits α -synuclein aggregation: a possible role as an anti-parkinsonian factor. Neuron. ISSN 0896-6273. 32:3, (2001), 213–223.
- Hashimoto, M et al. - β -synuclein regulates Akt activity in neuronal cells: A possible mechanism for neuroprotection in Parkinson's disease. Journal of Biological Chemistry. ISSN 00219258. 279:22, (2004), 23622–23629.
- Hegde, Muralidhar L. and Jagannatha Rao, K. S. - Challenges and complexities of α -synuclein toxicity: New postulates in unfolding the mystery associated with Parkinson's disease. Archives of Biochemistry and Biophysics. ISSN 00039861. 418:2, (2003), 169–178.
- Henkind, P., R.I. Hansen, and J. Szalay, Ocular circulation, in Physiology of the human eye and visual system, R.E. Records, Editor. Hagerstown, Md , (1979)
- Heydemann, Ahlke - An Overview of Murine High Fat Diet as a Model for Type 2 Diabetes Mellitus. Journal of Diabetes Research. ISSN 23146753. 2016 (2016).
- Humphreys, David T. et al. - Clusterin has chaperone-like activity similar to that of small heat shock proteins. Journal of Biological Chemistry. ISSN 00219258. 274:11, (1999), 6875–6881.
- Inzelberg, Rivka et al. - Retinal nerve fiber layer thinning in Parkinson disease. Vision Research. ISSN 00426989. 44:24, (2004), 2793–2797.
- Jain, Manish Kumar et al. - Comparative Analysis of the Conformation, Aggregation, Interaction, and Fibril Morphologies of Human α -, β -, and γ -Synuclein Proteins. Biochemistry. ISSN 15204995. 57:26, (2018), 3830–3848.
- Ji, Hongjun et al. - Identification of a breast cancer-specific gene, BCSG1, by direct differential cDNA sequencing. Cancer Research. ISSN 00085472. 57:4, (1997), 759–764.
- Jiang, Yangfu et al. - gSynuclein, a Novel Heat-Shock Protein-Associated Chaperone, Stimulates Ligand-Dependent Estrogen Receptor A Signaling and Mammary Tumorigenesis. Cancer Research. ISSN 00085472. 64:13, (2004), 4539–4546.
- Kahn, Barbara B. and Flier J.S.. - Obesity and insulin resistance. Journal of Clinical Investigation. 106:4, (2000), 473–481.

- Kalia, Lorraine V., Lang, Anthony E. - Parkinson's disease. The Lancet. ISSN 1474547X. 386:9996, (2015), 896–912.
- Kalia, Suneil K. et al. - Deep brain stimulation for Parkinson's disease and other movement disorders. Current Opinion in Neurology. ISSN 13507540. 26:4, (2013), 374–380.
- Katsarou, Anna-Maria et al. - Interneuronopathies and their role in early life epilepsies and neurodevelopmental disorders. Epilepsia Open. ISSN 24709239. 2:3, (2017), 284–306.
- Kaushik, Susmita, Cuervo, Ana Maria - Proteostasis and aging. Nature Medicine. 21 (2015), 1406.
- Kern, Timothy S., Engerman, Ronald L. - Pharmacological Inhibition of Diabetic Retinopathy: Aminoguanidine and Aspirin. Diabetes. ISSN 00121797. 50:7, (2001), 1636–1642.
- King, Aileen J. F. - The use of animal models in diabetes research. British Journal of Pharmacology. ISSN 00071188. 166:3, (2012), 877–894.
- Kharroubi, Akram T. - Diabetes mellitus: The epidemic of the century. World Journal of Diabetes. ISSN 1948-9358. 6:6, (2015), 850.
- Khoo, Tien K. et al. - The spectrum of nonmotor symptoms in early Parkinson disease. Neurology. ISSN 00283878. 80:3, (2013), 276–281. Ahre, Bo - The High-Fat Diet–Fed Mouse. Diabetes. 237 (2004), 215–219.
- Kleinridders, Andre et al. - Insulin resistance in brain alters dopamine turnover and causes behavioral disorders. Proceedings of the National Academy of Sciences. ISSN 0027-8424. 112:11, (2015), 3463–3468.
- Koga, Hiroshi et al. - Protein homeostasis and aging: The importance of exquisite quality control. Ageing Research Reviews. ISSN 15681637. 10:2, (2011), 205–215.
- Kokhan, Viktor S. et al. - Differential involvement of the gamma-synuclein in cognitive abilities on the model of knockout mice. BMC Neuroscience. ISSN 14712202. 14 (2013).
- Kõks, Sulev et al. - Mouse models of ageing and their relevance to disease. Mechanisms of Ageing and Development. ISSN 18726216. 160 (2016), 41–53.
- Kolb, Helga - How the Retina Works. American Scientist. (2003).
- Kolb, H. et al. - The synaptic organization of the dopaminergic amacrine cell in the cat retina. Journal of Neurocytology. ISSN 03004864. 19:3, (1990), 343–366.
- Kolb H, Fernandez E, Nelson R, editors. Webvision: The Organization of the Retina and Visual System [Internet]. Salt Lake City (UT): University of Utah Health Sciences Center; (1995).
- Kuilman, Thomas et al. - The essence of senescence. Genes Dev. 24, (2010), 2463–2479.
- Lavedan, C. - The synuclein family. Genome Research. ISSN 10889051. 8:9, (1998), 871–880.

- Lavedan, C. et al. - Identification, localization and characterization of the human gamma-synuclein gene. Human genetics. ISSN 0340-6717. 103:1, (1998), 106–112.
- Lawrence, Toby - The nuclear factor NF-kappaB pathway in inflammation. Cold Spring Harbor perspectives in biology. ISSN 19430264. 1:6, (2009), 1–10.
- Lee, F. S. et al - Direct binding and functional coupling of alpha-synuclein to the dopamine transporters accelerate dopamine-induced apoptosis. The FASEB Journal. ISSN 15306860. 15:6, (2001), 916–926.
- Lee, H. J. - Clearance of α -Synuclein Oligomeric Intermediates via the Lysosomal Degradation Path way. Journal of Neuroscience. ISSN 0270-6474. 24:8, (2004), 1888–1896.
- Leger, François et al. - Protein aggregation in the aging retina. Journal of Neuropathology and Experimental Neurology. ISSN 00223069. 70:1, (2011), 63–68.
- Lesage, Suzanne, Brice, Alexis - Parkinson's disease: From monogenic forms to genetic susceptibility factors. Human Molecular Genetics. ISSN 09646906. 18:R1, (2009), 48–59.
- Li, Ying C., Kavalali, Ege T. - Synaptic Vesicle-Recycling Machinery Components as Potential Therapeutic Targets. Pharmacological Reviews. ISSN 0031-6997. 69:2, (2017), 141–160.
- Li, Jie Qiong et al. - The role of the LRRK2 gene in Parkinsonism. Molecular neurodegeneration. ISSN 17501326. 9:47 (2014)
- Liu, Bin et al. - Parkinson ' s Disease and Exposure to Infectious Agents and Pesticides and the Occurrence of Brain Injuries : Role of Neuroinflammation. Environmental Health Perspectives 111:8, (2003), 1065–1073.
- Lou, Xiaochu et al. - α -Synuclein may cross-bridge v-SNARE and acidic phospholipids to facilitate SNARE-dependent vesicle docking. Biochemical Journal. ISSN 0264-6021. 474:12, (2017), 2039–2049.
- López-Otín, Carlos et al. - The hallmarks of aging. Cell. ISSN 10974172. 153:6, (2013).
- Lücking CB et al. – Association between early-onset Parkinson's disease and Mutations in the Parkin Gene. The New England Journal of Medicine. (2000).
- Lytkina, O. A. et al. - Gamma-synuclein binds synaptic vesicles but does not interact with SNARE-complex proteins. Doklady Biochemistry and Biophysics. ISSN 1607-6729. 456:1, (2014), 108–110.
- Maroteaux, L. et al. - Synuclein: a neuron-specific protein localized to the nucleus and presynaptic nerve terminal. The Journal of neuroscience: the official journal of the Society for Neuroscience. ISSN 0270-6474. 8:8, (1988), 2804–2815.
- Matsunaga D, Yi J, Puliafito C, Kashani A. - OCT Angiography in Healthy Human Subjects. Ophthalmic Surg Lasers Imaging Retina. 45 (2010) 510-515.

- Maxwell, Michele M. et al. - The Sirtuin 2 microtubule deacetylase is an abundant neuronal protein that accumulates in the aging CNS. Human Molecular Genetics. ISSN 09646906. 20:20, (2011), 3986–3996.
- McCoy, Melissa K., Cookson, Mark R. - Mitochondrial Quality Control and Dynamics in Parkinson's Disease. Antioxidants & Redox Signaling. ISSN 1523-0864. 16:9, (2012), 869–882.
- Mendoza-Santesteban, Carlos E. et al. - The retina in multiple system atrophy: Systematic review and meta-analysis. Frontiers in Neurology. ISSN 16642295. 8, (2017).
- Meredith, Gloria E., Rademacher, David J. - MPTP Mouse Models of Parkinson's Disease: An Update. J Parkinsons Dis. ISSN 1877-718X. 1:1, (2012), 19–33.
- Middleton, Elizabeth R., Rhoades, Elizabeth - Effects of curvature and composition on α -synuclein binding to lipid vesicles. Biophysical Journal. ISSN 15420086. 99:7, (2010), 2279–2288.
- Mosharov, Eugene V. et al. - Interplay between Cytosolic Dopamine, Calcium, and α -Synuclein Causes Selective Death of Substantia Nigra Neurons. Neuron. ISSN 08966273. 62:2, (2009), 218–229.
- Muresan, Zoia, Besharse, Joseph C. - D2-like dopamine receptors in amphibian retina: Localization with fluorescent ligands. Journal of Comparative Neurology. ISSN 10969861. 331:2, (1993), 149–160.
- Murphy, D. D. et al. - Synucleins are developmentally expressed, and alpha-synuclein regulates the size of the presynaptic vesicular pool in primary hippocampal neurons. The Journal of neuroscience. ISSN 1529-2401. 20:9, (2000), 3214–3220.
- Nadal-Nicolás, Francisco M. et al. - The aging rat retina: from function to anatomy. Neurobiology of Aging. ISSN 15581497. 61: (2018), 146–168.
- Nakajo, S. et al. - a new brain specific 14-kDa protein is phosphoprotein in its complete amino acid sequence and evidence for phosphorylation. Molecular Brain Research. (1993), 1057–1063.
- Nakajo, S et al. - Localization of phosphoneuroprotein 14 (PNP 14) and its mRNA expression in rat brain determined by immunocytochemistry and in situ hybridization. Molecular Brain Research. ISSN 0169328X. 27:1, (1994), 81–86.
- Nalls, Mike A. et al. - Large-scale meta-analysis of genome-wide association data identifies six new risk loci for Parkinson's disease. Nature Genetics. ISSN 15461718. 46:9, (2014), 989–993

- Nemani, Venu M. et al. - Increased Expression of α -Synuclein Reduces Neurotransmitter Release by Inhibiting Synaptic Vesicle Reclustering after Endocytosis. Cell Press. ISSN 08966273. 65:1, (2010), 66–79.
- Ninkina, Natalia et al. - Synucleinopathy: Neurodegeneration associated with overexpression of the mouse protein. Human Molecular Genetics. ISSN 09646906. 18:10, (2009), 1779–1794.
- Nishimura, Chihiro, Kuriyama, Kinya - Alterations in the Retinal Dopaminergic Neuronal System in Rats with Streptozotocin-Induced Diabetes. Journal of Neurochemistry. (1985), 448–455.
- Nguyen-Legros, J. et al. - Dopamine inhibits melatonin synthesis in photoreceptor cells through a D2-like receptor subtype in the rat retina: biochemical and histochemical evidence. Journal of neurochemistry. ISSN 0022-3042. 67:6, (1996), 2514–2520.
- Nguyen-Legros, J. - Functional neuroarchitecture of the retina: hypothesis on the dysfunction of retinal dopaminergic circuitry in Parkinson's disease. Surgical and radiologic anatomy: SRA. ISSN 0930-1038. 10:2, (1988), 137–44.
- Noda, Kousuke et al. - Leukocyte adhesion molecules in diabetic retinopathy. Journal of Ophthalmology. ISSN 2090004X. (2012).
- Normando, Eduardo Maria et al. - The retina as an early biomarker of neurodegeneration in a rotenone-induced model of Parkinson's disease: Evidence for a neuroprotective effect of rosiglitazone in the eye and brain. Acta Neuropathologica Communications. ISSN 20515960. 4:1, (2016), 1–15.
- Nuñez, Gabriel et al. - Caspases: The proteases of the apoptotic pathway. Oncogene. ISSN 09509232. 17:25, (1998), 3237–3245.
- Nuscher, Brigitte et al. -Synuclein Has a High Affinity for Packing Defects in a Bilayer Membrane. The Journal of Biological Chemistry. 279:21, (2004), 21966–21975.
- Noyce, Alastair J. et al. - Meta-Analysis of Early Nonmotor Features and Risk Factors for Parkinson Disease. American Neurologic Association. (2012).
- Ohtake, H. et al. - α -Synuclein gene alterations in dementia with Lewy bodies. Neurology (2004), 805–811.
- Oliveira, Rita Machado De et al. - The mechanism of sirtuin 2–mediated exacerbation of alpha-synuclein toxicity in models of Parkinson disease. PLoS Biology. ISSN 15457885. 15:3, (2017), 1–27.
- Oueslati, Abid et al. – Role of post-translational modifications in modulating the structure, function and toxicity of α -synuclein: Implications for Parkinson's disease pathogenesis and therapies. Progress in Brain Research. ISSN 0079-6123. 183 (2010).

- Outeiro, Tiago Fleming et al. - Formation of toxic oligomeric α -synuclein species in living cells. PLoS ONE. ISSN 19326203. 3:4, (2008), 1–9.
- Owsley, Cynthia et al. - Delays in rod-mediated dark adaptation in early age-related maculopathy. Ophthalmology. ISSN 01616420. 108:7, (2001), 1196–1202.
- Parihar, M.S. et al. - Mitochondrial association of alpha-synuclein causes oxidative stress. Cell and Molecular Life Sciences 65 (2008), 1272–1284.
- Park, S. H. et al. - Apoptotic death of photoreceptors in the streptozotocin-induced diabetic rat retina. Diabetologia. ISSN 0012186X. 46:9, (2003), 1260–1268.
- Peng, Xiangmin M. et al. - α -Synuclein activation of protein phosphatase 2A reduces tyrosine hydroxylase phosphorylation in dopaminergic cells. Journal of Cell Science. (2005).
- Perez, Ruth G. et al. - A role for α -synuclein in the Regulation of Dopamine Biosynthesis. The Journal of Neuroscience. ISSN 1529-2401. 22:8, (2002), 3090–3099.
- Perrin, Richard J. et al. - Interaction of human α -synuclein and Parkinson's disease variants with phospholipids: Structural analysis using site-directed mutagenesis. Journal of Biological Chemistry. ISSN 00219258. 275:44, (2000), 34393–34398.
- Peters, Owen M. et al. - Selective pattern of motor system damage in gamma-synuclein transgenic mice mirrors the respective pathology in amyotrophic lateral sclerosis. Neurobiology of Disease. ISSN 09699961. 48:1, (2012), 124–131.
- Peterson, R. G. et al. - Zucker Diabetic Fatty Rat as a Model for Non-insulin-dependent Diabetes Mellitus. ILAR Journal. ISSN 1084-2020. 32:3, (1990), 16–19.
- Petrie, Emma J. et al. - Conformational switching of the pseudokinase domain promotes human MLKL tetramerization and cell death by necroptosis. Nature Communications. ISSN 20411723. 9:1, (2018).
- Phillips, Michael S. et al. - Leptin receptor missense mutation in the fatty Zucker rat. Nature Genetics. ISSN 15461718. 13:1, (1996), 18–19.
- Pick, A. et al. - Role of apoptosis in failure of beta-cell mass compensation for insulin resistance and beta-cell defects in the male Zucker diabetic fatty rat. Diabetes. 47:3, (1998), 358 LP-364.
- Pissadaki, Eleftheria et al.- The energy cost of action potential propagation in dopamine neurons: clues to susceptibility in Parkinson's disease. Frontiers in Computational Neuroscience. ISSN 1662-5188 (2013), 1–17.
- Polymeropoulos, Mihael H. et al. - Mutation in the α -synuclein gene identified in families with Parkinson's disease. Science. ISSN 00368075. 276:5321, (1997), 2045–2047.
- Popova, Blagovesta et al. - Sumoylation Protects Against β -Synuclein Toxicity in Yeast. Frontiers in Molecular Science. 11 (2018), 1–17.

- Poewe, Werner et al. – Parkinson’s disease. Primer. 3 (2017).
- Price, Diana L. et al. - Longitudinal live imaging of retinal α -synuclein::GFP deposits in a transgenic mouse model of Parkinson’s Disease/Dementia with Lewy Bodies. Scientific Reports. ISSN 20452322. 6:July, (2016), 1–10.
- Quilty, M. C. et al. - Localization of α -, β -, and γ -synuclein during neuronal development and alterations associated with the neuronal response to axonal trauma. Experimental Neurology. ISSN 00144886. 182:1, (2003), 195–207.
- Rapin I. et al. - Cockayne Syndrome in Adults: Review With Clinical and Pathologic Study of a New Case. Journal of Child Neurology. ISSN 08966273. 8:9, (2014), 1385–1395.
- Reeve, A. K. et al. - Aggregated α -synuclein and complex I deficiency: Exploration of their relationship in differentiated neurons. Cell Death and Disease. ISSN 20414889. 6:7, (2015), e1820-10.
- Ribelayga, Christophe et al. - The Circadian Clock in the Retina Controls Rod-Cone Coupling. Neuron. ISSN 08966273. 59:5, (2008), 790–801.
- Roy, M.S. et al. - Color Vision Defects in Early Diabetic Retinopathy. Archives of Ophthalmology. ISSN 15383601. 104:2, (1986), 225–228.
- Sang, Myun Park et al. - Distinct roles of the N-terminal-binding domain and the C-terminal-solubilizing domain of α -synuclein, a molecular chaperone. Journal of Biological Chemistry. ISSN 00219258. 277:32, (2002), 28512–28520.
- Santos, Gabriela Vilaça Cruz Cerqueira dos - Qual o papel das sinucleínas na neurodegeneração da retina?. Lisboa : Faculdade de Ciências Médicas, 2017. Tese de Mestrado.
- Senior, Steven L. et al. - Increased striatal dopamine release and hyperdopaminergic-like behaviour in mice lacking both alpha-synuclein and gamma-synuclein. European Journal of Neuroscience. ISSN 0953816X. 27:4, (2008), 947–957.
- Siderowf, Andrew, Lang, Anthony E. - Premotor Parkinson’s disease: Concepts and definitions. Movement Disorders. ISSN 08853185. 27:5, (2012), 608–616.
- Simó, R., Hernández, C. - Intravitreal anti-VEGF for diabetic retinopathy: Hopes and fears for a new therapeutic strategy. Diabetologia. ISSN 0012186X. 51:9, (2008), 1574–1580.
- Schmidt, Robert E. et al. - Analysis of the Zucker Diabetic Fatty (ZDF) Type 2 Diabetic Rat Model Suggests a Neurotrophic Role for Insulin/IGF-I in Diabetic Autonomic Neuropathy. AM J Pathol. 163:1, (2003), 21–28.
- Sokol, Samuel et al. - Contrast Sensitivity in Diabetics with and Without Background Retinopathy. Archives of Ophthalmology. ISSN 15383601. 103:1, (1985), 51–54.

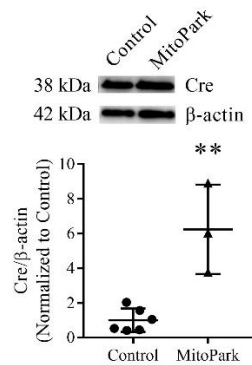
- Söllner, Thomas et al. - A protein assembly-disassembly pathway in vitro that may correspond to sequential steps of synaptic vesicle docking, activation, and fusion. Cell. ISSN 00928674. 75:3, (1993), 409–418.
- Souza, José M. et al. - Chaperone-like activity of synucleins. FEBS Letters. ISSN 00145793. 474:1, (2000), 116–119
- Spillantini, M. G. et al. - Assignment of human alpha-synuclein (SNCA) and beta-synuclein (SNCB) genes to chromosomes 4q21 and 5q35. Genomics. ISSN 0888-7543. 27:2, (1995), 379–81.
- Srinivasan, K., Ramarao, P. - Animal models in type 2 diabetes research: an overview. The Indian journal of medical research. ISSN 0971-5916. 125:3, (2007), 451–472.
- Stitt, A. W. et al. - Substrates modified by advanced glycation end-products cause dysfunction and death in retinal pericytes by reducing survival signals mediated by platelet-derived growth factor. Diabetologia. ISSN 0012186X. 47:10, (2004), 1735–1746.
- Surwit, R. S. S. et al. - Diet-induced type II diabetes in C57BL/6J mice. Diabetes. ISSN 00121797. 37:9, (1988), 1163–1167.
- Surwit, R. S. et al. - Differential effects of fat and sucrose on body composition in C57BL/6 and A/J mice. Metabolism: clinical and experimental. ISSN 0026-0495. 47:11, (1998), 1354–1359.
- Sung, Yoon Hui, Eliezer, David - Residual Structure, Backbone Dynamics, and Interactions within the Synuclein Family. Journal of Molecular Biology. ISSN 00222836. 372:3, (2007), 689–707.
- Surgucheva, I. et al. - Effect of γ -synuclein silencing on apoptotic pathways in retinal ganglion cells. Journal of Biological Chemistry. ISSN 00219258. 283:52, (2008), 36377–36385.
- Surgucheva, I. et al. - New alpha- and gamma-synuclein immunopathological lesions in human brain. Acta Neuropathol Commun. ISSN 2051-5960 (Electronic). 2 (2014), 132.
- Surgucheva, I. et al. - Synucleins in glaucoma: Implication of γ -synuclein in glaucomatous alterations in the optic nerve. Journal of Neuroscience Research. ISSN 03604012. 68:1, (2002), 97–106.
- Surguchov, Andrei et al. - Synucleins in ocular tissues. Journal of Neuroscience Research. ISSN 03604012. 65:1, (2001), 68–77.
- Tang, Johnny, Kern, Timothy S. - Progress in Retinal and Eye Research Inflammation in diabetic retinopathy. Progress in Retinal and Eye Research. ISSN 1350-9462. 30:5, (2011), 343–358.
- Taschenberger, Grit et al. - B-Synuclein Aggregates and Induces Neurodegeneration in Dopaminergic Neurons. Annals of Neurology. ISSN 03645134. 74:1, (2013), 109–118.

- Thayanidhi, N. et al. - α -Synuclein Delays Endoplasmic Reticulum (ER)-to-Golgi Transport in Mammalian Cells by Antagonizing ER/Golgi SNAREs. Molecular biology of the cell. ISSN 1939-4586. 21:22, (2010), 4042–4056.
- Tenreiro, Sandra et al. - Protein phosphorylation in neurodegeneration: friend or foe? Frontiers in Molecular Neuroscience. ISSN 1662-5099. 7:May, (2014), 1–30.
- Tenreiro, Sandra et al. - Yeast reveals similar molecular mechanisms underlying α - and β -synuclein toxicity. Human Molecular Genetics. ISSN 14602083. 25:2, (2016), 275–290.
- Tian, Jane et al. - Advanced glycation endproduct-induced aging of the retinal pigment epithelium and choroid: a comprehensive transcriptional response. Proceedings of the National Academy of Sciences of the United States of America. ISSN 0027-8424. 102:33, (2005), 11846–11851.
- Tian, Tian et al. - Common pathophysiology affecting diabetic retinopathy and Parkinson's disease. Medical Hypotheses. ISSN 15322777. 85:4, (2015), 397–398.
- Trifunovic A. et al. - Premature ageing in mice expressing defective mitochondrial DNA polymerase. Nature. ISSN 0028-0836. 395, 429 (1998), 272–274.
- Samuel, Melanie A. et al. - Age-related alterations in neurons of the mouse retina. The Journal of neuroscience. ISSN 1529-2401. 31:44, (2011), 16033–44.
- Ulusoy, Ayse et al. - Dysregulated dopamine storage increases the vulnerability to α -synuclein in nigral neurons. Neurobiology of Disease. ISSN 09699961. 47:3, (2012), 367–377.
- Uversky, Vladimir N. et al. - Biophysical Properties of the Synucleins and Their Propensities to Fibrillate. 277:14, (2002), 11970–11978.
- Vanguilder, Heather D. et al. - Diabetes downregulates presynaptic proteins and reduces basal synapsin i phosphorylation in rat retina. European Journal of Neuroscience. ISSN 0953816X. 28:1, (2008), 1–11.
- Varanese, Sara et al. - Apathy, but not depression, reflects inefficient cognitive strategies in Parkinson's disease. PLoS ONE. ISSN 19326203. 6:3, (2011).
- Vecino, Elena et al. - Glia-neuron interactions in the mammalian retina. Progress in Retinal and Eye Research. ISSN 18731635. 51 (2016), 1–40.
- Veruki, Margaret L. - Dopaminergic Neurons in the Rat Retina Express Dopamine D2 / 3 Receptors. (1997), 1096–1100.
- Versaux-Botteri, Claudine et al. - Morphology, density and distribution of tyrosine hydroxylase-like immunoreactive cells in the retina of mice. Brain Research. ISSN 00068993. 301:1, (1984), 192–197.
- Vicente Miranda, Hugo et al. - Glycation potentiates α -synuclein-associated neurodegeneration in synucleinopathies. Brain. ISSN 14602156. 140:5, (2017), 1399–1419.

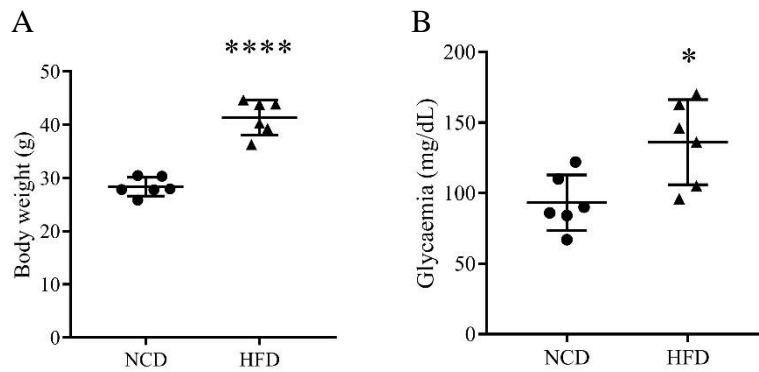
- Vicente Miranda, Hugo, Outeiro, Tiago Fleming - The sour side of neurodegenerative disorders: the effects of protein glycation. J Pathol. ISSN 00223417. 221:1, (2010), 13–25.
- Wakabayashi, Koichi et al. - The Lewy Body in Parkinson's Disease and Related Neurodegenerative Disorders. Molecular Neurobiology. 47 (2013), 495–508.
- Wales, Pauline et al. - Limelight on Alpha-Synuclein: Pathological and Mechanistic Implications in Neurodegeneration. Journal of Parkinson's Disease. 3, (2013), 415–459.
- Wang, Chunxin, Youle, Richard J. – The role of mitochondria in apoptosis. Annu Rev Genet. 43 (2016), 95–118.
- Wang, Huayi et al. - Mixed Lineage Kinase Domain-like Protein MLKL Causes Necrotic Membrane Disruption upon Phosphorylation by RIP3. Molecular Cell. ISSN 10974164. 54:1, (2014), 133–146.
- Wersinger, Christophe, Sidhu, Anita - Differential cytotoxicity of dopamine and H₂O₂ in a human neuroblastoma derived cell line transfected with alpha-synuclein and its familial Parkinson's disease-linked mutants. Neuroscience letters. ISSN 0304-3940. 342:1–2, (2003), 124–128.
- Wersinger, Christophe, Sidhu, Anita - Partial regulation of serotonin transporter function by gamma-synuclein. Neuroscience letters. ISSN 1872-7972. 453:3, (2009), 157–61.
- Wild S. et al. - Estimates for the year 2000 and projections for 2030. Diabetes Care. 27:5, (2004).
- Winzell M.S., Ahre, B. - The High-Fat Diet–Fed Mouse. Diabetes. 237:3 (2004), 215–219.
- Wishart, Thomas M. et al. - Synaptic Vulnerability in Neurodegenerative Disease. Journal of Neuropathology Experimental Neurology. 65:8, (2018), 733–739.
- Wong, T.Y. et al. - Diabetic retinopathy. Nature Reviews Disease Primers. ISSN 2056676X. 2 (2016).
- Wood, Stephen J. et al. - α -Synuclein Fibrillogenesis is Nucleation-dependent. Biochemistry. ISSN 0021-9258. (1999), 19509–19512.
- Wu, Dong Mei et al. - Purple sweet potato color repairs d-galactose-induced spatial learning and memory impairment by regulating the expression of synaptic proteins. Neurobiology of Learning and Memory. ISSN 10747427. 90:1, (2008), 19–27.
- Xie, Weilin, Chung, Kenny K. K. - Alpha-synuclein impairs normal dynamics of mitochondria in cell and animal models of Parkinson's disease. Journal of Neurochemistry. ISSN 00223042. 122:2, (2012), 404–414.
- Xu, Heping et al. - Para-inflammation in the aging retina. Progress in Retinal and Eye Research. ISSN 13509462. 28:5, (2009), 348–368.

- Yamauchi, Tomofusa et al. - Inhibition of glutamate-induced nitric oxide synthase activation by dopamine in cultured rat retinal neurons. Neuroscience Letters. ISSN 03043940. 347:3, (2003), 155–158.
- Yamin, Ghiam et al. - Forcing nonamyloidogenic b-synuclein to fibrillate. Biochemistry. ISSN 00062960. 44:25, (2005), 9096–9107.
- Yue, Xuejing et al. - Risk of Parkinson Disease in Diabetes Mellitus. Medicine. ISSN 0025-7974. 95:18, (2016), e3549.
- Yung, K. L. et al. - Immunocytochemical localization of D1 and D2 dopamine receptors in the basal ganglia of the rat: Light and electron microscopy. Neuroscience. ISSN 03064522. 65:3, (1995), 709–730.
- Zhang, Hong et al. - Role of gamma-synuclein in microtubule regulation. Experimental Cell Research. ISSN 10902422. 317:10, (2011), 1330–1339.
- Zhang, Ling et al. - Semi-quantitative analysis of α -synuclein in subcellular pools of rat brain neurons: An immunogold electron microscopic study using a C-terminal specific monoclonal antibody. Brain Research. ISSN 00068993. 1244, (2008), 40–52.
- Zhang, Nan Yan et al. - α -synuclein protofibrils inhibit 26 S proteasome-mediated protein degradation: Understanding the cytotoxicity of protein protofibrils in neurodegenerative disease pathogenesis. Journal of Biological Chemistry. ISSN 00219258. 283:29, (2008), 20288–20298.

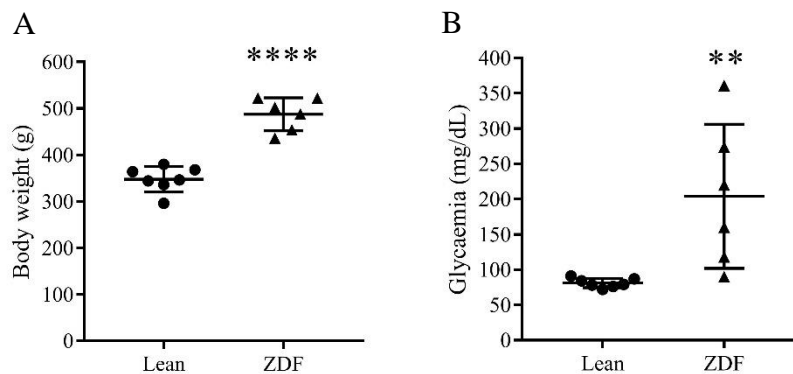
6. Appendices



Supplementary Figure 1 – Assessment of Cre recombinase levels by Western Blot in Control and MitoPark mice whole retina protein extracts. Upper panel corresponds to the western blot and the lower panel corresponds to densitometry analysis. A representative image of the western blot is shown. Data are presented as Mean ± SD. **p<0.01 MitoPark compared with Control; T-test.



Supplementary Figure 2 – Body weight and glycaemic characterization of NCD and HFD mice. N=6 for both groups. Data are present as Mean±SD. *p<0.05, ****p<0.0001 HFD compared to NCD; T-test.



Supplementary Figure 3 – Body weight and glycaemic characterization of Lean and ZDF rats. N=7 for Lean and N=6 for ZDF rats. Data are present as Mean±SD. **p<0.01, ****p<0.0001 ZDF compared to Lean; T-test.